



HAL
open science

Bio-sourced particles for soft matter physics

Thomas Gibaud

► **To cite this version:**

Thomas Gibaud. Bio-sourced particles for soft matter physics. Soft Condensed Matter [cond-mat.soft]. Université de Lyon, 2018. tel-01934851v2

HAL Id: tel-01934851

<https://hal.science/tel-01934851v2>

Submitted on 16 Dec 2018

HAL is a multi-disciplinary open access archive for the deposit and dissemination of scientific research documents, whether they are published or not. The documents may come from teaching and research institutions in France or abroad, or from public or private research centers.

L'archive ouverte pluridisciplinaire **HAL**, est destinée au dépôt et à la diffusion de documents scientifiques de niveau recherche, publiés ou non, émanant des établissements d'enseignement et de recherche français ou étrangers, des laboratoires publics ou privés.

1722_309_7_m 10 nm ceiling, Ekod: BG_10_0916_1717_44_3-frames



UNIVERSITÉ
DE LYON



Thomas Gibaud

Univ Lyon, Ens de Lyon, Univ Claude Bernard, CNRS, Laboratoire de Physique, F-69342 Lyon, France

Bio-sourced particles for soft matter physics

Manuscript submitted to obtain the grade
« Habilitation à Diriger des Recherches »
and presented the 23/11/2018 at the Ens de Lyon

Jury composition:

Laurence Ramos, Université de Montpellier 2, Fr
Paul Menut, Sup'Agro Montpellier, Fr
Giuseppe Foffi, Université de Paris Sud, Fr
Laurent Heux, Université Grenoble Alpes, Fr
Olivier Sandre, Université de Bordeaux, Fr
Denis Bartolo, Ens de Lyon, Fr
Eric Fréssingéas, Ens de Lyon, Fr

Bio-sourced particles for soft matter physics.

Manuscript presented the 23/11/2018 by Thomas Gibaud to obtain the grade "Habilitation à Diriger des Recherches".

Abstract – I use, purify or engineer nanometer to micron particles which serve as building blocks to create innovative soft materials. The particles specific properties cascade to macroscopic scales and are the cornerstone for designing new materials. I then put efforts in understanding the soft material response to external solicitations. To do so, I use devices such as rheometer, optical tweezers or high power ultrasound. I also take advantage of built-in sensitivity of the particles to pH or temperature to continuously morph the dispersion's properties. This bottom up approach combined with external solicitation of the self assembled soft materials allows me to tackle fundamental issues in self-assembly, gels and active matter and mimics many phenomena observed in biology or hard condensed matter. In this manuscript, I focus on two examples, namely, the use of filamentous bacteriophages as building block for reconfigurable self-assembly and instabilities such as yielding, rupture and wrinkling in colloidal gels.

Particules bio-sourcées pour la physique de la matière molle.

Manuscrit présenté le 23/11/2018 par Thomas Gibaud pour obtenir le grade "Habilitation à Diriger des Recherches".

Résumé – J'utilise, purifie ou conçois des particules du nanomètre au micron qui servent de brique élémentaire de construction pour créer des matériaux mous innovants. Les propriétés spécifiques des particules se répercutent à l'échelle macroscopique et constituent la pierre angulaire de la conception de nouveaux matériaux. Je m'efforce ensuite de comprendre la réponse de ces matériaux mous à des sollicitations externes. Pour ce faire, j'utilise des appareils comme des rhéomètres, des pinces optiques ou des ultrasons de haute puissance. Je profite également de la sensibilité propre des particules au pH ou à la température pour modifier en continu les propriétés de la dispersion. Cette approche ascendante combinée à des sollicitations externes de ces matériaux mous auto-assemblés me permet d'aborder les questions fondamentales sur auto-assemblage, les gels et la matière active. Par ailleurs, ces matériaux mimiquent de nombreux phénomènes observés en biologie ou en matière condensée dure. Dans ce manuscrit, je me concentre sur deux exemples, à savoir l'utilisation de bactériophages filamenteux comme éléments constitutifs de l'auto-assemblage reconfigurable et des instabilités telles que la fluidization, la rupture et le plissement de gels colloïdaux.

Contents

I	Preamble	
1	Foreword and acknowledgements	7
II	Defense report	
III	Self-assembly	
2	Introduction	14
3	Filamentous phages - versatile building blocks	16
3.1	Synthesis	16
3.2	A model system?	16
3.3	A versatile library of colloid rods	18
3.3.1	Chirality	18
3.3.2	DNA backbone	18
3.3.3	Major coat proteins	18
3.3.4	Cap proteins	19
4	Condensation of colloidal rods	20
4.1	Colloidal rod and depletion	20
4.1.1	Nematic droplets	20
4.1.2	Colloidal membranes	20
4.2	Colloidal membranes and chirality	23
4.2.1	Tuning the edge chirality	23
4.2.2	Twisted ribbons	23
4.3	Colloidal membranes and chiral coalescence	26
4.3.1	Homo chiral coalescence – π -walls, pores, Möbius anchors and colloidal skyrmions	26
4.3.2	Hetero chiral coalescence – scalloped membranes and gaussian curvature	29
4.4	Asymmetric mixtures of colloidal rods	30
4.4.1	Phase separation in colloidal membranes	30
4.4.2	Membrane rafts	31
5	Conclusion and perspectives	33
IV	Other projects synopses	
6	Triggering instabilities in Gels	36
6.1	Introduction	36
6.2	Fatigue and yielding in soft gels	37
6.2.1	Challenges associated with the determination of the yield stress	37
6.2.2	Yielding characteristic time scales	37

6.3	Predicting rupture in strong gels	39
6.3.1	Challenges associated with the prediction and assessment of rupture	39
6.3.2	Rupture and phase separation	39
6.3.3	How strain non-linearities point toward the rupture point	39
6.4	Wrinkling gels	41
6.4.1	Investigating new wrinkling mechanisms in a model system	41
6.4.2	Experiments with yogurt-like gels	41
6.4.3	A new wrinkling mechanism related to the gel porosity	41
7	Futur projects	43
7.1	(StruBaDy) Structure Bacteria Dynamics	43
7.1.1	Global objective	43
7.1.2	Context and aim	43
7.1.3	Impact of the project	45
7.1.4	Organization of the project and means implemented	45

V

Curriculum Vitae

8	Short CV	48
9	Long CV	50
9.1	Short Biography	50
9.2	Research statement	50
9.3	Scientific production	50
9.4	Media coverage	53
9.5	People	53
9.6	Services	54
9.7	Teaching and Outreach	54
9.8	Grants	55

VI

Bibliography



Preamble

1. Foreword and acknowledgements

The Habilitation à Diriger des Recherches (HDR) is a national qualification of higher education delivered by French University level organisms. In France, this diploma is required to apply for a university professor position or directeur de recherche at the CNRS. It is a recognition of the candidate's high scientific level, the originality of his approach in a field of science, his ability to master a research strategy in a sufficiently broad scientific or technological field, and its ability to supervise young researchers [Arrêté du 23 novembre 1988 relatif à l'habilitation à diriger des recherches].

This HDR presents some of my research work in the field of physics from 2012 to 2017. The research is centered on soft matter physics. The common thread rely in the use, the purification or the engineering of organic and living matter to design smart colloids which serve as building blocks to create materials with fine tuned dynamics and structures. Those materials are not only a venue to study self-assembly, gels and active matter but they also mimics many phenomena observed in biology or hard condensed matter physics.

The work presented in the HDR results from long standing collaborations. The people involved in those collaborations shaped my research projects and allowed me to progress though out the years to become not only a better scientist but also a better person. I'm lucky to have cross your way. It has been a pleasure to work with you all. I look forward continuing research with you.

I decided to pass my HDR when I was invited by the journal J. Phys Cond. Mat. to write a review on self assembly and phages for the winter 2017. This review constitute the core of my HDR (Part III) and allows me to kill two birds with one stone. Part III Chapters 2-3-4-5 deals with self-assembly, the phenomenon in which a collection of particles spontaneously arrange themselves into mesoscopic structures. Through the use of filamentous phage as building block for self assembly we mainly discuss two fundamental questions. Can the global behavior of a system be engineered using local rules set by the building blocks properties? And how do local rules interlace with physics principles and determine global behavior? The results presented come from a fruitful collaboration mainly with Zvonimir Dogic at Brandeis University (USA). I sincerely thank Zvonimir Dogic who introduce me to microscopy and the subject of self-assembly/filamentous phages. Many thanks to Edward Barry, Anna Modlińska, Prerna Sharma, Andrew Ward and Mark J. Zakhary for countless hours spend together in the lab making those experiments work; to C. Nadir Kaplan, Louis Kang, Tom C. Lubensky, Robert B. Meyer, Robert A. Pelcovits, Thomas R. Powers and Hao Tu for their theoretical insight; and Seth Fraden, Eric Grelet, Pavlik Lettinga and Rudolf Oldenbourg for useful discussions.

Although Part III is the main subject of this HDR, I have added in part IV synopses of other projects. Part IV Chapter 6 presents results on proteins gels, soft solids composed of a space spanning protein network in water. The works is centered around three distinct questions. How gels fatigue? Is it possible to predict rupture in gels under repetitive loads way before the gels are damaged? And what are the protein properties necessary to spontaneously wrinkle a thin sheets of gel? This work is a collaborative effort mainly with Sébastien Manneville at the Ens de Lyon (France). I sincerely thanks Sébastien Manneville who has introduce me to rheology and ultrasound techniques. Many thanks to Nicolas Taberlet, Christophe Perge, Mathieu Leocmach, Brice Saint-Michel, Thibaut Divoux and Stephan Lindstrom for their precious help on those gels experiments.

Part IV Chapter 7 presents preliminary results on one of my futur projects. It is a collaborative effort mainly with Denis Bartolo at Ens de Lyon (France). I sincerely thanks Denis Bartolo who was very enthusiast to initiate this new collaboration in unknown territory for both of us. Thanks to Antoine Lagarde, Pierre-Henri Delville and Noémie Dagès who helped me start the project on bacteria.

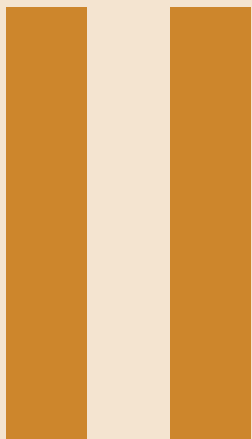
Part V is dedicated to my CV.

I acknowledge and thank the jury members, Laurence Ramos as referee (Université de Montpellier 2, Fr), Paul Menut as referee (Sup'Agro Montpellier, Fr), Giuseppe Foffi as referee (Université de Paris Sud, Fr), Laurent Heux (Université Grenoble Alpes, Fr), Olivier Sandre as president (Université de Bordeaux, Fr), Denis Bartolo (Ens de Lyon, Fr) and Eric Fréssingeas (Ens de Lyon, Fr) for accepting to evaluate my HDR.

I thanks the funding agencies (Agence National de la Recherche, the région Rhône Alpes Auvergne, the fédération Ampère and the CNRS) which grants have allowed me to recruit scientists and buy research equipment. I also thanks the CNRS which is my employer and has given the liberty to tackle many subjects. I finally thanks the Ens de Lyon and the Laboratoire de Physique which as welcomed me and hosted me.

Finally, this work is all the more meaningful and enjoyable that I have a family and friends with whom to share my free time. I am grateful to Florence for her love. Sharing the down and the up of life with you is immensely rewarding. I feel lucky and proud to build a family life with you.

Thomas Gibaud,
Lyon (France),
August 2018



Defense report

de l'HABILITATION À DIRIGER DES RECHERCHES en PHYSIQUE à l'ENS de Lyon

de Monsieur Thomas GIBAUD,

le 23 novembre 2018

sur le thème suivant :

« Soft matter with bio-sourced particles »

Arrêté du 23 novembre 1988 relatif à l'Habilitation à Diriger des Recherches

[Le président du jury, après avoir recueilli l'avis des membres du jury, établit un rapport qui est contresigné par l'ensemble des membres du jury. Le Rapport de soutenance est communiqué au candidat.]

Dans une présentation claire et dynamique, Thomas Gibaud a présenté une série de trois sujets représentatifs de ses travaux depuis la fin de sa thèse. La présentation très pédagogique a mis en évidence le large spectre de techniques expérimentales et de systèmes physico-chimiques qu'il maîtrise. La cohérence des travaux est apparue clairement autour du fil conducteur des instabilités, aussi bien sur des auto-assemblages à l'équilibre et forcés hors équilibre par des écoulements. Le niveau de ses recherches se situe au premier plan international.

Le projet que Thomas Gibaud a élaboré s'appuie sur son expertise dans l'utilisation d'objets biologiques comme "atomes modèles" pour la formation d'objets auto-assemblés.

En conclusion le jury considère unanimement que Thomas Gibaud présente toutes les qualités requises pour encadrer de jeunes chercheurs au travers de projets ambitieux et novateurs.

Arrêté du 23 novembre 1988 relatif à l'habilitation à diriger des recherches

Monsieur Thomas GIBAUD

Né le : 15 février 1979, à Le Mans (FRANCE)

Nationalité : Française

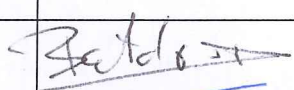
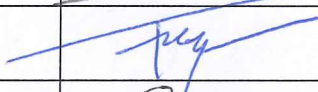
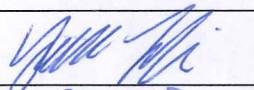
Candidat à l'**Habilitation à Diriger des Recherches** en **PHYSIQUE**, (Section CNU n°28)

a présenté publiquement en soutenance une habilitation à diriger des recherches sur le thème suivant :

« **Soft matter with bio-sourced particles** »

Après délibération, le jury présidé par (Prénom - NOM) : Olivier SANDRE

et composé de :

Membres du jury		Signatures
Monsieur Denis BARTOLO	Professeur des universités	
Monsieur Éric FREYSSINGEAS	Maître de conférences - HDR	
Monsieur Laurent HEUX	Directeur de recherche	
Monsieur Olivier SANDRE	Directeur de recherche	
Monsieur Paul MENUT	Maître de conférences - HDR	
Monsieur Giuseppe FOFFI	Professeur des universités	
Madame Laurence RAMOS	Directrice de recherche	

Article 7 de l'arrêté du 23 novembre 1998 modifié par l'arrêté du 13 juillet 1995 :

L'admission ou l'ajournement est prononcé après délibération du jury. Le président du jury établit et signe le rapport de soutenance qui est contresigné par l'ensemble des membres du jury. Le rapport de soutenance est communiqué au candidat.

déclare le candidat :

ADMIS à l'**Habilitation à Diriger des Recherches**

AJOURNÉ

À Lyon, le 23 novembre 2018.

1^{er} rapporteur (NOM et prénom) : RAMOS Laurence 

2^{ème} rapporteur (NOM et prénom) : FOFFI Giuseppe 

3^{ème} rapporteur (NOM et prénom) : MENUT Paul 

ATTESTATION DE RÉUSSITE

Je soussigné, Jean-François PINTON, Président de l'École Normale Supérieure de Lyon, certifie que :

Monsieur Thomas GIBAUD

Né le **15 février 1979** à **Le Mans (FRANCE)**

a présenté publiquement en soutenance le **23 novembre 2018**

une **Habilitation à Diriger des Recherches** en **PHYSIQUE**

sur le thème suivant :

« **Soft matter with bio-sourced particles** »

et a été déclaré **admis**.

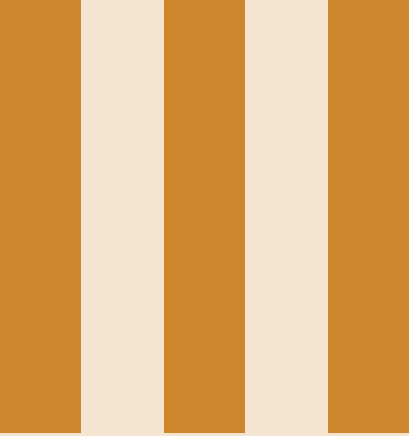
Attestation établie pour valoir ce que de droit.

Fait à Lyon, le **04 DEC. 2018**

Pour le Président de l'ENS de Lyon,
par délégation,
la vice-présidente aux Études

Sylvie MARTIN





Self-assembly

2	Introduction	14
3	Filamentous phages - versatile building blocks	16
3.1	Synthesis	
3.2	A model system?	
3.3	A versatile library of colloid rods	
4	Condensation of colloidal rods	20
4.1	Colloidal rod and depletion	
4.2	Colloidal membranes and chirality	
4.3	Colloidal membranes and chiral coalescence	
4.4	Asymmetric mixtures of colloidal rods	
5	Conclusion and perspectives	33

2. Introduction

Self-assembly is the phenomenon in which a collection of particles spontaneously arrange themselves into mesoscopic structures [1, 2, 3, 4, 5, 6]. The complexity of the mesoscopic structure is encoded in the building blocks and the physics that drive its condensation. Although the fundamental and driving questions in self-assembly have persisted from the birth of the field up to the present – Can the global behavior of a system be engineered using local rules set by the building blocks properties? How do local rules interlace with physics principles and determine global behavior? – the complexity has drastically increased over the years.

Complexity is in part driven by the properties of the building blocks. In this respect colloidal building blocks have a peculiar savor. Contrary to polymers, copolymers, surfactants or molecular liquid crystals [7, 8], colloids can be considered as giant atoms [9, 10] where the solvent mediate the interactions. Consequences are many fold. First, it is a convenient experimental system. Since colloids can be quite big, both the shape and the structure of the condensate at the colloidal level can be visualized under a microscope. Second colloids and their condensates may be manipulated using microfluidics and external fields such as optical traps. Third, due to their large size, the colloids dynamics is also quite slow which permits to probe local kinetics and mechanisms leading to their condensation and their restructuring. Finally colloids come with a large toolbox that permits to engineer their shape and interactions. The last decades have seen an explosion of strategies to obtain synthetic and biological colloids. Colloidal may come in various shape from spheres to anisotropic geometries [11, 12] such as colloidal polyhedra [13, 14], tetrapods [15], dumbbell [16] and triangles [17] or cubes [18, 19]. Classical techniques to tailor isotropic interactions include tuning the Van der Waals attraction via the Hamaker constant, grafting polymers to the colloid surface for entropic repulsion, screening the surface charge with the salt, the use of polymers to induce depletion interactions [20], etc. . . . Anisotropic interactions are common in proteins [21] and may be induced just by the shape of the colloid [22] or by functionalizing the particle surface [23] with lock and key groups, such as topological patch, DNA oligonucleotides [24, 25, 26, 27], protein-based cross-linkers like biotin–avidin or antibody–antigen binding pairs [28], and metallic patches [29]. Depending on the strength and topology of the patchy interactions, the bounding of two colloids may lead to super colloids with internal degree of freedom such articulated bond for instance obtained in 'lock and key' colloids [30] or by grafting DNA onto liquid interfaces of emulsions [31]. Anisotropic interactions may also come from the solvent. Small water droplets dispersed in a nematic liquid crystal exhibit short-range repulsion and a long-range dipolar attraction which lead to the formation of anisotropic water droplets chainlike structures [32]. Interaction that can be triggered externally is one essential knob to study reconfigurable self-assembly and sequential or layer by layer self-assembly. It allows to navigate in the phase diagram of colloidal dispersions in a continuous way, providing reversible pathway to induce transition between different structures. Divers strategies are adopted to have interactions which can be sensitive to temperature (DNA coated colloids [33, 34], proteins [35]), magnetic fields [36, 37, 38], or electric fields [39, 40].

Complexity also comes from the interplay between thermodynamics and kinetics. Self-assembly is a stochastic process and the thermal energy $k_B T$ plays a particular role. It unable the particles to diffuse and probe the energy landscape of the dispersion. In principle, according to thermodynamics, the preferred self-assemble structures are the ones that minimize the free energy of the dispersion. However the actual order obtained may depend on non-equilibrium effects, local fields, kinetic traps, and pathway-dependent ordering. Hard sphere crystallization is a simple case of self assembly directed by entropy that can be hindered by the glass transition [41]. Assembly strategies have complexified in recent years. In directed assembly, external fields are used as template to order the colloids [42, 43, 40]. In template-assisted self assembly, a substrate is used to order colloids [44, 45]. In reconfigurable self-assembly, tunable interactions permits transition from one state to another [46, 47]. In programmable self-assembly, information is added to the colloids to direct their organization [48, 27, 49, 48, 50, 51]. Sequential self-assembly is based on colloids with selective interactions and their sequential activation to form material through multistep kinetics [52, 53]. Those strategies may lead to simple structures like homogeneous crystals or to hierarchical assembly where the building blocks organization takes place over distinct multiple levels leading to material structuration at length scales much larger than the building blocks [54, 55, 56, 57, 47, 58, 59].

In the quest to complex structures, one has to deal the possibility to flatten the configuration energy landscapes. This leads to diverging assembly times and increased probability of forming kinetically trapped structures as shown in the following examples.

- Colloids with unspecific and low binding energy produce a zoology of configurations which make it hard to target one specific structure. Colloidal clusters containing a few particles bound together by weak attractive interactions are among the simplest, nontrivial systems for investigating collective phenomena in condensed matter. For example a cluster of six colloids may form eight-bond polyhedra with various configurations: three of which lie in a ground state and eight in the excited state [60].

- Kinetically driven process may induce strong local order but inhibit restructurations or self healing processes. Capillary driven self-assembly consists of suspending small objects at the water–air interface. Due to the balance between gravity and surface tension, the interface is slightly deformed, inducing a net force between the particles. By inducing liquid curvatures with specific cross and curved particles it is possible to assemble various fivefold symmetry structures [61]. Due to the strong attraction between the particles such approach depends very much on the initial conditions and may produce a considerable amount of defective structures. This is also the case in over crowded systems which lead to dynamical arrest or particles with a large number of specific interactions such as DNA origamis which permit to produce well-defined complexes structures where thousands of locations can be independently functionalized with nanometer-scale precision, but have a very low yields[62].

Here we focus on filamentous phages. Filamentous bacteriophages such as fd-like viruses are monodisperse rod-like colloids that have well defined properties: diameter, length, rigidity, charge and chirality. Engineering those viruses leads to a library of colloidal rods which can be used as building blocks for self-assembly, section 3. Their condensation in aqueous solution with additive depletants to mediate attraction between the rods leads to a myriad of fluid-like micronic structures ranging from isotropic/nematic droplets, colloid membranes, achiral membrane seeds, twisted ribbons, π -wall, pores, colloidal skyrmions, Möbius anchors, scallop membranes to membrane rafts. Those structures and the way they shape shift not only shed light on the role of entropy, chiral frustration and topology in soft matter but it also mimics many structures encountered in different fields of science, section 4.

Finally we discuss a road map using an isotropic aqueous suspensions of filamentous phages and depletion to rationalize the phages hierarchical and reconfigurable self-assembly upon variations of attraction via the depletion interaction, chirality and rods composition, section 5.

3. Filamentous phages - versatile building blocks

A bacteriophage or phage is a virus that infects and replicates within a bacterium. They were discovered by Twort [63] and d'Hérelle [64] in the early 20th century. Bacteriophages are among the most common and diverse entities in the biosphere [65] and are widely distributed in locations populated by bacterial hosts, such as soil or the intestines of animals or sea water. In the latest, up to $\sim 10^8$ virions per milliliter were found in microbial mats at the water surface, [66]. The impact of phage research in biology is huge: from novel biochemical mechanisms for replication, maintenance and expression of the genetic material and new insights into origins of infectious disease to their use as therapeutic agents [67]. Here, we focus on fd-like phage and their use as building block for self-assembly, [68].

3.1 Synthesis

The fd-wt virus was originally isolated from sewage [70]. fd-wt ($M_w = 16.4 \times 10^6$ g/mol) are identical to one another and composed of a single strand DNA surrounded by a protein layer of about 2700 identical protein p8 subunits. The protein p8 has a molecular mass of 5240 g/mol and accounts for about 99% of the total protein mass. The rest of the protein mass belongs to the minor coat proteins and are located at the tips of virus [71]. At one end of the filament there are five copies of the protein p9 and p7. At the other end of the phage, there are five copies of p3 and p6. p3 proteins are the first to interact with the E. coli host during infection. p3 is also the last point of contact with the host as a new phage bud from the bacterium, Fig. 3.1.

Bacteriophage viruses were named based on their observed ability to lyse bacterial cells (in greek, 'bacteria eaters'). However not all phages lyse bacteria. In particular, fd-wt use a lysogenic cycle. Lysogeny is characterized by the integration of the bacteriophage nucleic acid into the host bacterium's genome or formations of a circular replicon in the bacterial cytoplasm. In this condition, the bacterium continues to live and reproduces normally. The genetic material of the bacteriophage is transmitted to daughter cells at each subsequent cell division. Once infected the cell and its descendants are thus turn into a virus manufacture.

fd-wt are grown using standard biological techniques [72, 73]. In short, an overnight starter culture taken from a single colony of the bacteria ER2738 is incubated at 37°C and shaken at 250 rpm in 5 mL of sterile 2xYT (yeast extract tryptone) growth medium. 200 μ L from the resulting overnight E. coli culture is then grown in 5 mL of a fresh growth medium until it reaches an optical density $OD = 0.5$ at 600 nm measured with a UV-Vis spectrophotometer. The sample is then inoculated with 10 μ L fd-phage stock at approximately 1 mg/mL. The suspension is incubated and shaken 30 minutes then transferred to a 250 mL conical flask with 30 mL of froth media for 2 hours and finally transferred in a 2 L flask with 500 ml of growth and media and grown until $OD = 1$. From the 500 mL growth cycle, E. coli cells and debris are removed by centrifuging the cultures twice at 8300g for 15 minutes, harvesting the supernatant each time. A precipitant solution is added (146.1 g/L NaCl and 200 g/L PEG 8000) in a ratio of 3 parts precipitant to 10 parts supernatant. After refrigeration for at least an hour, the supernatant is centrifuged as before, and the clear supernatant is removed, leaving the precipitated pellet of viruses. Viral pellets are resuspended in 10 mL of sterile phosphate buffered saline (PBS) solution. Ultracentrifuge (1h at 90000 rpm) is then used to exchange the buffer and concentrate the viruses. The virus concentration is determined using absorption spectroscopy. The optical density of fd-wt at 269 nm for 1 mg/ml solution in a 1 cm cuvette is $OD = 3.84$ [74]. This procedure yields a virus stock solution with some multimers, such as dimers that have a contour length that is twice that of fd-wt, Fig. 3.2. To select the monomers, the stock solution is fractionated. Samples are concentrated to reach the isotropic-nematic phase coexistence so that 20% of the sample is nematic and the rest is isotropic. Longer rods preferentially dissolve in the nematic phase [75]. The isotropic fractions is isolated and used as a stock of monodisperse viruses. For the study presented in the review, the viruses are dispersed in a buffer that contains 100 mM/mL NaCl and 20 mM/mL Tris at pH = 8.05.

For the study presented in the review, in addition to fd-wt, the filamentous phages fd-y21m and m13KO7 are also used. Their synthesis follow the same protocol as for fd-wt and their unique properties are details in Tab. 3.1.

3.2 A model system?

There are unique advantages of this particular system. First, fd-wt are monodisperse. This eliminates complications related to the polydispersity of rods and facilitates direct quantitative comparison with theory. Second, fd-wt have a diameter of 6.6 nm for a contour length of 880 nm [80, 81] conferring them a large aspect ratio, ~ 130 which is similar to the one of spaghetti (~ 150). Finally viruses are quite rigid: fd-wt has a persistence length of $\sim 2.8 \mu$ m and the mutant fd-y21m has an even greater persistence length, $\sim 9.9 \mu$ m [77]. Therefore,

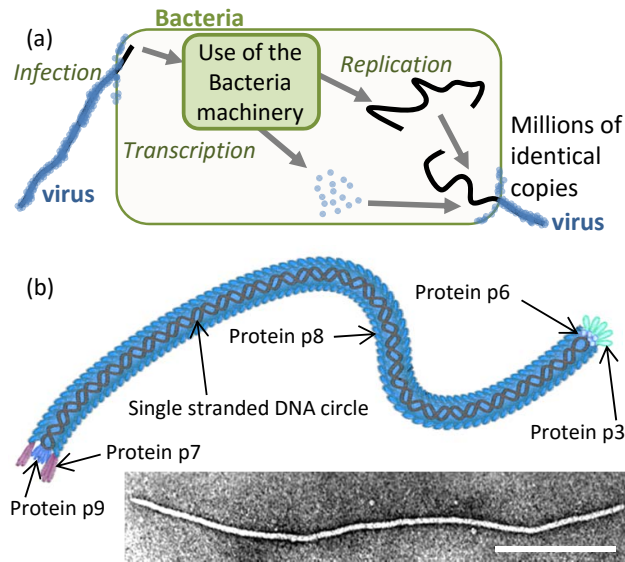


Figure 3.1: Phage virus like fd-wt use the machinery of *E. coli* to reproduce itself. (a) Schematic of the reproduction cycle of fd-wt. (b) Schematic, [69] and electron microscopy image of fd-wt virus. Scale bar 200 nm.

	fd-wt	fd-y21m	M13KO7
D (nm)	6.6	6.6	6.6
L (μm)	0.88	0.88	1.2
L_p (μm)	2.8	9.9	2.8
C (e^-/nm)	10	10	7
Chirality	right	left	right

Table 3.1: Properties of the filamentous phages fd, fd-y21m and M13KO7: diameter D , Contour length L , Persistence length L_p , Charge density at pH=8.05 C and chirality [76, 77, 78, 79].

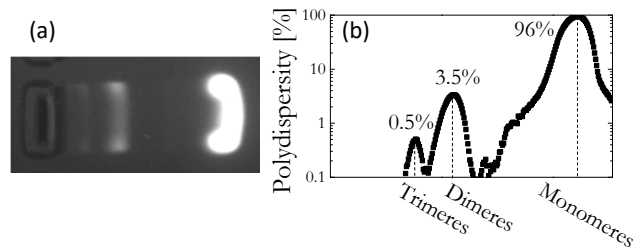


Figure 3.2: Gel electrophoresis of a typical fd-wt preparation [47]. (a) Ethidium Bromide stained gel viewed under UV illumination. The bottom bright band consists of 880 nm long fd-wt monomers, while the middle and top bands contain fd-wt dimers and trimers, respectively. (b) Virus polydispersity is quantified by plotting the normalized intensity profile of the gel, [47].

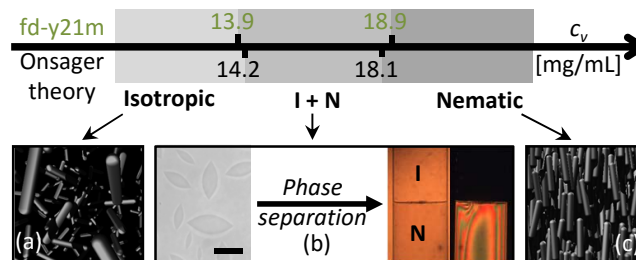


Figure 3.3: Comparison between the phase diagram of fd-y21m and the Onsager prediction [77]. (a) schematic of the isotropic phase, (b) I-N phase separation process starting with tactoids and eventually leading to two homogenous isotropic and nematic phase separated by a single interface and (c) a schematic of the nematic phase. Due to their higher flexibility, the coexistence region for fd-wt is narrower and shifted toward higher concentrations: $c_{Iso} = 19.8$ and $c_{Nem} = 22.6$ mg/mL.

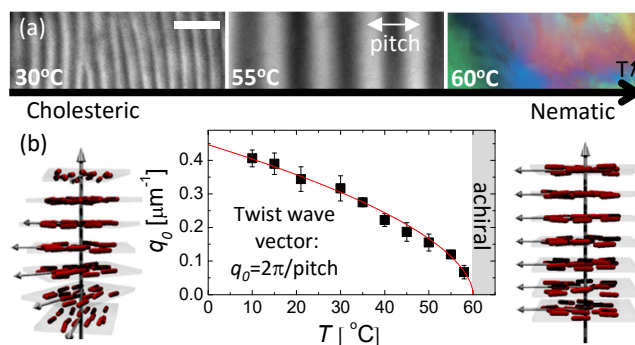


Figure 3.4: Effect of temperature on the chirality of an aqueous suspensions of fd-wt at $c_v=100$ mg/mL [47]. (a) Cross polarized microscopy pictures of the nematic and cholesteric phases. Scale bar 30 μm. (b) Measurements of the twist wave vector of the cholesteric phases as a function of temperature. Left: sketch of the cholesteric phase. Right: sketch of the nematic phase.

viruses, and fd-y21m in particular, can be considered as a model liquid crystal system in the framework defined by Onsager. At low concentrations, colloidal rods form an isotropic phase with no direction or orientation order. However as the concentration is increased, the isotropic dispersion becomes metastable or unstable: orientation fluctuations drive concentration gradients which lead to phase separation. During this transition, transient nematic droplets or tactoids nucleate in an isotropic background and coalesce to minimize the interface between the isotropic and the nematic phases. This leads to the thermodynamically stable state: two homogeneous phases, the isotropic and nematic phase separated by a single interface, Fig. 3.3. Onsager has established that this transition is purely entropic in nature [82, 83]. The entropy loss due to the orientation ordering in the nematic phase is over compensated by the increase in translational entropy: the free volume for any one rod increases as the rods align. Moreover, he established that the transition volume fractions for rigid rods with an aspect ratio larger than 75 and repulsive interactions are: $\phi_{Iso} = 3.289D/L$ for the isotropic phase and $\phi_{Nem} = 4.192D/L$ for nematic phase [82]. D is the diameter of the rod and L its contour length. These predictions are remarkably close to experimental results [77], Fig. 3.3.

3.3 A versatile library of colloid rods

A challenge associated with hierarchical assembly is to control the final macroscopic assemblage by specific modification of relevant microscopic parameters. Thanks to nature diversity, genetic engineering and chemistry, it is possible to collect and create a large library of fd-like particles with slight variations in their physical properties, like their contour length, diameter, rigidity or interactions [68, 84].

3.3.1 Chirality

fd-wt is chiral and left-handed: in close contact with one another fd-wt tend to twist preferentially clockwise. Therefore fd-wt, at room temperature, form a cholesteric phase instead of nematic [85, 47], Fig. 3.4. Moreover, fd-wt chirality is temperature sensitive. Chirality decreases with temperature and eventually vanishes at 60 °C, Fig. 3.4. Deriving the virus chirality and its temperature dependence and its propagation at the macroscopic length scale remains a challenge [86, 87, 88, 89, 71]. Day and Meyer proposed that the cholesteric twist derives from a 'cork screw' shape of the virus due to the interplay between its major coat proteins and its DNA backbone [71].

3.3.2 DNA backbone

The contour length of phage virus scales linearly with its genome size. The virus length impacts the dynamics of the virus. Maguire *et al.* have shown that the rotational diffusion coefficient of rods in the isotropic phase scales linearly with the length [90]. Alvarez *et al.* have shown that the mobility of long rods immersed in a smectic phase composed of short rods is enhanced compared to the short rods [91]. The virus length also affects the phase diagram. It shifts the location of the isotropic-nematic phase transition toward higher volume fractions and it stabilizes the smectic phase [92, 76, 93]. So far, physicists have used viruses whose lengths range from ~ 0.4 to 1.2 μm. However, using molecular cloning techniques it is possible to engineer viruses that are as short as 50 nm and as long as 8000 nm [94, 95, 96, 97, 98].

3.3.3 Major coat proteins

The major coat proteins confer to fd-wt a net linear charge density of $10 e^-/\text{nm}$ at pH=8.05 [99, 76]. It is possible to label the major coat proteins with chemical compounds. This is very convenient to make the virus fluorescent and track their individual dynamics within an assemblage. Coatings such as PEG [100], SiO₂, TiO₂, [101], PNIPAM [102], DNA [103], gold [104], carbon nanofiber [105] or fluorescent dyes [106] obviously

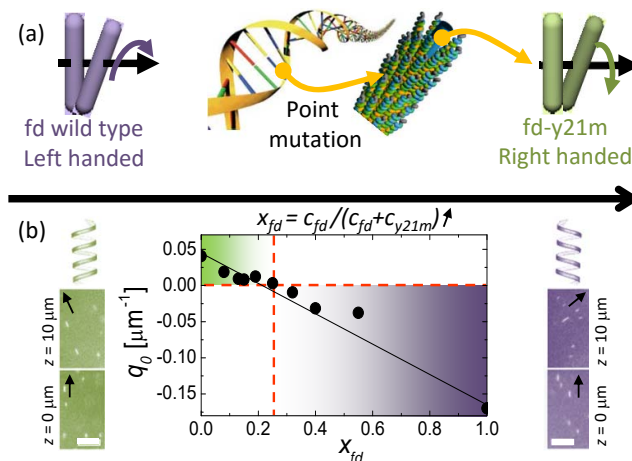


Figure 3.5: Effect of the ratio of fd-wt to fd-y21m on the chirality of aqueous mixtures of fd-wt and fd-y21m, $c_v=55$ mg/mL, $T = 22$ °C [77]. (a) Sketch of the chiral interaction between two fd-wt and the point mutation on the major coat proteins that induce opposite chiral interaction between fd-y21m. (b) Measurements of the twist wave vector of the cholesteric phases as a function $x_{fd} = c_{fd} / (c_{fd} + c_{fdy21m})$ where c_{fd} and c_{fdy21m} are the concentration of fd-wt and fd-y21m. Side figures: z -stack of a cholesteric phase which helicoidal structure oriented along the z -axis. A few fluorescently labeled viruses are embedded in the structure to indicate the local director and hence the sense of the chirality. Scale bar $5 \mu\text{m}$.

increases the diameter of the virus but may also drastically change the interactions between the viruses and therefore the way they self-assemble.

Genetic mutation represents another way to act on the major coat proteins [107]. For example, structural biologists have genetically engineered fd-wt into fd-y21m, a mutant virus in which the 21st amino acid out of the 50 composing the major coat protein is changed from tyrosine to methionine [108]. fd-y21m is not only stiffer as mentioned above, but it also makes left-handed cholesteric state as opposed to fd-wt which forms right-handed cholesteric state [77] and contrary to fd-wt, fd-y21m chirality is temperature independent [47]. By mixing fd-wt and fd-y21m at a controlled ratio x_{fd} , it is possible to design cholesteric phases with the desired pitch and chirality, Fig. 3.5. The phase space of all possible mutations of the major coat protein is huge. It could be investigated using phage display technology [109] to better understand the impact of the coat protein structure on the coarse-grained properties of the filament [110].

3.3.4 Cap proteins

Another attractive feature of filamentous bacteriophages is the presence of cap protein which are distinct from the major coat protein, thus enabling selective labeling of the virus end and in particular normal anchoring of the phage. On one hand this feature is used to create new materials. For instance using phage display, filamentous phages were organized into smectic layers that are intercalated with layers of end-bound inorganic nanoparticles [111, 112]. On the other hand this feature is also used to design new particles such as star colloids where filamentous phages were pinned to the colloid surface [113] or filamentous ring-like structures by labeling the two ends of the virus with distinct labels that stick to each other [114]. This last example paves the road toward specific and sequential self-assembly.

Nature is capable of assembling structures of colloidal size that are frequently unmatched by chemical synthesis. fd-like virus is one of them and it makes fd-like viruses unique building blocks for reconfiguration self-assembly. In particular, their anisotropic shape, colloidal size and the already existing large library of viruses permit to dig into the combined field of liquid crystal physics, surfactant and colloidal physics for self-assembly concept. Finally, the possibility to trigger externally chiral interactions, which are luckily of the order of $k_B T$, is appealing as a knob to continuously move in their phase diagram and study structural transitions.

4. Condensation of colloidal rods

4.1 Colloidal rod and depletion

In mixture of colloidal rods and polymers depletants there is a region which surrounds every colloidal rod that is unavailable for the centers of the depletants. As two rods approach each other, this excluded volume overlap and additional free volume becomes available to the polymers, thus increasing the overall entropy of the mixture, Fig. 4.1. This results in an effective attractive (depletion) potential between the rods, whose strength and range can be tuned by changing the polymer concentration and size, respectively [115]. Under high-salt conditions, hard-core repulsive interactions dominate the behavior of virus/polymer mixtures, and consequently all phase transitions in this system are entropically driven.

For rod-like particles, the depletion interaction is anisotropic. It tends to align the viruses [116] so that the overlap volume is maximized. The obvious consequence in the introduction of polymers in suspensions of phages is that it tends to shift the isotropic boundary to lower volume fractions. Due to the level rule, the nematic state is consequently shifted to higher volume fractions. Using fd-wt and dextran mixtures this behavior is quantitatively confirmed and modeled [117], Fig. 4.2. Depletion is an ideal tool to promote condensation.

4.1.1 Nematic droplets

Nematic droplets are composed of elongated molecules that adopt a nematic order. Due to this inner structuration and the interplay between the interfacial tension and the splay and bend elastic constants of the nematic phase [82], rather than being spherical, the droplets display a spindle shape called tactoid [118, 119, 120]. Tuning the morphology and order within the droplets represent a corner stone for applications such as light modulators or more generally as photonic materials [121, 122, 123, 124].

Most paths which lead to tactoids formation are kinetically driven. For example, Lettinga *et al.* prepared samples in the I-N coexistence region and used shear to dissolve the tactoids and then study their condensation. To circumvent kinetics issues, Modlińska *et al.* engineered a colloidal system where one can continuously tune the attraction between the rods to condensate tactoids in a reversible and quasi static way starting from an equilibrium isotropic state [125]. They replaced the depletants Dextran by thermo-sensitive and non-adsorbing pnipam microgel particles [126]. The effective attraction between the rods is then controlled externally by temperature. Navigating the phase diagram in a continuous way, they showed that tactoids formation is preceded by the nucleation and growth of dense isotropic spherical droplets within the isotropic background. This scenario is analogous to the enhanced protein crystallization spot located above the liquid-liquid phase separation suggested by ten Wolde and Frenkel [127]. Just as the critical density fluctuations and in particular fluctuations of high densities behave as a micro reactor to lower the energy barrier for crystal nucleation, the dense isotropic droplets layout the ideal nucleation spot for the nematic phase.

4.1.2 Colloidal membranes

Fig. 4.2 shows that it is possible to promote rods condensation but it does not reveal any new phases compared to the case without depletant. Barry and Dogic extended this phase diagram to higher dextran concentrations ($M_w = 500\,000$ g/mol) [128] and showed that, starting from an isotropic rods suspension at $c_v = 1$ to 10 mg/mL, it is possible to assemble a new phase: 2D colloidal membranes composed of a one-rod length thick mono-layer of aligned rods which diameter range from a few microns to hundreds of microns, Fig. 4.4. For dextran concentrations

Fig. 4.2 shows that depletion interactions promote rods condensation but it does not reveal any new phases

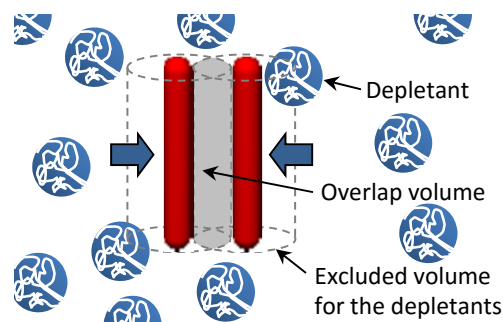


Figure 4.1: Sketch of the depletion interaction between two colloidal rods.

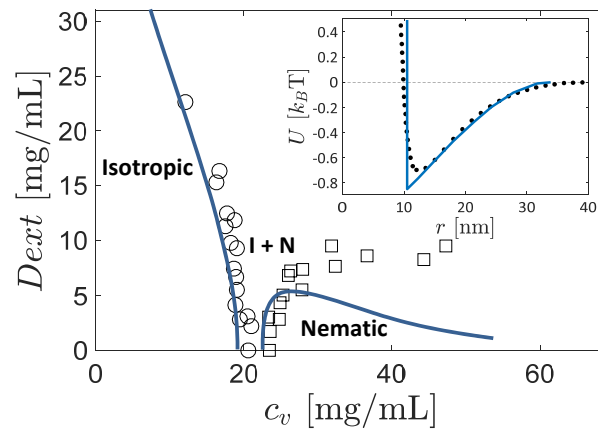


Figure 4.2: Influence of the depletant dextran ($M_w = 500\,000$, radius of gyration $R_g = 17.6$ nm, concentration D_{ext}) on an aqueous dispersion of fd-wt at a concentration c_v [117]. Circles delimit the isotropic state from the I-N coexistence region. Squares delimit the I-N coexistence region from the nematic state. The blue line corresponds to the predictions from the second virial theory with attraction (SVTA). Inset: interaction potential between two viruses separated by a distance r and oriented at 90° . The interaction potential is a sum of the electrostatic repulsion and the depletion interaction. Dot are the results of computer simulation. The line correspond to the approximate intermolecular potential between rods with an effective hard core diameter $D_{eff} = 10.5$ nm. The attractive part of the potential is modeled by Asakura-Oosawa penetrable spheres whose effective radius and concentration best fits the potential obtained through computer simulation. SVTA use this approximated potential as input.

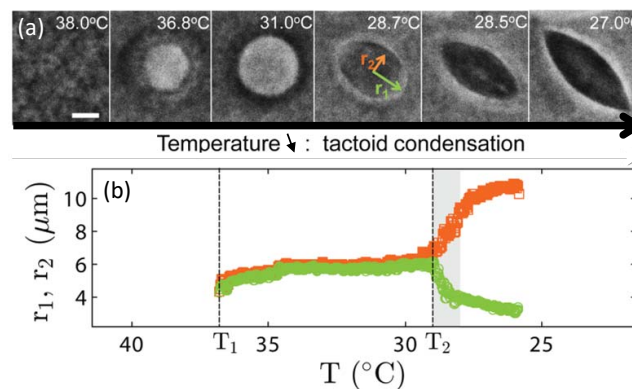


Figure 4.3: Condensation of nematic droplets in dispersions of colloidal rods with thermo-sensitive depletants [125]. (a) Phase contrast images of a suspension of M13K07 viruses at $c_v = 1$ mg/mL mixed with pnpam microgel particles at $c_p = 30$ mg/mL. As temperature is lowered ($0.09^\circ\text{C}/\text{min}$), the attraction increases and the condensation of nematic droplets is observed. The process is fully reversible when temperature is increased. Scale bar, $5\ \mu\text{m}$. (b) Measurements of the long and short semi-axis of the droplet, r_1 and r_2 as a function of temperature T . T_1 and T_2 are respectively the temperatures that separate the isotropic state, the spherical droplets regime and the tactoids regime.

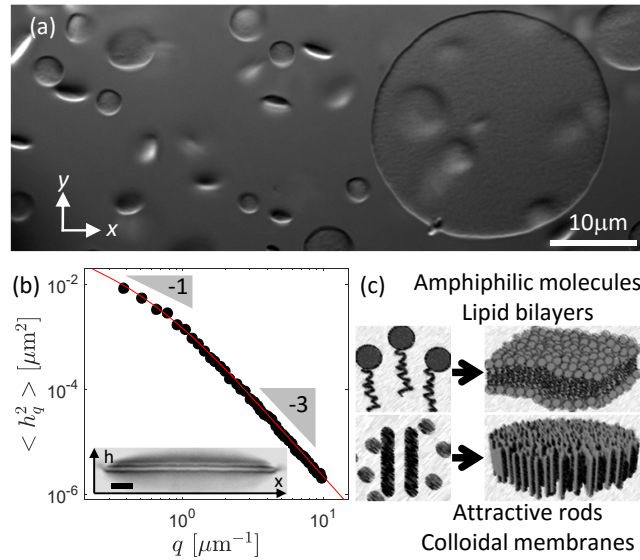


Figure 4.4: fd-wt colloidal membranes, $T = 22^\circ\text{C}$, $Dext = 45 \text{ mg/mL}$ [128]. (a) DIC micrograph colloidal membranes. Scale bar is $10\mu\text{m}$. (b) Fluctuation spectrum resulting from the Fourier analysis of a sequence of uncorrelated membrane conformations. The red line is the best fit to the Helfrich equation, which yields a lateral bending modulus of $135 k_B T$ and a surface tension of $100 k_B T/\mu\text{m}^2$. Inset: DIC micrograph of a colloidal membrane edge-on. Scale bar $2 \mu\text{m}$. (c) Sketch of lipid bilayer and colloidal membrane which on a coarse grain level are similar and obey the Helfrich equation.

compared to the case without depletant. Barry and Dogic extended this phase diagram to higher dextran concentrations ($M_w = 500\,000 \text{ g/mol}$) [128] and showed that, starting from an isotropic rods suspension at $c_v = 1$ to 10 mg/mL , it is possible to assemble a new phase: 2D colloidal membranes composed of a one-rod length thick mono-layer of aligned rods. The membrane diameter is not controlled and varies from a few microns to hundreds of microns, Fig. 4.4. On a coarse grain level the self-assembled fluid-like and equilibrium monolayers have the same symmetry as lipid bilayers and one can develop many analogies. First, like lipid bilayers, the instantaneous and average projected colloidal membrane area A are proportional, $\langle A - \langle A \rangle \rangle^2 = k_B T \langle A \rangle / \chi$ where the compressibility is $\chi \sim 4500 k_B T/\mu\text{m}^2$ [128, 129, 130, 131, 132]. For comparison, the compressibility of lipid membrane is 2 to 3 orders of magnitude higher $\sim 10^7 k_B T/\mu\text{m}^2$ [133]. Second, the colloidal membranes viewed in edge-on configurations, exhibit thermal undulations. The Fourier analysis of these fluctuations can be model using the elastic free energy written down by Helfrich, originally developed for lipid bilayers [134]. Finally, the stability of colloidal membranes is similarly related to the way lipid bilayers interact [135, 136, 137]. Indeed, From $Dext = 45$ to 53 mg/mL , colloidal membrane remain isolated from each other: as two membranes approach each other in suspension, protrusion fluctuations lead to an effective repulsive interaction and promote the stability of isolated membranes. At higher dextran concentrations, the depletion interaction becomes sufficiently large to overcome this effective repulsion and colloidal membranes stack on top of each other [128] and eventually crystallize [138, 139].

However, from a microscopic perspective the forces driving the assembly of colloidal membranes and lipid bilayers are very distinct. Colloidal membranes are assembled from micron length hydrophilic rod-like molecules, whereas lipid bilayers are assembled from nanometer amphiphilic lipids. This leads to orders of magnitude difference in their compressibility, lateral bending modulus or lateral tension. Nonetheless, being a robust assemblages stable over a wide range of parameters [140], colloidal membranes represent a unique opportunity to investigate membrane biophysics from an entirely new perspective on a length scale where it is possible to visualize and follow under a microscope the constituent building blocks, the membrane dynamics or reconfigurable processes.

We first discuss the edge properties of colloidal membranes which are described at a macroscopic level by the interfacial tension γ [141]. For 2D colloidal membranes, γ is 1D and is the equivalent of surface tension for 3D objects like emulsion for instance. This a thermodynamic quantity that results from the greater affinity of the colloidal membrane particles to each other than to the particle isolated in the solvent. The net effect is an inward force at the membrane circumference that causes the edge to behave elastically. The control of interfacial tension is manifold. It justifies that colloidal membranes adopt a circular shape. Its control, in analogy with micro-emulsion, could lead to fine tune the size of colloidal membranes.

The edge structure of achiral colloidal membrane is determined using three complementary imaging techniques, namely two-dimensional (2D) and three-dimensional (3D) polarization microscopy and electron microscopy [47]. 2D-LC-PolScope [142] of a membrane lying normal to the z -axis of the microscope produces images in which the intensity of a pixel represents the local retardance and indicates the local tilt of the rods with respect to the z -axis. Rods in the bulk of a membrane are aligned along the z -axis, and it follows that 2D

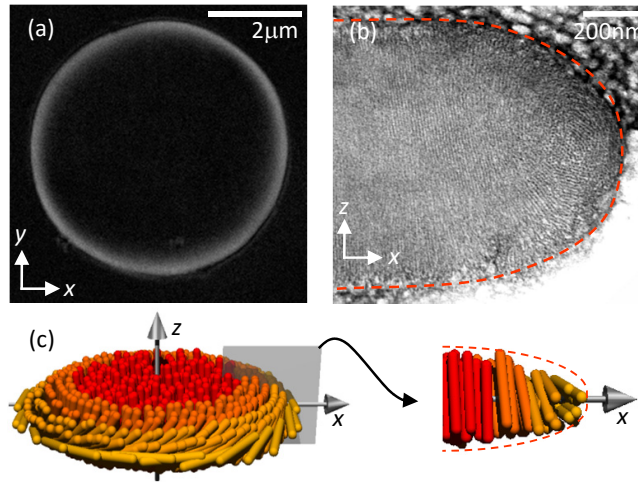


Figure 4.5: Structure of a colloidal membrane, $T = 22^\circ\text{C}$, $Dext = 45 \text{ mg/mL}$ [47]. (a) 2D LC-PolScope retardance map of a colloidal membrane. The bright band associated with the edges indicates local rod tilting. (b) Electron micrograph cross section of a membrane directly visualizing the tilt of the rods and the curved edge profile. (c) Sketch of a colloidal membrane indicating that its edge adopts a curved profile, forcing rods to locally twist.

LC-PolScope images appear black in that region. By contrast, the bright, birefringent ring along the membrane's periphery reveals local tilting of the rods at the edge. The 3D reconstruction of the membrane structure using electron tomography [143, 144], shows that the virus tilt by 90° , from being normal to the membrane surface in the bulk to tangential to the edge along the membrane periphery. This behavior is corroborated by 3D LC-PolScope [145]. This twist goes with a hemi-toroidal curved edge. The twisted edge makes the membrane a chiral object. For achiral virus dispersions, the spontaneous twist at the edges is equally likely to be clockwise or anticlockwise [47]. For chiral virus suspensions, the edge adopts the chirality of the virus. By comparison with an untilted edge, a curved edge structure lowers the area of the rod-polymer interface, thus reducing interfacial tension, at the cost of increasing the elastic energy due to a twist distortion. Saying that we already see the potential of the virus chirality to affect the edge energy.

4.2 Colloidal membranes and chirality

4.2.1 Tuning the edge chirality

A classical way to measure the interfacial tension consist in analyzing the membrane's edge thermal fluctuations in the Fourier space [148, 149, 150]. A typical fluctuation spectrum for an achiral edge is shown in Fig. 4.6. In the thermodynamic limit which corresponds to small wave vectors, q , the mean square Fourier amplitudes of the edge fluctuations, $\langle a_q^2 \rangle$, is q -independent, and yields the effective line tension, $\langle a_q^2 \rangle = k_B T / \gamma$ [148]. In the large- q limit, fluctuations scale as $1/q^2$ and yield the bending rigidity of the interface, κ . In the range of temperatures and dextran concentrations explored, for fd-wt colloidal membranes, $\kappa \sim 100 k_B T \cdot \mu\text{m}$ while γ varies from ~ 100 to $800 k_B T / \mu\text{m}$

Next we evidence the role of chirality on γ . Using mixture of dextran and fd-wt viruses the self-assembly of colloidal membranes is driven by entropy alone and therefore athermal as apposed to the chiral interaction which depends solely on temperature. We thus have a unique system where it is possible to decorelate the effect of attraction (dextran concentration) from chirality (temperature): $\gamma(Dext, T) = \gamma_{bare}(Dext) - \gamma_{chiral}(T)$, where γ_{bare} is the line tension of a membrane edge composed of achiral rods and γ_{chiral} is the chiral contribution to the line tension [47]. In Fig. 4.6, we observe that the effect of chirality drastically modify the fluctuation spectrum of the edge of a colloidal membrane, $\langle a_q^2 \rangle$ as expected from the edge structure. First, $\langle a_q^2 \rangle$ is shifted upward at low q which indicate that the line tension decreases with chirality as hypothesize. This is further demonstrated using dextran series which show that γ decreases with the same slope as temperature decreases confirming that the two contributions to γ are uncorrelated. Second, a peak appears at intermediate q . This peak is attributed to out of plane fluctuations. Indeed the effect of chirality at the edge of colloidal membranes is twofold. 2-D layered geometry cannot support twist and chirality is consequently expelled to the edges in a manner analogous to the expulsion of a magnetic field from superconductors [151, 152]. Moreover, to palliate the 2D frustration [153, 152, 154], chirality forces the edge fluctuations to escape in the z -direction [155] which vouch for the existence of a positive Gaussian curvature, $\bar{k} \sim 150 k_B T$ [146].

4.2.2 Twisted ribbons

The chiral control of line tension raise the possibility that at sufficiently low temperatures the chiral contribution to interfacial energy could dominate the bare line tension, lowering the energetic cost of creating edges and

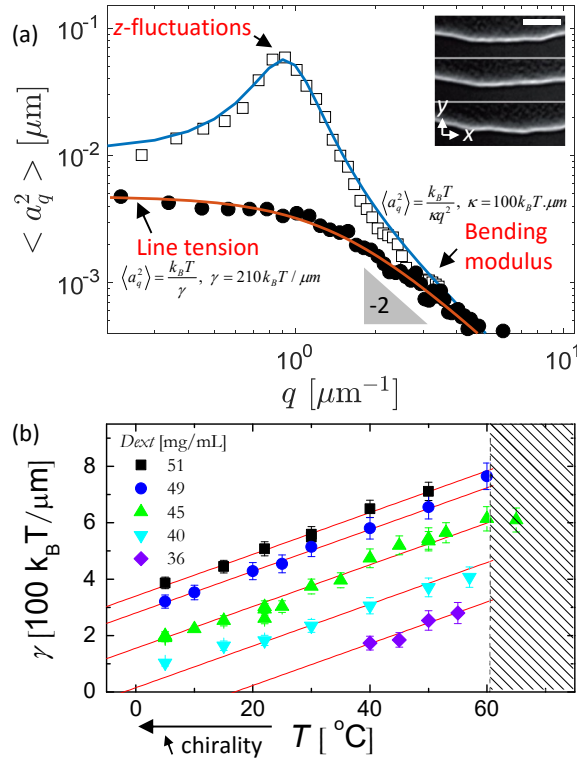


Figure 4.6: Chiral control of interfacial tension of colloidal membranes composed of fd-wt [47, 146, 147]. (a) Fluctuation spectrum of the membrane edge $\langle a_q^2 \rangle$ at $T = 20^\circ\text{C}$ (square) and 50°C (circle) for $Dext = 36$ mg/mL. For small wave number q , $\langle a_q^2 \rangle$ is independent of q and inversely proportional to the effective line tension γ . For large q , $\langle a_q^2 \rangle$ are independent of $Dext$ and T and scale as $1/q^2$. For very chiral samples a peak is observed at intermediate q which is attributed to Gaussian curvature which enable out of plane fluctuations. Red lines are fits using equation (3). Inset: DIC images, taken 1s apart, illustrating the fluctuations of the membrane's edge. Scale bar, $5\mu\text{m}$. (b) Line tension as a function of temperature for different dextran concentrations. In the achiral limit at 60°C , $\gamma_{chiral} = 0$ and $\gamma_{bare} = \gamma$. Increasing the Dextran concentration increases γ_{bare} . Decreasing the temperature reduces γ because γ_{chiral} decreases. The red lines of fixed slope are guides to the eyes illustrating the universal scaling of γ with chirality.

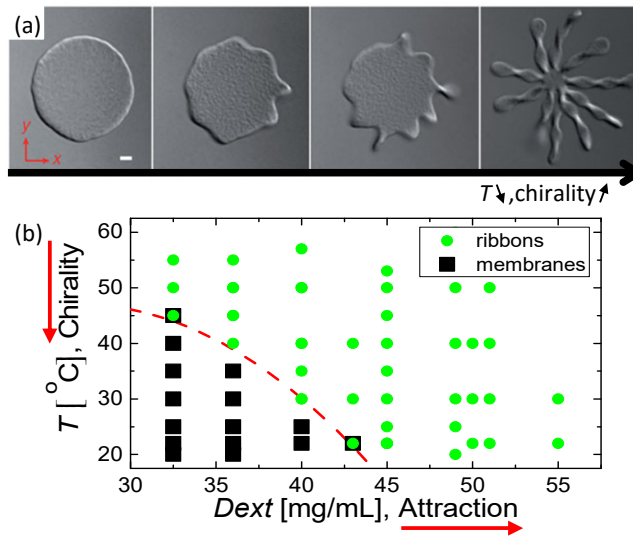


Figure 4.7: Reconfigurable self-assembly through chiral control of interfacial tension – colloidal membrane to twisted ribbons transition, [47]. (a) DIC micrographes of a temperature quench which show the transition of the 2D membrane into twisted ribbons. Scale bar, $2\mu\text{m}$. (b) The stability diagram indicates regions of phase space where twisted ribbons and membranes are observed as a function of T and $Dext$. The dash boundary is a guide to the eye. circle: membranes and squares ribbons.

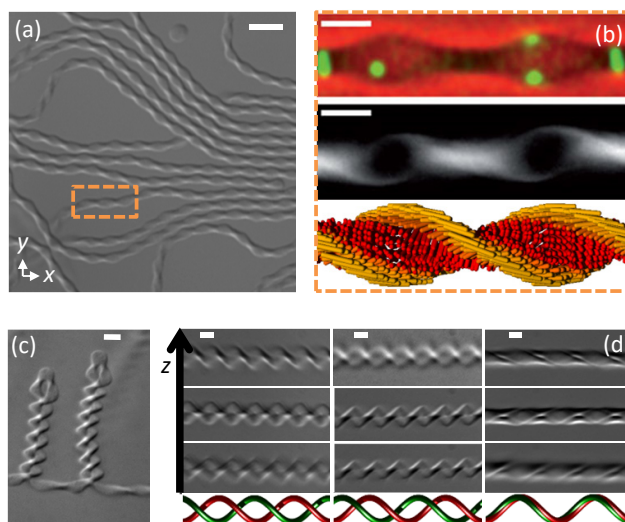


Figure 4.8: fd-wt twisted ribbons, $T = 22^{\circ}\text{C}$, $Dext = 36 \text{ mg/mL}$. [47]. (a) DIC micrograph of twisted ribbons Scale bar $5 \mu\text{m}$. (b) From top to bottom. An overlaid phase contrast (red) and fluorescence (green) image of a stable ribbon containing a low volume fraction of fluorescently labeled rods. LC-PolScope image indicating rod tilting that penetrates from the edge of the ribbon towards its center. Schematic structure of twisted ribbons as deduced from optical microscopy. (c) Doubly twisted ribbons consist of two twisted ribbons wrapped around each other. (d) z -stack DIC micrographs of doubly twisted ribbons with three different conformation. The red and green sinusoids follow the outer edges of each of the two ribbons comprising the double twisted ribbon, respectively and illustrate the phase shift between the two twisted ribbons can vary from being out of phase to being in phase. Scale bar $2 \mu\text{m}$.

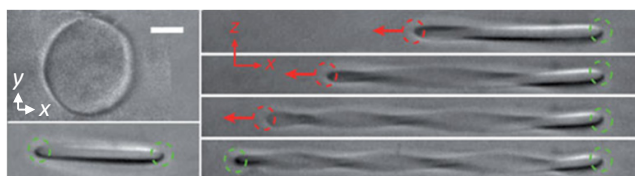


Figure 4.9: fd-wt colloidal membrane manipulation with optical tweezers, $T = 22^{\circ}\text{C}$, $Dext = 45 \text{ mg/mL}$ [47]. A colloidal membrane is trapped with a dual-beam optical trap and stretched, inducing the transition to a twisted ribbon. Red circles indicate moving traps and green circles indicate fixed traps. Scale bar, $2 \mu\text{m}$.

leading to their spontaneous formation. It is thus expected that chirality has a role similar to that of amphiphilic surfactants in oil–water mixtures. Such surfactants lower surface tension and lead to the stabilization of microemulsions. Fig. 4.7 shows that this is not the case. With decreasing temperature, the membrane edge eventually becomes unstable, resulting in a remarkable polymorphic transition. Twisted ribbons grow along the entire periphery of the disk from the out of plane fluctuations of the membrane edge, generating a starfish-shaped membrane. This polymorphic transition is reversible and twisted ribbons form equilibrium structures at high chirality and low dextran concentrations. Twisted ribbons are a beautiful example of hierarchical assembly, Fig. 4.8. It consists in a twisted monolayer of aligned rods which form a helicoidal structure perpendicular to the rod twist. As observed by Efrati and Irvine, such object is simultaneously right and left handed [156]. The rod twist at the edge is left handed while on larger length scales the helicoidal structure of the ribbon is right handed. As such it differs from other twisted ribbons observed in the literature [157, 158, 159, 160, 161, 162]. The twisted ribbons can be seen on a coarse grain level as polymers with a persistence length of the order of the pitch of the helicoidal structure and may form a zoology of structures ranging from branched polymer, to loop polymer or entangled phone cord like structures reminiscent of DNA double helix [47]. Twisted ribbons stability with respect to colloidal membranes is attributed to a structure where all rods twist to form an edge object with low line tension. Given the 3D structure of the ribbons, Gaussian curvature may also be an important parameter that justifies the twisted ribbon stability [146].

It is possible to use laser tweezers to manipulate the self-assembled structures. For instance in Fig. 4.9, the two opposite sides of a colloidal membrane are trapped with a dual-beam optical trap. The viruses align with the electric field of the laser and the membrane turns sideways. Using a static trap and an extensional displacement with the other optical trap, the membrane is stretched, causing the transition to a twisted ribbon. This mechanically induced disk-to-ribbon transition is reversible; on removal of the optical trap, the highly elastic ribbon relaxes back into its original shape. This experiment paved the way to study mechanical properties of self-assembled objects [163].

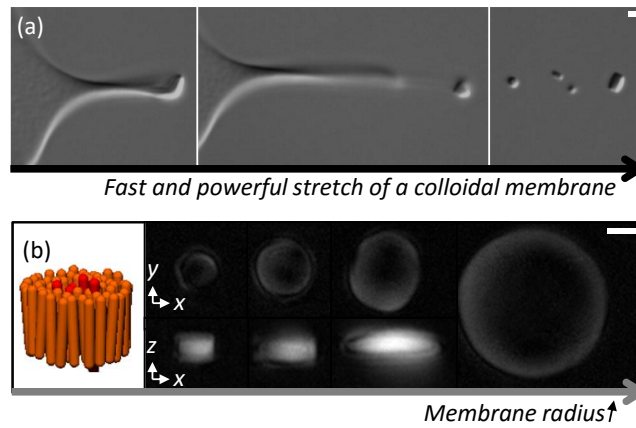


Figure 4.10: fd-wt membrane seeds, $T = 22^\circ\text{C}$, $D_{\text{ext}} = 45 \text{ mg/mL}$ [147]. (a) DIC micrographs time sequence: using 2 Watt optical tweezers, it is possible to grab a colloidal membrane and detach membrane seeds. (b) Schematic of a membrane seed. 2D-LC-Polscope of membrane seed observed from the top and sideways. Scale bars $1 \mu\text{m}$.

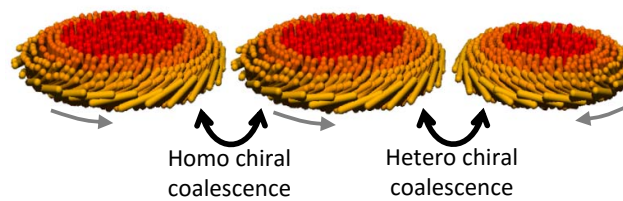


Figure 4.11: Chiral coalescence of colloidal membranes.

4.3 Colloidal membranes and chiral coalescence

Driven by the balance between interfacial tension and bulk energy, a pair of liquid droplets, when sufficiently close to one another, may coalesce to form a single daughter droplet. The coalescence process is complex and involve the rupture and the fusion of the droplets surfaces associated with energy barrier and local rearrangements [164, 165, 166, 167, 168, 169, 170, 171, 172]. In most cases, it is an ‘all-or-none’ process; once initiated, the reaction proceeds to completion. However, there is also the possibility of incomplete coalescence. For example, vesicles coalesce into hemi-fused state [173] and nanotubes into a defect-ridden structure [174]. Taking advantage of the chiral edge, colloidal membranes coalescence enlighten the role of geometrical frustrations [175] in the self-assembly of new structures [176, 177].

The edge chirality of colloidal membranes can be controlled in various ways. First, if the colloidal membrane is small enough, a diameter smaller than the virus length, the viruses stand straight at the edge and those membrane seeds are achiral, Fig. 4.10. Second, for larger membranes the edge adopt the chirality of the virus. Third, it is possible to compose achiral virus suspensions, for instance using fd-wt at $T = 60^\circ\text{C}$ or mixtures of fd-wt and fd-y21m at $x_{fd} = 0.26$, Fig. 3.5 and in this case, the symmetry being broken, colloidal membranes self assemble either with left- or right-handed edge. For chiral membranes, we can divide the coalescence in two families: homo and hetero chiral coalescence, Fig. 4.11. In homo chiral coalescence two coplanar membranes have the same chirality. The rods at the coalescence point are tilted in opposite directions, trapping 180° of twist between the two membrane. In hetero chiral coalescence both coplanar membranes have the opposite chirality and viruses at the edge need only to straiten in the z -direction at the coalescence point.

4.3.1 Homo chiral coalescence – π -walls, pores, Möbius anchors and colloidal skyrmions

Homo chiral coalescence [163] is at the center of chiral topological frustration. In Fig. 4.12, the coalescence between two homo chiral membrane may result in a defect-free daughter membrane. Similar to liquid droplets, the thermal fluctuations are sufficient to form a bridge between the two membranes. In this one rod-length-wide bridge, the rods twist by 180° to match the orientations of the joining edges. The twisted bridge induces a torque which enable the two membranes to rotate along the axis formed by the bridge and expel the trapped twist. As the membranes twist around each other, the connecting bridge expands in width, eventually leading to a circularly shaped defect-free daughter membrane. In an other pathway, coalescence is initiated by the formation of two twisted anchors, which bind the membranes together and initiate the nucleation of a continuous 1D line defect. This line defect, named a π -wall, quickly grows to its equilibrium size, pushing the two anchor apart. Once the π -wall is fully formed, it remains indefinitely. π -walls are stable with respect to two free membrane edges: the measurements of π -wall interfacial tension γ_π and the membrane edge interfacial tension γ shows that $\gamma < \gamma_\pi < 2\gamma$.

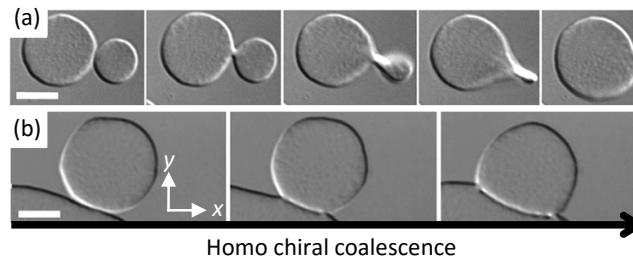


Figure 4.12: Homo chiral coalescence of fd-wt colloidal membranes, $D_{ext} = 45 \text{ mg/mL}$, $T = 22^\circ\text{C}$ [177]. (a) DIC micrographs time sequence showing a coalescence pathway resulting in a defect-free daughter membrane. The coalescing membranes initially form a twisted bridge that induces a torque and a rotation by 180° that expel the twist between the two membranes. (b) DIC micrographs time sequence showing another coalescence pathway resulting in the formation of a π -wall. Because the membranes lie on the bottom surface, the rotation required for defect-free coalescence is suppressed. Scale bars, $10 \mu\text{m}$.

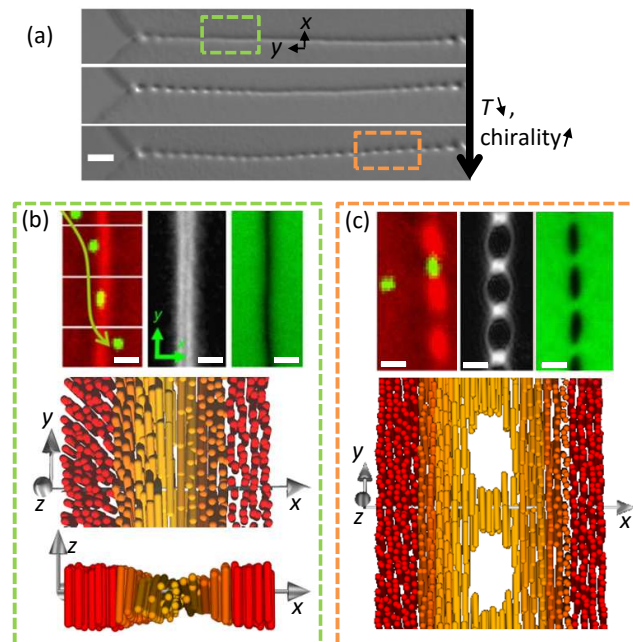


Figure 4.13: Reconfigurable self-assembly and chirality – π -wall to alternating bridge-pore arrays (ABPA) transition in fd-wt colloidal membranes [177]. (a) A temperature quench induces a transition from a π -wall to an ABPA. The colloidal membrane assembled at $D_{ext} = 45 \text{ mg/mL}$ is quenched from $T = 55$ to 22°C . During the quench, the π -wall morph into alternating bridge-pore arrays. Similarly to the membrane/twisted ribbon transition, this transition is reversible. Scale bar, $5 \mu\text{m}$. (b) π -wall structure. From left to right - A time sequence illustrates rotation of a fluorescently labeled virus (green) by 180° as it diffuses through a π -wall. Fluorescence images are superposed with simultaneously acquired phase-contrast images (red). The 2D-LC-PolScope image of a π -wall is compatible with the 180° twist of the viruses. A fluorescence image of a π -wall where all the rods are fluorescently labeled. The defect appears darker in its center which correspond to a decrease of the defect thickness. Bottom: sketch of π -wall. (c) ABPA structure. From left to right - The simultaneous fluorescence (green) and phase-contrast (red) imaging reveals that the rod twist by 180° within a bridge. A 2D-LC-PolScope confirms this twist. An ABPA image where all the rods are fluorescently labeled shows that the pores are empty of viruses. Bottom: sketch of ABPA. Scale bars, $2 \mu\text{m}$.

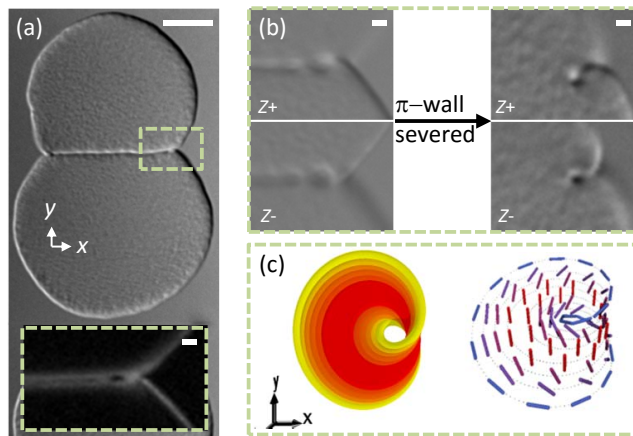


Figure 4.14: Möbius anchors in fd-wt colloidal membranes, $D_{ext} = 45$ mg/mL, $T = 22^\circ\text{C}$ [163]. (a) DIC micrograph of a π -wall, scale bar $5\mu\text{m}$. Inset: 2D-LC-PolScope anchor point of the π -wall at the edge of a colloidal membrane. We guess that this anchoring point forms a Möbius loop which prevents the π -wall to vanish. (b) DIC image of the Möbius anchors before and after the π -wall is severed with optical tweezers. $z+$ and $z-$ correspond to images focused slightly above and below the membrane plane. (c) Sketch of the Möbius anchor. Scale bars $2\mu\text{m}$.

However, in fd-wt systems where chirality can be controlled with temperature, π -wall can be continuously brought to regimes with high chiral interactions at low temperatures. In this case, $\gamma_\pi > 2\gamma$ and π -walls become metastable with respect to isolated membranes. In high chiral regimes, we do not observe the spontaneous dissociation of a π -wall into two defect-free membranes. We instead observe the opening of pores in the π -walls, Fig. 4.13. Those pores may form an alternating bridge-pore arrays (ABPA) structure which can be closed back into a π -wall by increasing the temperature. This behavior remains to be understood but seems reasonable, as pores create a large amount of edge interfaces which are favored at high chirality. More importantly, it empirically proves that with the right ingredient it possible to actuate pore upon external signaling in self-assembled membranes. Pore actuation is of primal importance through out the cell life cycle [178, 179].

Finally we discuss two structures related to π -walls: Möbius anchors and colloidal skyrmions. Both those structures rely on a robust on-demand method for imprinting defects into colloidal membranes with arbitrary spatial precision. Taking inspiration from recent work with thermotropic liquid crystals [180, 181, 182], we also use an optical trap.

A simple Möbius strip is a one-sided continuous surface, formed by twisting a long narrow rectangular strip of material through 180° and joining its ends. Such a structure can be made in liquid-crystal by knotting of microscopic topological defect lines with optical tweezers about colloids [183]. The Möbius strip we observe in colloidal membrane are Möbius anchors [176]. The Möbius anchor is associated with the way π -walls are anchored to the membrane edge, Fig. 4.14 and is mandatory for the π -wall to remain stable. For instance, it is possible with optical tweezers to imprint π -wall on a colloidal membrane. However, if the optical trap is released before the π -wall is anchored, the defect retracts. Based on 2D-LC-PolScope micrographs, it seems that the viruses follow a simple Möbius strip which tight the π -wall to both edges of the daughter membranes, Fig. 4.14. At this point this anchoring structure is only a guess. This hypothesis is however supported by the fact that it is necessary to produce a the back and forth motion with the optical trap to create the anchor which is reminiscent of the pathway depicted in soap film to create Möbius loop [184].

Colloidal skyrmions [176] are obtained using optical tweezers to cleave a π -wall in two places, and then quickly joining the two ends to form a closed ring embedded within the membrane, Fig. 4.15. The colloidal skyrmion shrink to an equilibrium diameter of about $\sim 1\mu\text{m}$. Note that for a similar size, an isolated colloidal membrane display an untwist edge. The colloidal skyrmion share properties with skyrmion excitations encountered in hard condensed matter physics [185, 186, 187, 188, 189]. It is topologically protected [190, 191]: it has a positive energy compared with the background field but the π -wall forming the skyrmion cannot be untrapped unless the π -wall is severed. Moreover, it is a 2D structure characterized by a vorticity $m = 1$ and a phase helicity $\varphi = \pm\pi/2$ which sign depends on the chirality of the π -wall. As such, it is very similar to singled out skyrmion from the hexagonal SkX state unveil by to neutron scattering experiments on MnSi [186] and $\text{Fe}_{1-x}\text{Co}_x\text{Si}$ [192, 193, 194] and seems to be the closest realization of a theoretical nematic skyrmions restricted to straight infinite lines in unbounded ideal materials [195]. It however differs from other liquid crystal skyrmion such as double twist cylinders “baby-skyrmions” [196, 197], skyrmion in cholesteric blue phases subjected to strong external fields [198, 199].

Understanding the principles that support or prevent membrane coarsening and defects formation such as π -wall is essential to grow large defect free membranes and consider applications. As chirality is at the center of π -walls, it suggests that producing achiral colloidal membranes would lead to defect-free coalescence and uniform monolayers.

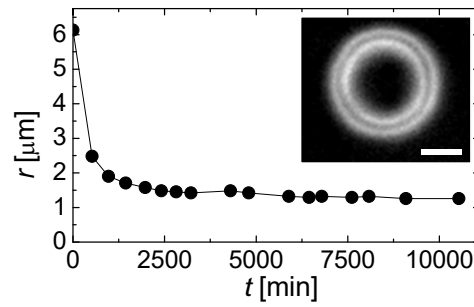


Figure 4.15: Colloidal skyrmion in fd-wt colloidal membranes, $D_{ext} = 45 \text{ mg/mL}$, $T = 22^\circ\text{C}$ [163]. Evolution of the radius of the colloidal skyrmion over time. $t = 0$ correspond to the time the colloidal skyrmion is imprinted with optical tweezers. Inset: 2D-LC-PolScope image of a colloidal Skyrmion using laser tweezers to close a π -wall on itself. Scale bar $1 \mu\text{m}$.

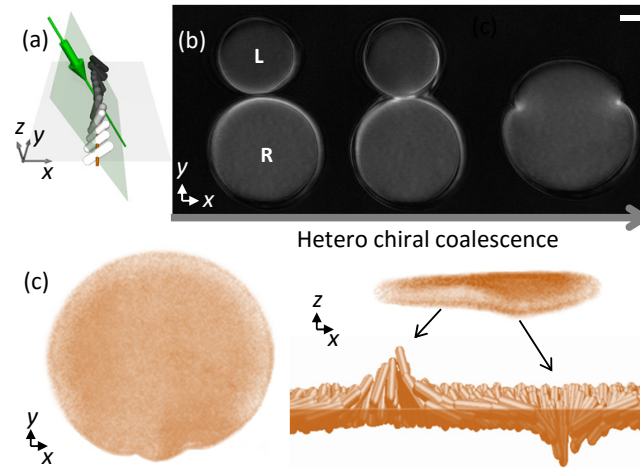


Figure 4.16: Hetero chiral coalescence leads to scalloped membranes [177], in mixtures of fd-wt and fd-y21m, $x_{fd} = 0.26$, $D_{ext} = 45\text{mg/mL}$, $T = 22^\circ\text{C}$. (a) Sketch of 2D-LC-PolScope Angled light illuminating a 1D cross-section of twisted rods. Because the direction of the incident light is tilted towards the x axis, rods twisting counter-clockwise along the light source are not birefringent and appear dark. In contrast, rods twisting clockwise, away from the incoming light, have higher optical anisotropy and thus appear bright. Tilting the light source breaks the symmetry of the 2D-LC-PolScope setup and allows us to distinguish between left-handed (L) and right-handed (R) membranes. The gray scale changes from dark to light with increasing retardance, where the rods aligned with the direction of incident light have zero retardance. (b) 2D-LC-PolScope Angled light micrographs time sequence showing the coalescence of a left-handed membrane with a right-handed membrane. The daughter membrane displays two cusps that separate the left-handed edge section from the right-handed one. Scale bars, $4 \mu\text{m}$. (c) Reconstruction of the membrane based on the confocal images and sketch of the point defects. Two adjacent point defect escape in the third dimension z with opposite direction.

4.3.2 Hetero chiral coalescence – scalloped membranes and gaussian curvature

To study hetero chiral coalescence [177], colloidal membranes composed of homogeneous mixtures of fd-wt and fd-y21m are used. For $0.04 < x_{fd} < 0.45$, in the early stages of the sample maturation, we observe colloidal membranes of either edge handedness, indicating spontaneously broken achiral symmetry. Over time, the intermediate-sized membranes with mixed edge twist continue to coalesce. Both homo and hetero chiral coalescence is observed. In both cases coalesced membrane display an homogeneous mixing of fd-wt and fd-y21m. In hetero chiral coalescence, as the two proximal edges of a pair of coplanar membranes merge, the twist of the edge-bound rods is expelled by aligning the constituent rods with the membrane normal. Hetero chiral coalescence leads to scalloped membranes. As compared to homo chiral coalescence, scalloped membrane form easily. Moreover, they are defect free in their bulk and may reach millimeter diameter. The hallmark of scalloped membrane is located on its edge. It displays two outward protrusions which separate a left from a right handed edge, Fig. 4.16. Using confocal microscopy, it is observed that the two protrusions escape in the z -direction in opposite directions. This 3D point-like singularity on the vertical axis vouch for the presence of Gaussian curvature κ_G associated with its Gaussian elastic modulus \bar{k} .

The distance δs between two adjacent edge protrusion greatly depends on x_{fd} , Fig. 4.17. Close to the achiral limit, at $x_{fd} = 0.26$, adjacent protrusions freely move along the edge and the variation of δs is diffusive. On the contrary, close to the boundary of stability of scalloped membranes at $x_{fd} = 0.04$ or 0.45 , adjacent protrusions pair and remains bound to each other at a well-defined distance δs_0 . To measure the entire binding potential, we performed active experiments where we moved one defect by δs using an optical trap, while

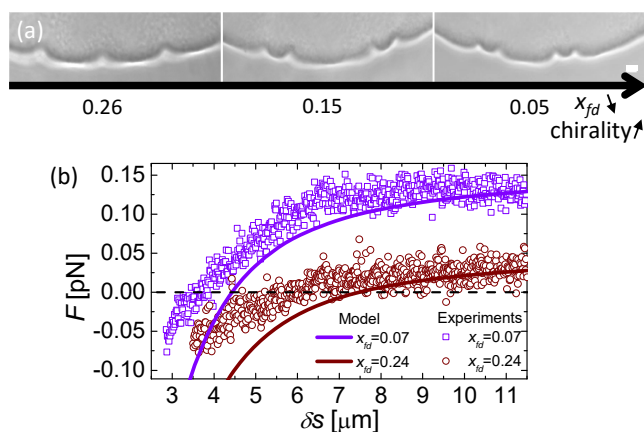


Figure 4.17: Measurement of the protrusion interactions in fd-wt/fd-y21m scalloped membranes, $T = 22^\circ\text{C}$, $D_{\text{ext}} = 45$ mg/mL [177]. (a) Phase contrast image of scalloped membranes at $D_{\text{ext}} = 40$ mg/mL. Decreasing ratio of x_{fd} (increasing the chirality) leads to a tighter coupling between two adjacent protrusion which then pair. Scale bars, $2 \mu\text{m}$. (b) Force measurements F (dots), obtained with laser tweezers, and fitted with a theoretical model (full curves) as a function of δs , the distance between two adjacent protrusions.

simultaneously measuring the force F exerted on the other defect. For this purpose, we embedded $1.5 \mu\text{m}$ diameter colloidal beads into two adjoining cusp defects. The force is negative below δs_0 , and positive above δs_0 . δs_0 is the stable equilibrium position. The force steeply increases for small separations and saturates at large separations, indicating that a defect pair is permanently bound, Fig. 4.17.

These observations can be mainly explained by the chirality of the edges. For instance, at $x_{fd} = 0.07$ the system is mostly composed of fd-y21m and right handed chirality is favored. Therefore right-handed edge have a lower energy than left handed edges. This leads, in scalloped membranes, to a finite difference in line tension $\Delta\gamma$ between the left-handed and right-handed outward protrusions. The edge free energy is minimized by reducing the length of the outward protrusions with the unfavored twist and the amplitude of $\Delta\gamma$ accounts for the strength of the long range attraction between two adjacent protrusion. Approaching the two protrusion close together has two consequences. It tends to over bend the edge separating the two adjacent protrusion and to flatten the protrusion in the z -direction. This works again the bending rigidity of the edge κ and against a negative Gaussian curvature κ_G , which lowers the free energy of elastic deformations if the Gaussian modulus is positive and sufficiently large, $\bar{k} = 200 k_B T$ [200, 201, 177].

This results display a striking difference with conventional bilayers which have a negative Gaussian modulus: saddle-shaped deformations increase the membrane energy [202, 203, 204, 205]. Moreover, scalloped membranes and the transition from membrane to twisted ribbons demonstrates that simple uniform elastic sheets lacking in-plane rigidity can spontaneously assume complex 3D folding patterns as opposed to thin elastic sheets with in-plane elasticity [206, 207, 208, 209] which require in-plane heterogeneities or imposing an external force to be fold or wrinkled. Finally achiral symmetry breaking has been observed in diverse soft systems with orientational order, ranging from lipid monolayers and nematic tactoids to confined chromonic liquid crystals (38-44). In particular the measured structure and interactions of the cusp-like defects in colloidal membranes resemble studies of point defects moving along a liquid crystalline dislocation line in the presence of chiral additives (45). the main difference is that in the colloidal membranes the achiral symmetry breaking leads to out-of-plane 3D membrane distortions that couples liquid crystal physics to membrane deformations. This is not possible for inherently confined liquid crystalline films.

4.4 Asymmetric mixtures of colloidal rods

4.4.1 Phase separation in colloidal membranes

Phase separation can be triggered by asymmetric force between the colloids. This force configuration can be achieved by mixing depletant with viruses of different lengths: fd-y21m virus (880 nm long) and M13KO7 virus (1200 nm long) [19]. The strength of the depletion force is proportional to the overlap of the excluded volume. In Fig. 4.18, two short rods and a short rod and long rod share the identical overlap of the excluded volume while two long rods have a large overlap of the excluded volume and therefore display greater attraction.

Colloidal membranes containing both fd-y21m (right handed) and M13KO7 (left handed) are assembled by adding a depletant to a dilute isotropic mixture of fd-y21m and M13KO7, [78]. After reaching a large enough size, membranes sediment to the bottom of the sample chambers; the constituent rods pointed in the z direction, Fig. 4.18. At low depletant concentrations, thermal energy is sufficient to overcome the attraction between the rods and the rods remain homogeneously mixed in the membrane. At high depletant concentrations the rods within the membrane separate into two phases: an enriched M13KO7 phase surround an enriched

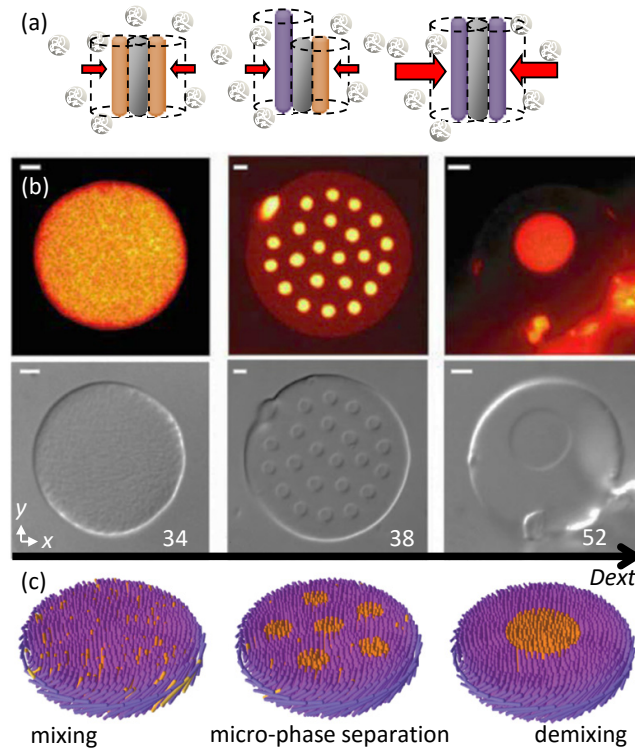


Figure 4.18: Phase separation and membrane rafts in mixture of viruses fd-y21m and MK13KO7 [78, 210]. (a) Sketch of the depletion interaction in mixture of long and short rods. (b) Dual view Fluorescence images of a fd-y21m (yellow)–MK13KO7 (red) and DIC micrograph of colloidal membrane as a function of dextran concentration. At $Dext = 34\text{mg/mL}$ the membrane is homogeneously mixed. At $Dext = 38\text{mg/mL}$, we observe the formation of finite-sized clusters enriched in fd-y21m embedded in a background enriched in MK13KO7. At $Dext = 52\text{mg/mL}$, complete separation of the bulk phase is observed. Scale bar, $5\mu\text{m}$. (c) Sketch of the colloidal membrane in (b).

fd-y21m phase. Both phase conserve the symmetry of the colloidal membrane. At intermediate concentrations, micro-phase separation is observed: colloidal rafts, highly monodisperse micrometre-sized 2D droplets enriched in fd-y21m, float in the background of M13KO7.

4.4.2 Membrane rafts

Colloidal rafts [78] do not coarsen with time, suggesting that they are equilibrium structures, Fig. 4.19. Particle tracking experiments show that the rods diffuse in and out of these rafts, allowing for equilibration to a preferred size. Using optical tweezers to create a raft population with heterogeneous radii, the raft growth rate is measured. Below a critical radius the raft the raft melt and above the raft converge toward an equilibrium radius of $\sim 1\mu\text{m}$.

Colloidal rafts seem similar to equilibrium clusters found in protein and colloidal dispersions [211, 212, 213]. The stability of equilibrium clusters is attributed to the mixed potential of the particles forming the cluster. This mixed potential is composed of a short range attraction and a long range repulsion. For the colloidal rods, the attraction is due to the depletion interaction. Contrary to equilibrium cluster particles, the electrostatic interactions of the colloidal rods are fully screened and the long range repulsion is attributed to virus chirality. Two raft are indeed in a homo chiral coalescence configuration which is not propitious for merging in 2D. The raft edge twist is further transmitted by the twisted structure of the background membrane which mediates a long range elastic repulsion between rafts. This interaction is measured quantitatively by bringing two rafts close together with optical traps and tracking their trajectories upon release of the traps [78]. This chiral repulsion stabilizes small rafts against an interfacial line tension that would otherwise promote coarsening to a single raft domain and establishes a preferred depletant-concentration-dependent raft size [210].

Those results fuel the ongoing discussion on the lipid raft which structure, properties and function constitute ongoing research [214, 215, 216, 217]. Lipid rafts have been proposed to be involved in the generation of the lipid gradients in the secretory pathway (Simons and Ikonen, 1997). Lipid raft coalescence can be induced by lipid-protein and protein-protein interactions to form ordered membrane microdomains involved in signal transduction [218], virus assembly [219], and membrane trafficking [220]. These membrane raft structures have evolved from controversial detergent-resistant entities to dynamic, nanometer-sized membrane domains formed by sterols, sphingolipids, saturated glycerophospholipids, and proteins [221, 222, 223, 215, 216]. Provided that the analogy between colloidal raft and lipid raft hold, it seems that short range attraction and chirality are the essential ingredient. A systematic study of the role a chirality in colloidal rafts with respect to the chiral

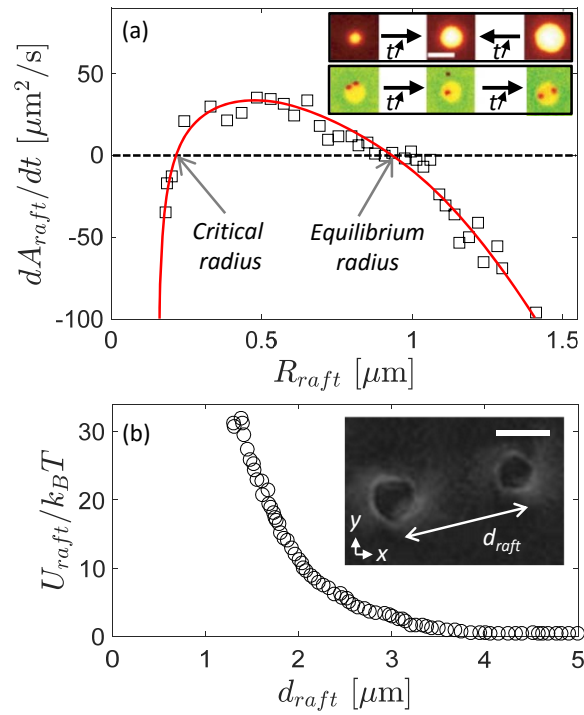


Figure 4.19: Equilibrium raft and their interaction in fd-y21m/M13KO7 colloidal membranes [78]. (a) The dependence of raft expansion rates on raft size directly reveals the critical nucleus size and equilibrium size. Inset top: Expansion of an undersized raft and contraction of an oversized raft. Inset bottom: Fluorescently labeled fd-y21m rods associate and dissociate from a raft, revealing binding kinetics at the single-molecule level. (b) Effective pair interaction potential obtained using the blinking trap technique for clusters with diameters of $1.6 \mu\text{m}$. Inset: 2D-LC-PolScope image of rafts embedded in a colloidal membrane.

molecule present in lipid raft remains to be done for a more refined analogy.

5. Conclusion and perspectives

Filamentous phage such as fd-like viruses are rod-like colloids that have well defined properties such as their diameter, length, rigidity, charge and chirality. Engineering those virus leads to a library of rods with slightly different properties which can be used as building blocks for self assembly, section 3. Their condensation in aqueous solution with additive depletants produces a myriad of structures ranging from isotropic/nematic droplets [125], colloid membranes [128, 140, 224], achiral membrane seeds [147], twisted ribbons [47], π -wall [163], pores, colloidal skyrmions, Möbius anchors, scallop membranes [177] to membrane rafts [78], section 4. First, those structure reinforce the general notion that through a careful choice of particle shapes, sizes, and concentrations it is possible to “engineer entropy” [4] and build structures of ever-increasing complexity. Second, the entropy driven condensation of millions of rods in finite liquid-like objects leads to dynamic equilibrium and allows the structures to permanently rearrange and test their energy landscape. Therefore, those structures are very sensitive to externally tunable interactions like chirality and attractions which trigger shape shifting transitions. Third, external forces like optical tweezers may be utilize to manipulate those structures and probe their mechanical properties and the transition between multiple metastable polymorphic forms with complex topologies. Fourth, those structures represent a showcase of analogies between objects which belong to different fields of science such as colloidal membranes and lipid bilayers, chiral pore actuation and pores in cells, colloidal rafts and membrane rafts, colloidal skyrmions and solid state skyrmion, the twist penetration length at the edge of colloidal membranes and the penetration depth of the magnetic field in superconductor, or the Möbius anchors and the Möbius strips. Fifth, this experiments work combined with theoretical inputs [210, 147, 146, 163, 201, 225, 226, 177, 227, 228, 200, 229] makes it well establish field in self-assembly. For all those reasons, fd-like phages constitute an attractive model system in soft matter physics, Fig. 5.1.

The subject is clearly open and many questions remain unanswered. 2D colloidal membranes do not form vesicles – would it possible with smaller viruses to reduce the lateral bending rigidity of the membranes and have them form vesicles? We have seen that chirality tends to produce 3D structures with gaussian curvature – is possible to enhance this effect to make 3D leather pouch like membranes? Raft are stabilized due to chirality – what happen to micro phase separation in homo chiral mixtures and in achiral mixtures? This review being only based on three different phages (fd-wt, fd-y21m and M13KO7) which is really far from being representative of phage diversity [230], there are many more structures to be discovered in such systems.

The phenomenology described in this review article should be relevant to diverse colloidal and nanosized rods that interact through excluded volume interactions. Indeed, as demonstrated in section 3, fd-like viruses are an excellent experimental realization of hard rods. The challenges for applications, especially in materials science, are threefold. Firstly, it lies in the development of monodisperse rods with interactions that exclude aggregation and permits equilibrium self assembly. Secondly, it necessitate robust rods that conserve their integrity in harsh conditions. Thirdly, large scale productions is required. Progress in these directions are clearly on their way [231, 232, 233, 234, 235] and material and bio-applications line up [236, 237, 238, 239]: templates for cells growth [240], colourimetric sensors [241], photovoltaic devices [242, 243], batteries [244, 245, 246], etc. . . .

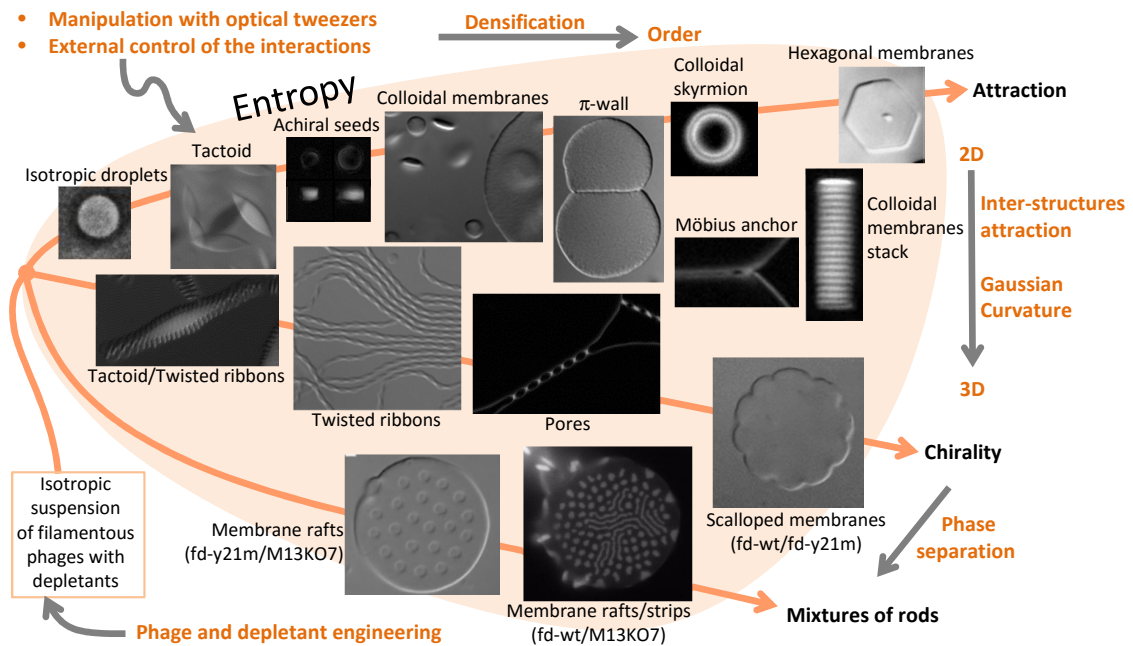


Figure 5.1: Filamentous phages as building block for reconfigurable and hierarchical self-assembly. Starting with isotropic suspensions of filamentous phages and depletion interactions, it is possible to drive the system to self assemble in a myriad of structures. Tuning the depletion interaction leads to condensate the virus with increasing density and order. Using the virus chirality, it is possible to turn 2D structures in 3D structures with Gaussian curvature. By mixing different type of rods the system may phase separate. Optical tweezers and external control over the interactions permits to navigate continuously in this state diagram and trigger shape-shifting structures.

IM Other projects synopses

6	Triggering instabilities in Gels	36
6.1	Introduction	
6.2	Fatigue and yielding in soft gels	
6.3	Predicting rupture in strong gels	
6.4	Wringling gels	
7	Futur projects	43
7.1	(StruBaDy) Structure Bacteria Dynamics	

6. Triggering instabilities in Gels

6.1 Introduction

Gels are composed of small particles at very low volume fractions that form an elastic space spanning three-dimensional network embedded in a solvent. Gel form through the sol-gel transition. Initially A fluid mixture is composed of solute (sol) particles suspended in a solvent. Then, under appropriate conditions, the particle aggregate until a percolating network is formed. The network often displays a large length scale signal associated with the fractal properties of its structure. By weight, gels are mostly fluid, but the network confer mechanical properties to the gel that fall into the category of viscoelastic solids. They display an elastic plateau at rest and flow only when solicited above a certain strain or stress.

The internal network structure result from bonds between the particles. Physical gels or soft gels are gels in which bonds originate from physical interactions of the order of $k_B T$, so that bonds can reversibly break and form many times during the course of an experiment. Physical gels are usually formed by colloidal and soft particles as well as associative polymers, and bonds are induced via depletion interactions, hydrogen bonds and hydrophobic effects to name a few. Chemical gels or strong gels in contrast are gels where the network bonds are irreversible. Chemical gels are usually formed by cross-linked polymers but also physical interactions much larger than $k_B T$ like in gelatin. Physical and chemical gels are out of equilibrium structures and their properties are driven by dynamical arrest during the sol-gel transition. The path employed during the sol-gel transition is therefore crucial and may affect the structure and mechanical properties of the gel.

In the next we discuss mechanical instabilities that are triggered by solicitations Fig. 6.1. Solicitations can be external to the gels and applied using rheometer, optical tweezers or high power ultrasound. Solicitations can also be internal, taking advantage of the built-in sensitivity of our particles to pH or temperature quenches to morph our dispassion's properties. Among the the systems I have studied, I choose to present three instabilities:

- The yielding transition of a soft colloidal gel, i.e. the transition from a solid state to a fluid state due to shear.
- The prediction of the rupture point in strong colloidal gels subject of oscillatory stress.
- The wrinkling pattern in strong colloidal gels triggered by a pH quench.

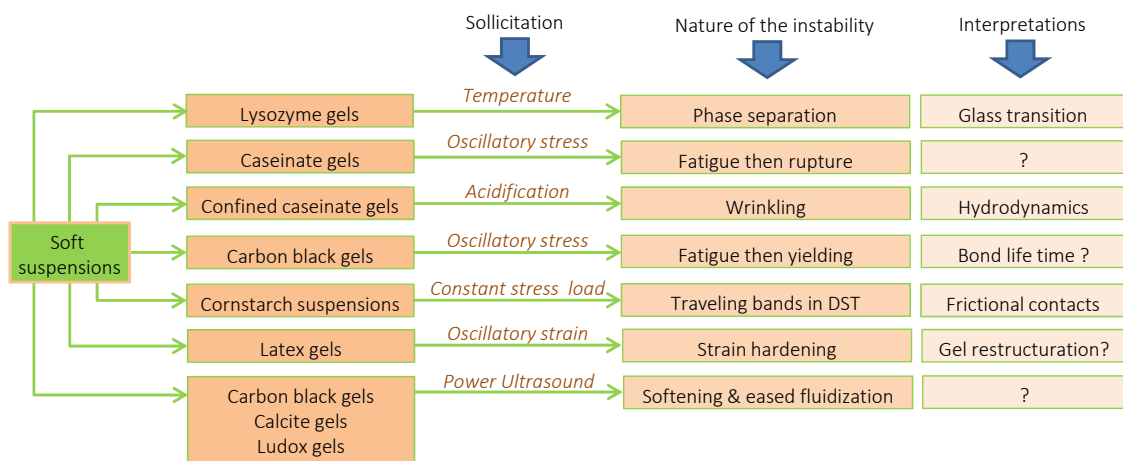


Figure 6.1: Soft materials under solicitations – how to trigger instabilities? Lysozyme gels [247]. Caseinate gels [248]. Confined caseinate gels [207]. Carbon black gels [249]. Cornstarch suspensions [250]. Latex gels [251]. Calcite and Ludox [252]

6.2 Fatigue and yielding in soft gels

6.2.1 Challenges associated with the determination of the yield stress

Fatigue refers to the changes in material properties caused by repeatedly applied loads [253]. Fatigue is quite universal and affects a broad range of materials from metals [254] to biomaterials such as adhesion clusters of cells [255]. In metals, the microscopic events associated with fatigue depend on the load and usually weaken the material. For example, if loads are above a certain threshold, microscopic cracks form at stress concentrators such as the surface, persistent slip bands, and grain boundaries [253, 256, 257, 258]. Eventually a crack reaches a critical size, propagates, and the structure fractures [259, 260]. Here, we address the question of fatigue in a soft material namely a colloidal gel. Under a constant stress, colloidal gels, like many other viscoelastic solids such as foams or emulsions, flow only above a critical stress referred to as the yield stress σ_y . This stress-induced fluidization is involved in virtually any application of colloidal gels, and it is essential to correctly measure and control this yield stress to ensure the safe and proper use of the material. Yet it has been shown in recent years that many phenomena may affect the way a material yields [261, 262, 263, 264]. Slippery boundary conditions may induce the solid-body motion of the material without bulk fluidization [264]. Long and complex transient regimes may show coexistence of fluid and solid phases before a liquid-like stationary state is reached [265]. In particular colloidal gels are prone to so-called “delayed yielding” where it may take a very long time for a weak gel to yield under a constant stress [266, 267, 268]. For instance, a gel can fail under its own weight after several hours or days [269, 270]. This “gravitational collapse” has been associated to the progressive weakening of the gel network due to thermally activated localized rearrangements [271] or to the interplay between the poroelasticity of the gel and gravitational compression [272, 273]. Delayed yielding has also been investigated in gels subjected to a constant shear stress imposed by a rheometer, including carbon black gels [274, 275], thermo-reversible protein gels [276] or weak gels of polystyrene particles [267]. In all cases, the gels are eventually fluidized after complex transient regimes. These dynamics have been related to activated processes: the applied shear stress σ decreases the energy barrier for bond breakage leading to failure times that decrease exponentially with σ [266, 268]. In this work we focus on the interplay between fatigue and yielding of carbon black gels under cyclic shear, a phenomenon which is comparatively much less documented in soft matter than the case of constant load.

Carbon black (CB) particles are colloidal, carbonated particles with a typical size range of 85 to 500 nm [277] that result from the partial combustion of hydrocarbon oils. These particles are widely used in the industry for mechanical reinforcement or to enhance the electrical conductivity of plastic and rubber materials [278]. When dispersed in a mineral oil (density $0.838 \text{ g}\cdot\text{cm}^{-3}$, viscosity $20 \text{ mPa}\cdot\text{s}$, Sigma Aldrich), these CB particles (Cabot Vulcan XC72R of density $1.8 \text{ g}\cdot\text{cm}^{-3}$) are weakly attractive with interactions of typical strength $U \sim 30k_B T$ [279]. From a dispersed state at weight concentrations of 6 % w/w., the particles aggregate to form sample-spanning networks of fractal dimension $d_f = 2.2$ even at very low concentrations [277].

6.2.2 Yielding characteristic time scales

Using oscillatory stress experiments with a constant stress amplitude σ_0 in a Couette cell combined with ultrasonic imaging, we have determined the yielding dynamics, Fig. reffig:cb1(a). Within the time interval $0 < t < \tau_w$ the gel remains solid, within $\tau_w < t < \tau_b$ the gel yields at the walls but remains solid in the bulk, and within $\tau_b < t < \tau_f$, we observe solid–fluid coexistence associated with negative normal forces. Beyond τ_f , the sample flows like a liquid. Those characteristic times scale differently with the oscillatory stress amplitude σ_0 at low and high stresses, Fig. reffig:cb1(b). However this difference vanishes when we scale the characteristic duration of each process τ_w , $\tau_b - \tau_w$, $\tau_f - \tau_b$ with σ_0 . Such a scaling allows us to distinguish three successive yielding processes: yielding at the wall, bulk yielding and clusters yielding, Fig. reffig:cb2.

Those durations are functions of the applied stress and can be empirically fitted by an exponential, although a power law cannot be ruled out due to the limited range of σ_0 . To gain insight into those multiple yielding processes, we have used the delayed yielding model [268] extended to oscillatory stress experiments ($\tau \sim \exp(-\sigma_0/\sigma^*)$) and the Basquin model [280] ($\tau \sim \sigma_0^{-\alpha}$). Both models fit reasonably well the data. This analysis shows that each successive yielding process requires a higher stress barrier, σ^* or a lower exponent α . According to the Basquin model, the CB gels are prompt to accumulate damage and are much more sensitive to stress than asphalt [281] or metals [282]. According to the delayed failure model, the CB particles have a weaker interaction with the walls than between themselves which justifies that the gel yields first at the wall and then in bulk. This work [283, 284] establish fatigue process in gels set bases for comparison with fatigue in hard materials such as composite or metals.

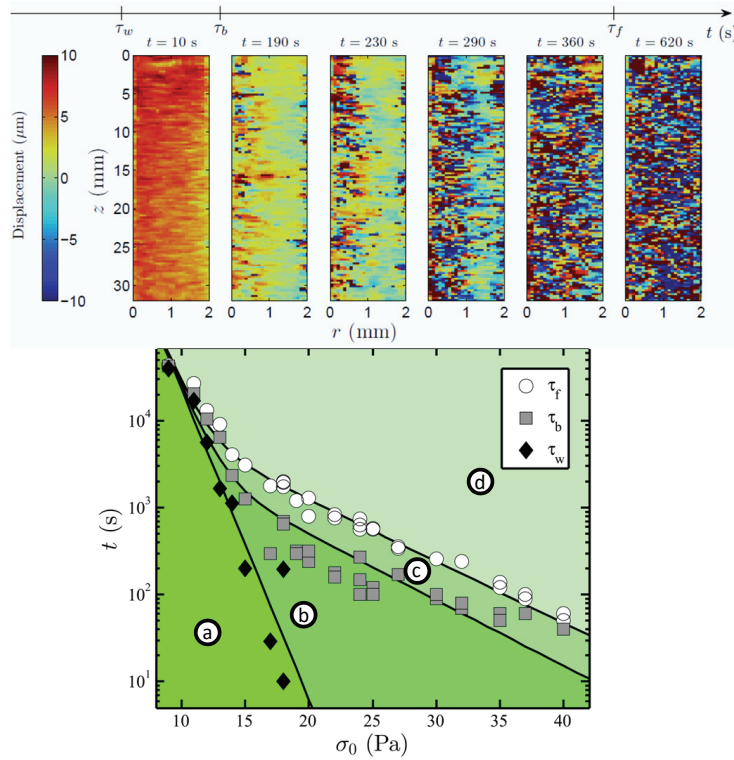


Figure 6.2: Fatigue dynamics, [283, 284]. (a) Time evolution of the displacement field $\Delta(r,z,t)$ as measured through ultrasonic imaging during the oscillatory stress experiment of amplitude $\sigma_0 = 27$ Pa at a frequency of $f = 1$ Hz. The ultrasonic imaging sampling frequency is 0.2 Hz so that $\Delta(r,z,t)$ is probed every five oscillation cycles. The rotor is at $r = 0$ mm and the stator at $r = 2$ mm. Depending on how the displacements are correlated between every five oscillations cycle we can infer the state of the gels. (b) Dynamic state diagram of the fatigue process of a CB gel at $c = 6\%$ w/w. The characteristic times $t = \tau_w$ (◆), $t = \tau_b$ (■) and $t = \tau_f$ (○) are determined from ultrasonic imaging and define the boundaries between different states encountered during the fatigue process: (a) solid-like state, (b) plug-like flow i.e. solid-body displacement with slip at the walls, (c) solid–fluid coexistence along the vorticity direction, and (d) a fluid-like state.

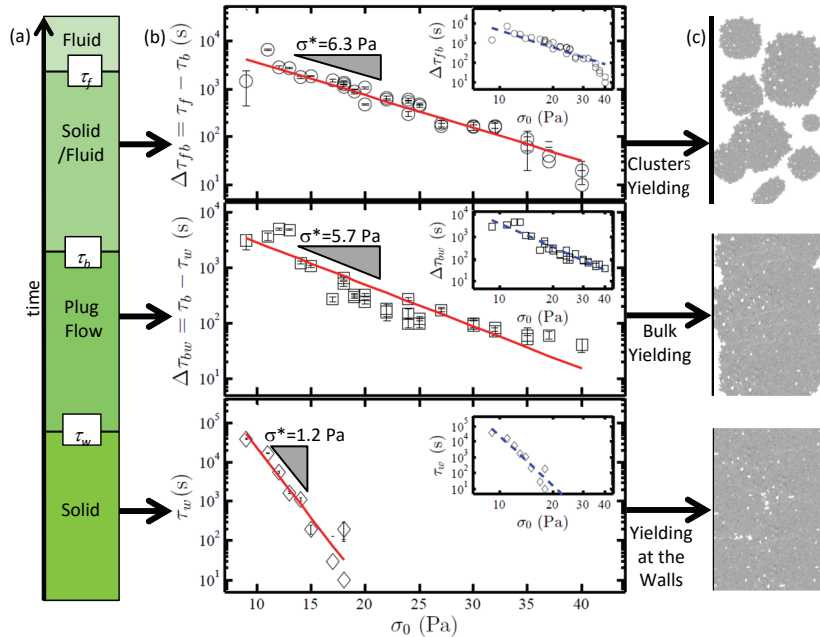


Figure 6.3: Scaling properties of the characteristic durations as a function of the applied stress amplitude σ_0 , [283]. (a) Flow state as a function of time. (b) τ_w , $\Delta\tau_{bw}$ and $\Delta\tau_{fb}$ vs σ_0 . Red solid lines are exponential fits ($\Delta\tau = Ae^{-\sigma_0/\sigma^*}$) to the data whereas blue dashed lines in the insets are power-law fits ($\Delta\tau = B\sigma_0^{-\alpha}$) to the same data. (c) Sketch of the gel structure between the stator and the rotor.

6.3 Predicting rupture in strong gels

6.3.1 Challenges associated with the prediction and assessment of rupture

Under sufficiently large stresses, solid materials may either flow or break. In hard solids, such as metals or composite structures, these highly nonlinear phenomena have a century of history, in an engineering context, it is critical to understand failure mechanisms in order to improve mechanical performance and ensure a safe usage. For soft solids, like gels or pastes, the topic is more recent yet nonetheless important. Most soft materials, including colloidal gels [285, 286, 287, 288, 289, 290, 291, 249], colloidal glasses [292], foams [293, 294], star polymers [295] and emulsions [296, 297, 298], display a *yielding* transition where they evolve from a solid-like state to a fluid-like state as the stress is increased [299, 300]. This transition is reversible and the material regains its elasticity once brought back to rest. Yielding has tremendous implications for food and cosmetics, including industrial processing and texturing [301, 302, 58]. It is also relevant to biology, for instance to the mechanosensing properties of cellular tissues [303]. However, when strong interparticle bonds are involved, soft solids rather develop fractures and *irreversibly break* under stress. This is the case for a number of biopolymer gels, such as gelatin [304], agar [305] and casein gels [306].

Experimental characterization of the yielding transition is not always easy for soft solids, as discussed in the previous section. Predicting failure in soft solids is even more difficult and remains an open problem. The onset of yielding and/or rupture under a stress load has been associated with a diverging correlation length scale [297], plasticity [307], “hot spots” [308, 309], and complex avalanche-like statistics [310]. Nevertheless, such features are insufficient to predict failure due to slippery boundary conditions [311, 312, 288, 313, 314, 315], long transient regimes or spatial heterogeneities [288, 291, 249, 316].

A large number of studies have been devoted to cracks and fractures induced by a *constant* load or strain in various soft materials including gels [317, 304, 306], fibrous materials such as fiberglass and wood [318] or paper [319, 320, 321] and harder composite materials [322] or even basalt [323]. Surprisingly, the irreversible rupture of soft solids under *oscillatory* shear remains much less explored, although oscillations provide a convenient way to follow the build-up of nonlinearity as a function of load amplitude, frequency and time [289, 291, 324, 325, 326, 327]. Oscillatory loads are also frequently involved in applications and often involve damage accumulation prior to rupture, a phenomenon known as “fatigue” that is still poorly understood [328, 329, 330, 331, 249].

Here, we focus on sodium caseinate protein gels under oscillatory stress. The protein gels is an aqueous dispersion of milk proteins, sodium caseinates, and GDL, molecules causing a gradual acidification of the environment in time [332, 333]. This acidification causes the condensation of the proteins into a homogeneous gel which fills the Couette cell. Acoustic contrast for the echography is provided by the addition of neutrally buoyant polyamide spheres (Orgasol 2002 ES3 NAT3, diameter 30 μm , density $d = 1.03$, Arkema). Casein gels are known to stick to PMMA so that wall slip or syneresis is not an issue in the present geometry [306]. The samples are gelled in the rheometer and subsequently submitted to an imposed oscillatory shear $\sigma(t) = \sigma_1 \cos(2\pi ft)$ with frequency f and amplitude σ_1 . Two types of oscillatory shear experiments are performed at $f = 0.1$ Hz: (i) “instantaneous” experiments where the gel is solicited over a short duration and (ii) “fatigue” experiments where oscillations are applied with a given stress amplitude for much longer durations. On the one hand, “instantaneous” experiments gives us an quasi-instantaneous snapshot of the gel mechanical properties. On the other hand, “fatigue” experiments allow us to monitor the evolution of the material as it accumulates damage over time. We use those two sets of experiments to predict and probe rupture.

6.3.2 Rupture and phase separation

Such gels are reported to display brittle-like rupture both under constant stress or strain [334, 306, 335]. Using a recently-developed echography technique, LORE, Fig. 6.4(a), we measure the local viscoelastic properties of the system and find that they remain homogeneous up to rupture, at least on length scales larger than 50 μm . At the rupture the gel suddenly gives way to a solid–fluid phase separation upon, Fig. 6.4(b-c).

6.3.3 How strain non-linearities point toward the rupture point

The sample strain response $\gamma(t)$ is recorded by the rheometer. Under medium and large amplitude oscillatory stresses, $\gamma(t)$ becomes nonlinear [337]. This results in the presence of harmonics in the Fourier series decomposition of $\gamma(t)$: $\gamma(t) = \sum_k \gamma_k \cos(2\pi kft + \phi_k)$ where γ_k is the amplitude of the k^{th} harmonics and ϕ_k its phase with respect to $\sigma(t)$. In our experiments, even harmonics are always negligible as expected from symmetry considerations in the absence of wall slip [338, 339, 340, 337, 341, 336] so that we only focus on odd harmonics $k = 3, 5, 7$ and 9.

Following “instantaneous” experiments and upon increasing the stress amplitude σ_1 the build-up of harmonic modes in the strain response, σ_1 can be rescaled for all gel concentrations ($[cas]$). This rescaling yields an empirical criterion to predict the rupture point way before the samples are significantly damaged, Fig. 6.5. First, for $0.1 \lesssim \sigma_1/G' \lesssim 0.5$, γ_1 keeps following the same linear law while higher harmonic modes are now clearly measurable and nicely described by power laws of σ_1/G' . More quantitatively, fitting γ_3 and γ_5

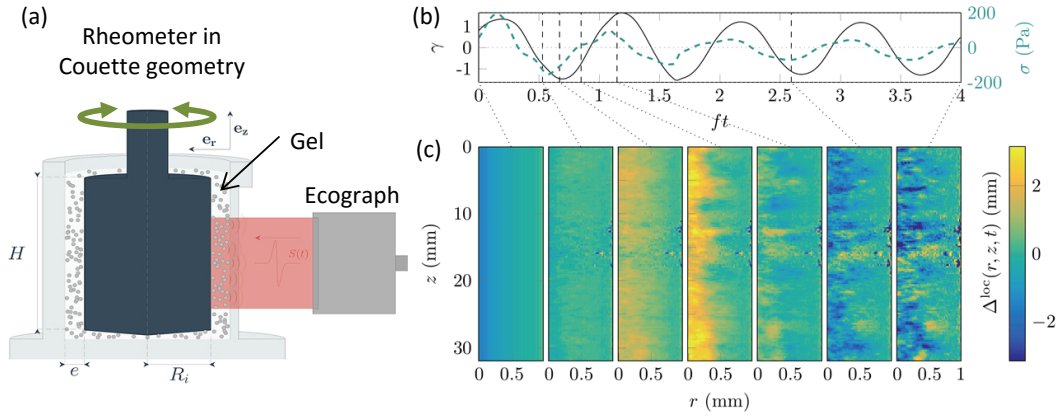


Figure 6.4: Large Oscillatory Rheology from Echography (LORE) to study rupture of a casein gel. (a) LORE [336]. (b) Strain γ and stress σ as a function of ft during the rupture of a casein gel. Note that the rheometer fails to apply a perfectly constant amplitude. (c) Local displacement maps Δ^{loc} obtained with LORE [248] during gel breakdown.

by power laws of σ_1/G' along this NLVE regime, $\gamma_k = A_k \left(\frac{\sigma_1}{G'}\right)^{n_k}$, yields the exponents $n_3 = 2.7 \pm 0.1$ and $n_5 = 4.1 \pm 0.6$ with prefactors $A_3 = 0.6$ and $A_5 = 0.4$. Most strikingly, the extrapolation of both these power-law fits and of the linear regime $\gamma_1 = \sigma_1/G'$ to higher stress amplitudes all intersect at a single point. This point corresponds to $(\sigma_c/G' = 1.33 \pm 0.24, \gamma_c = 1.37 \pm 0.23)$ and matches remarkably well the experimental rupture point $(\sigma_c/G' = 1.06 \pm 0.25, \gamma_c = 1.32 \pm 0.20)$. This empirical analysis of the nonlinear strain response thus yields a criterion to *predict* the rupture point based on oscillatory shear experiments at intermediate stresses way before the gels is damaged. Moreover, “fatigue” experiments follow the same scenario and can be mapped perfectly well onto the previous “instantaneous” oscillatory experiments when considering $\gamma_{k>1}$ as a function of γ_1 . This proves that the rupture pathway is controlled by strain rather than time.

We expect this work [248] to trigger numerical modeling and theoretical efforts to explain the power-law evolution of the higher harmonic modes as well as the rupture criterion. We believe those scalings and the rupture prediction to be also relevant for biological networks and biopolymer gels made of, e.g., actin, alginate, gelatin or agar. Further experiments on these various systems are in line to check for generality. Our work also opens the way to deeper local investigations of the damage process of soft materials under oscillatory shear.

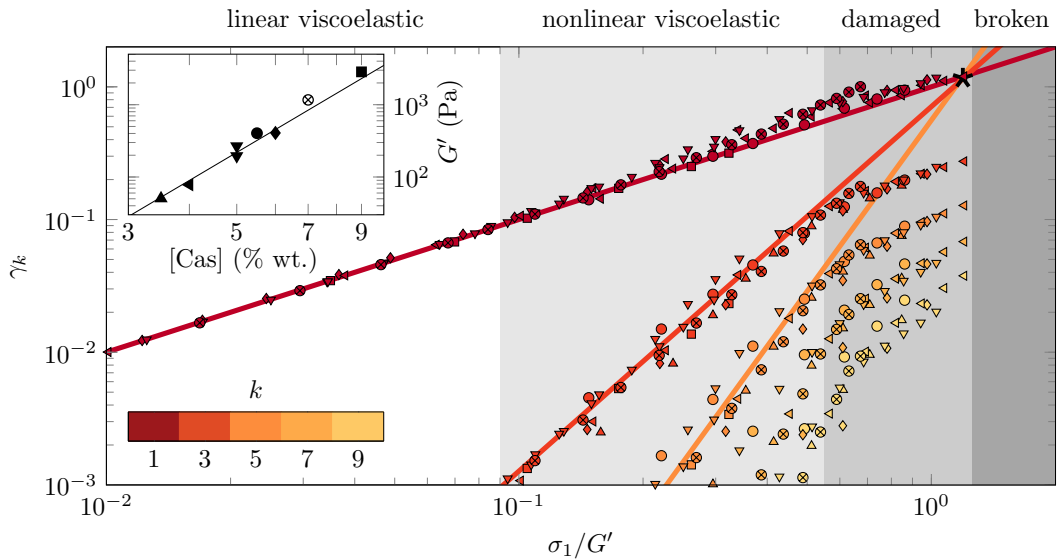


Figure 6.5: Build-up of nonlinear modes γ_k of the strain response of casein gels subject to an oscillatory stress of amplitude σ_1 for various casein concentrations, [248]. Colors code for $k = 1$ to 9. The stress amplitude is normalized by the elastic modulus G' of the gel measured in the LVE regime. Solid lines show the best power-law fits of γ_k for $\sigma_1/G' < 0.5$. Background colors delimit the various regimes discussed in the text. Inset: G' as a function of $[cas]$. The symbols code for casein concentration in the main graph. The solid line is $G' \sim [cas]^4$.

6.4 Wrinkling gels

6.4.1 Investigating new wrinkling mechanisms in a model system

What makes a soft film buckle or wrinkle? A film may buckle and wrinkle in many ways and for various reasons Fig. 6.6. When compressed along its length a plastic ruler bends. It is said to buckle. When a carpet is compressed, it does not buckle on its entire length but instead forms small ripples, or wrinkles. The weight of the carpet, which is exerted perpendicular to the compression, disfavors long undulations. It is the competition between the weight and the elasticity that define the wrinkling wavelength. The causes of wrinkling are always a combination between excess surface, responsible of the buckling, and a constraint perpendicular to the selected wrinkling wavelength. For example, the skin of an apple which flesh dries out is in excess and must buckle, but the skin is retained by the elasticity of the apple flesh and therefore it wrinkles. It has been predicted that in the case of an elastic film in contact with a very thin layer of liquid, the viscosity of this liquid would resist the long undulations and wrinkles could appear. This has not been observed yet because in experimentally convenient situations, the film is at the top of the liquid and the weight of the film plays the larger role so as in the carpet situation.

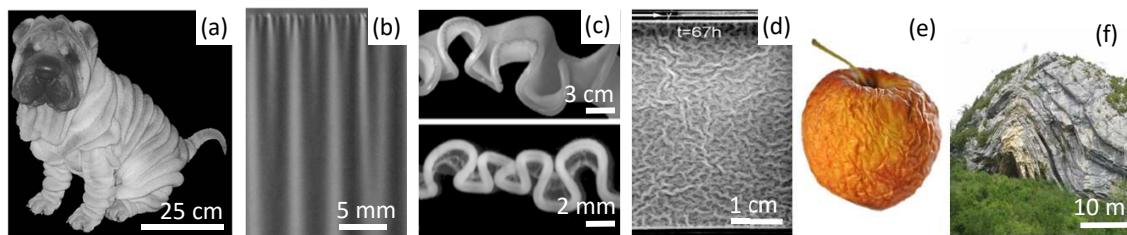


Figure 6.6: Wrinkling. An elastic film buckles because of excess area and wrinkles when a substrate hinders buckling. The selection of the preferred wrinkling wavelength is peculiar to the situation and is related to a mismatch of elastic properties between the surface and the substrate [342, 343, 344, 345, 206, 346]. In biology, wrinkling-controlled morphogenesis is ubiquitous. Aging and loss of elastic fibers make our skin wrinkle [346, 347]. (a) The Chinese Shar-Pei, the dog that is “too small to fit properly into its own fur”. (b) The difference in growth rate between the gut tube and its dorsal anchoring is responsible for the villification of guts [348, 349, 350]. (c) Localized cell death in biofilms focuses on mechanical forces and initiates a three-dimensional labyrinth pattern [351, 352]. (e) drying apple. In physics, the last two decades have seen the development of methods used to obtain well-controlled patterns via linear (bowden1998, genzer2006, hu1998, kim2010, vandeparre2011, li2013) or nonlinear wrinkling [353, 354, 355, 356]. Such patterns can be triggered by temperature dilation (bowden1998), swelling [357, 358], or removal of prestrain [346]. (e) Smooth Cascade of Wrinkles at the Edge of a Floating Elastic Film. (f) Le Chapeau du Gendarme near Septmoncel (Jura, France). The birth of the Alps straightened the strata vertically. At this point, the base of the folding broke along a horizontal axis. As the push from the Alps continues, the straightened strata will then slide along this break. They will push the Lower Cretaceous stratum without moving the strata of the Jurassic below. Close to the break, the cretaceous stratum will detach from that of the Jurassic and will strongly wrinkle forming the a napoleon hat like structure.

6.4.2 Experiments with yogurt-like gels

To circumvent this issue, we took inspiration from the yogurt-making process to create thin porous biogel films immersed in a viscous medium which density is close to the one of the biogel Fig. 6.7. In a cell consisting of two microscopy lamellas separated by 100 microns, we enclose an aqueous dispersion of milk proteins, sodium caseinates, and GDL, molecules causing a gradual acidification of the environment in time. This acidification causes the condensation of the proteins into a homogeneous gel which fills the cell and contracts within minutes in a thin elastic porous film of a few tens of microns thick and separated from the microscopy lamella by layers of water. As the acidification continues, the gel film inflates, develops an excess of surface and wrinkles. Furthermore, in this confined geometry, the wrinkles soon meet the lamellas and flatten on it. To gain further area, the gel wrinkles inside the preceding wrinkles as seen on the left hand side of the illustration next page, Fig. 6.8.

6.4.3 A new wrinkling mechanism related to the gel porosity

The three-dimensional conformation of gel film is reconstructed by confocal microscopy and is displayed on the right hand side of the illustration. By analyzing the dynamics of the formation of folds and by comparing it to a theoretical model, we were able to show that the porosity of the gel is selecting the wrinkling wavelength. Indeed when the film is very close to one of the lamella, it is easy for the water to go through the porous gel. The new wrinkling mechanism identified in this work [207] may be relevant to wrinkles that appear in membranes inside our body which are immersed in body fluids and partially permeable to them. This may have some important consequence during morphogenesis.

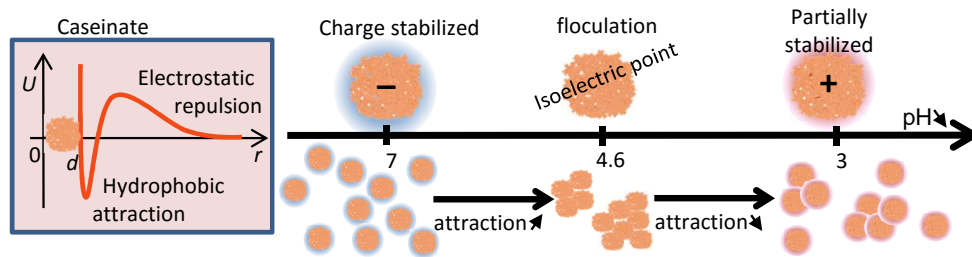


Figure 6.7: The stability of casein dispersions strongly depends on pH. At neutral pH, caseins are charged negatively and repel one another. As pH decreases to the isoelectric point of caseins ($\text{pH} = 4.6$), casein molecules lose their negative net charge and tend to stick to one another [332, 333, 359]. Beyond the isoelectric point, caseins acquire a positive net charge and therefore partially redissolve.

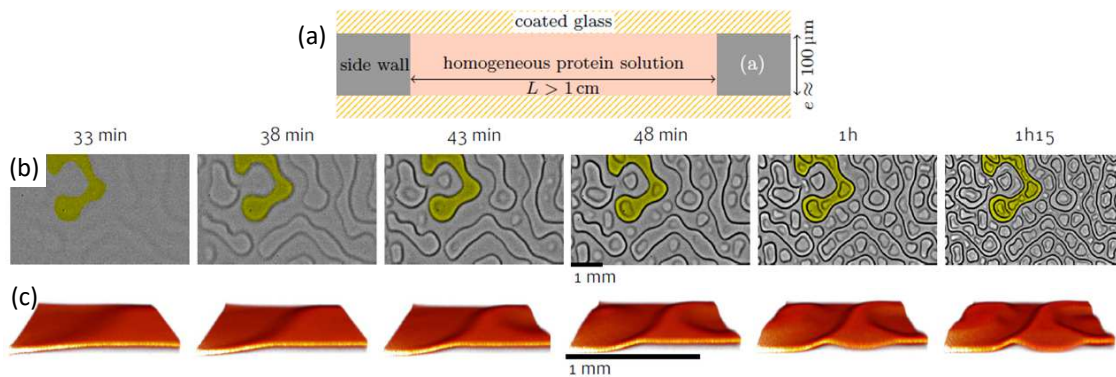


Figure 6.8: Dynamics of pattern formation in a confined film of casein gel, [207]. (a) Initial configuration: the sealed optical cell contains a homogeneous caseinate protein (Firmenich) and GDL (Firmenich) a molecule that will slowly and homogeneously release protons H^+ dispersed in deionized water. The gel only attaches to the side walls because the bottom and top glasses are coated with polyacrylamide brushes to prevent caseinate adsorption. (a) Light transmission microscopy. (b) Three-dimensional reconstruction from fluorescent confocal microscopy. This scenario is robust and is observed over a large range of dispersions. We used concentrations such that GDL and sodium caseinate weight concentrations are equal, $[\text{GDL}] = [\text{cas}]$ ranging from 2 to 8% wt and mixture of water and glycerol to change the dispersion viscosity.

7. Futur projects

Recently, we got lucky; we got several project funded: on bacteria dispersions (grant ANR JCJC 2018), gels and power ultrasounds (grant Rhône-Alpes-Auvergne 2017) and people behavior in ice breaker games (grant CNRS 2016). In the next, I only present the project on bacteria.

7.1 (StruBaDy) Structure Bacteria Dynamics

7.1.1 Global objective

Our goal is to lay out the design principles of active mesophases. These states of active matter will be self-assembled from swimming bacteria with externally controlled interactions. Firstly, we will add attractive interactions in initially repulsive dispersions of bacteria. Using cutting edge strategies from colloidal science, the attraction will be mediated using thermo-sensitive depletants. Taking advantage of this externally tunable attraction via temperature, we will investigate active mesophases of different symmetries and determine the kinetic pathways to shape shift one active mesophases to another. Secondly, we will establish the structural and transport properties of active mesophase in patterned media. We will take advantage of micro-patterning techniques to design cylindrical pillars with controlled spatial repartitions. In practice, in dilute dispersions of bacteria, counting on the depletants, we aim to channel bacteria to orbit around pillars. Fine tuning the bacteria orbit time with depletion, we will study the bacteria hopping dynamics in lattices of pillars. Finally, in dense suspensions of bacteria suspensions with depletants, we aim at nucleating condensates of swimming bacteria around micro-pillars. We will take advantage of collective bacterial effects to mimic atomic structures such as atoms, molecules and solids. The mesoscopic atom will be composed of a cloud of bacteria orbiting around a pillar. The mesoscopic molecule will be composed of two mesoscopic atoms in interaction. The strength of the molecular bound will correspond to the degree of synchronization between the orbiting bacteria of the two mesoscopic atoms. Mesoscopic solids will correspond to mesoscopic atoms in interaction on a lattice. Playing with the pillar organization and the direction of rotation of the bacteria around the pillars, we will generate long range order. We aim at self-assembling ferromagnetic and anti-ferromagnetic ordered structures as well as chiral mesophases by utilizing geometrical frustrations. To sum it up, this project will bring to the next level the concept of colloids as giant atoms using the synergy between bacteria, depletants and micro-pillars.

7.1.2 Context and aim

State of the art and originality of the project — Over the last five years, a major attention has been paid to novel classes of colloidal liquids made of motile units: from living bacteria and algae, to synthetic active particles, see [360] and references therein. Apart from very rare exceptions [361, 362], we do lack of model systems allowing a continuous control over the interactions between the motile units of active materials. This limitation strongly hinders the systematic exploration and understanding of their collective behavior. In this project we will rectify this situation and create active materials based on smooth running bacteria capable of self-assembling into mesophases of unprecedented structural and dynamical properties. Our strategy consists in taking advantage of 30 years of successful research in colloidal science and self-assembly. In the 80's, the drastic expansion of colloidal science was sparked by the development of attractive interactions induced by depletion. This tool has resulted in understanding of a host of phases: from arrested structures like gels [363], to complex thermodynamics structures like empty liquids [364], colloidal membranes [128] and twisted ribbons [47]. For example, based on our own research, using thermo sensitive polymers as depletion agents, we managed to continuously tune the attraction between hard rods to trigger and understand the pathway leading to the condensation of anisotropic droplets (tactoids) [125]. Firstly, building on this work, we will continuously explore the multidimensional phase diagram of active mesopases (WP1). Secondly, using micro patterning techniques, we will address and elucidate their interplay with geometrical boundaries (WP2).

WP1: From bacteria suspensions to bacteria mesophases — In stark contrast with passive colloids, the phase behavior of bacterial fluids remains rather poor. The sole mesophase found in bacterial fluids is the well-established (and unstable) active nematics phase [365, 366, 367]. Until now, pioneering attempts to tailor the interaction between the swimming cells by means of depletants has only yield the formation of dense bacterial cluster having a rather short lifetime prior to cell death due to lack of nutriments and oxygen [361]. In this project we will explore the pathways between the existing, and unanticipated phases of bacterial liquids using continuously tunable interactions. We will achieve this goal by building on two experimental expertises. First, we will use homemade thermo sensitive PNIPAM microgel particles [125] as depletion agents which will make it possible to continuously tune the attraction between the bacteria upon minute temperature changes. Second, by handling the bacteria in dedicated agar cells [368] or micro-channels allowing a flow-free

continuous supply of oxygen and nutrients [369, 370], we will be able to explore stationary regimes at very high bacteria concentrations, up to 20% volume fractions.

WP2: Bacterial mesophases in micro-patterned geometries — We then aim to tame a bacteria so that it swim around a pillar, Fig. 7.2. 10-50 μm size pillars will be designed using lithography and used as nucleation spot to form bacteria clusters. Indeed, due to hydrodynamics interactions, a bacteria is attracted by surfaces and will therefore tend to swim naturally around the pillars [371, 372, 373]. As hydrodynamics interactions might not be sufficient, depletion interactions will be added to enhance and better control the orbit lifetime of the bacteria around the pillars. This system would then be the Hydrogen atom: a nucleus with an orbiting electron, Fig. 7.1(a-b) We will focus adding bacteria to the orbit and study the dynamic equilibrium properties of the cluster as well as its coherence.

Building on the bacteria/depletion/pillar system we will add other pillars and ask the following questions. How does the cluster behave when other pillars are in their close vicinity? At low attraction the bacteria would diffuse though the pillar network as free electron in a metal and at high attraction the bacteria would be localized around the pillars as electrons in an insulator. If pillars are close enough so that bacteria diffuse from one pillars to the other would it possible to synchronize the handedness of the rotational motion of the bacteria between all the pillars and create chiral dynamics? If the pillars lattice is triangular then the rotation sense of the bacteria around the pillar is frustrated. How then does the system organize?

Methodology — All our experiments will rely on fluorescence, and confocal video-microscopy to characterize the structure and dynamics of the bacteria/depletent suspensions. Micro-channels and micro-structures will be fabricated using soft-lithography methods already mastered in the Bartolo group. We reiterate that one of the major problems with bacteria dispersions is to keep them alive during experiment at high concentrations. To do so we have already used simple agar optical cell [368] and microfluidic stickers [369, 370] making it possible to maintain bacteria in a stationary state for at least 90 mins even at volume fractions as high as 20%, Fig. 7.1(c).

Risk managements — The first risk concerns the introduction of depletion interactions between bacteria. T. Gibaud has a very strong experience in tailoring depletion-induced interactions in passive colloidal systems [125]. In addition, W. Poon group has demonstrated that polysulfonated and PEG polymers can be effectively used as depletent agents to induce phase separation in E-coli suspensions [361]. Given the quite similar structure of PNIPAM, we believe PNIPAM microgel particles can also be used as depletent agents. They will provide the unique advantage of a continuous control of the attraction strength in a given sample. In case of (unlikely) failure, we would use PEG or Dextran polymers.

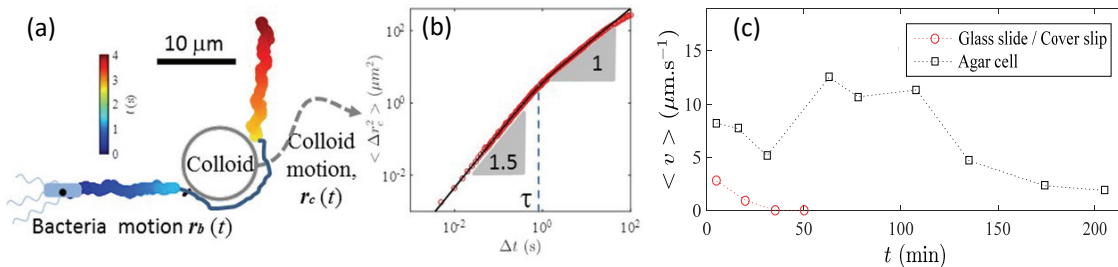


Figure 7.1: Preliminary experiments, unpublished. (a) Scattering of a swimming E-coli bacterium by a 10 μm colloidal particle. (b) The bacteria perturb the colloid dynamics r_c [374]. For $\Delta t < \tau$, $\langle r_c^2 \rangle \sim \Delta t^{1.5}$. We demonstrate that this is due to the transient orbiting motion of the bacteria around the colloid. This evidence a novel transport mechanism and settle a long-standing debate about the origin of enhance diffusion. (c) Mean individual velocity of a concentrated bacteria suspension measured with differential dynamic microscopy [375]. At high concentrations ($\sim 10\%$ volume fraction) bacteria have life time of about 5min between glass slide and a cover slip whereas this life time is extended to 1h30 in our agar cells.

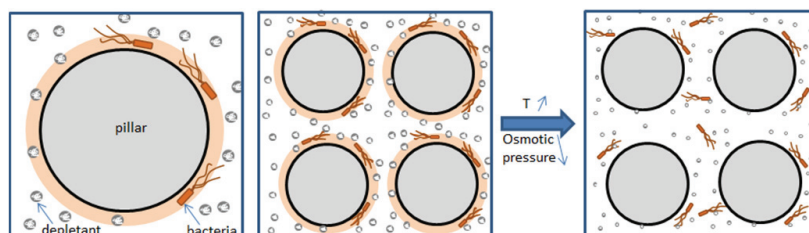


Figure 7.2: Taming bacteria motility to mimic the transport properties of electrons in conductor and insulator

7.1.3 Impact of the project

Microscopy platform — A wet lab as well as the microscope of T. Gibaud are open to scientists in Lyon so that they can check their sample and/or perform quantitative experiments including particles tracking, -rheology, birefringence measurement or Differential Dynamic Microscopy.

Scientific communications — We aim at publishing the results of such a fundamental-science project in high-impact peer-reviewed journals. In addition, our results will be presented in international scientific conferences. PhD students will be encouraged to attend international soft-matter conferences to get well integrated in the soft matter community, a key parameter to initiate their career in the field.

Contributions to the content of higher education courses — This project will fuel lab courses. Currently T. Gibaud is setting up a lab course where a pair of students comes to the lab and performs experiments during 1 week. Over the past years, We studied Brownian motion [376], bacteria motility [375], gelation [377], schlieren methods [378]. The students learn to optimize the microscope setup, to handle the analysis of the acquired images coding in matlab [379, 380, 381, 382, 383]. We will pursue this fruitful strategy.

Promotion of scientific culture — We will also pay attention to the dissemination of our research to the public. At a local level, we will actively participate to ‘la fête de la science’ allowing non-specialists to visualize living bacteria and gain a better understanding of how they move and proliferate. At a larger scale, given the increasing impact of social media we will communicate on our latest results on our Youtube channels (<https://www.youtube.com/user/GibaudLab>), Tweeter and LinkedIn, creating dedicated channels and feeds for the present project. T. Gibaud will also continue to communicate his results to the ‘actualité scientifique du CNRS’ as done for previous work on self-assembly of colloidal rods and wrinkling gels, he will also benefit from the experience of D. Bartolo to disseminate his work through general French and international media (Newspaper, radio and TV).

Intellectual property — Intellectual property issues will be addressed, if necessary, according to the rules set by our employers: CNRS and ENS de Lyon.

7.1.4 Organization of the project and means implemented

Thomas Gibaud (implication 70%) — Principal Investigator. This project relies on a set of skills that T. Gibaud has developed during his career: the use of biological colloids and the use of external stimuli to tune colloids interactions and move continuously in their state diagram. During his PhD with P. Schurtenberger, he used lysozyme and its temperature dependent attraction as model colloids to explore the interplay between the glass transition and the spinodal decomposition. He constructed a coherent framework that bridged the gap between the hard sphere glass and the gel phases [21, 247], shed light into protein crystallization [384] and provided a new pathway to assemble amorphous solid-like networks characterized by a specific correlation length [385, 386] and rheological properties [387]. After ATER with S. Manneville at the Ens de Lyon, he went to the USA for a 3 years post doc. During his post-doc with Z. Dogic and ANR-retour postdoc at the ENS de Lyon, he used viruses with thermosensitive chirality interactions and dextran as a depletent to open a new paradigm on colloidal membranes to twisted ribbon transition [47], membrane rafts formation [78] and chiral coalescence [177, 163]. As a sole PI, he used PNIPAM as thermosensitive depletent to understand the condensation pathway leading to nematic droplet [125]. More recently, using caseinate with pH induce syneresis, He uncover a new wrinkling mechanism in gels [207], and developed a rheology analysis to experimentally predict caseinate gels rupture point before the gels get irreversibly damaged [336, 248].

Team — The team will be composed of two researchers, two PhD and master students. T. Gibaud and D. Bartolo, have started an informal collaboration that has already lead to very promising results on the manipulation of bacteria in microchips, Fig. 7.1.

Denis Bartolo (implication 30%) — Partner. Denis Bartolo is Professor at ENS de Lyon and a world expert in synthetic active-matter physics and microfluidics (see CV). The collaboration with D. Bartolo will make it possible to combine our non-redundant and complementary expertise to tackle this ambitious long-term research program.

Students — In order to complete our project T. Gibaud will recruit a PhD student at a very early stage of the project (Co-supervised with D. Bartolo). He will host one Master student (M1 or M2) per year. We will seek a talented experimentalist with a strong background in Soft-condensed matter physics, fluid mechanics, biophysics and statistical physics. We plan to hire a second PhD student at the beginning of year 4 (Funding from Ecoles Doctorales or Ens de Lyon). Ens de Lyon is an ideal institution to source high profile students.

Equipment and facilities — Experiments will be performed in the Gibaud lab already equipped with an optical and fluorescent microscope. Microfluidics and micro-patterning will be developed in the clean room facility of ENS de Lyon. We will also rely on the microscopy platform at Ens de Lyon (Platim). We will have access to 10 confocal microscopes, and benefit from the help of five full-time engineers. We stress that this solution is much cheaper than buying a fast confocal head for our microscopes.

Estimated cost —

- PhD student 100 k€
- Master students: 1 student/year (5 month/year, gratification of 500€/month) 10 k€

• Traveling costs and conferences: 2000€/pers/year	22 k€
• Computers for data acquisition, storage and analysis	10 k€
• Confocal time at the platform PLATIM for 4 years	10 k€
• Temperature control platform for microscopy	10 k€
• Consumable, small equipment and microfluidics: 12.5 k€/year	50 k€
• Grant management by the host institution: 15% of the total cost	33 k€
	Total over 4 years: 255 k€



Curriculum Vitae

8	Short CV	48
9	Long CV	50
9.1	Short Biography	
9.2	Research statement	
9.3	Scientific production	
9.4	Media coverage	
9.5	People	
9.6	Services	
9.7	Teaching and Outreach	
9.8	Grants	

8. Short CV

Thomas Gibaud

Research scientist – CNRS

Curriculum Vitae

✉ Laboratoire de Physique, Ens de Lyon,
46 allée d'Italie, 69007 Lyon, Fr

☎ 0761520550

@ thomas.gibaud@ens-lyon.fr

🌐 <http://perso.ens-lyon.fr/thomas.gibaud>

Links :  -  -  -  -  - 

→ *underlined cyan* : active link

Employments

Research scientist (CNRS), *Ens de Lyon, Fr* 12/2011 → present
Invited scholar at *Brandeis University* (2 months, 2014)
Invited lecturer at *East China Normal University* (1 month, 2013)
Invited scholar at *Brandeis University* (4 months, 2012)
Post-Doc with Z. Dogic, *Brandeis University, USA* 01/2009 → 12/2011
ATER (100%), *Ens de Lyon, Fr* 09/2007 → 01/2009
Post-Doc with S. Manneville and Teaching Assistant
Teaching Assistant, *Université de Fribourg, CH* 09/2004 → 09/2007

Education

PhD in Physics with P. Schurtenberger, *Université de Fribourg, CH* 2008
Agrégation in Physics, *Université J. Fourier, Grenoble, Fr* 2004
Master in Materials Sc., *UPMC-X-ENS-Centrale-ESPCI, Paris, Fr* 2002
Bachelor in Physics, *Université du Maine, Le Mans, Fr* 2001

Research

[Experiments in soft condensed-matter physics](#) – I use, purify or engineer organic and living matter to design smart colloids which serve as building blocks to create materials with fine tuned dynamics and structures. We then put efforts in understanding the material response to external solicitations using devices such as rheometer, optical tweezers or high power ultrasound. We also take advantage of built-in sensitivity of our particles to pH or temperature to continuously morph our dispersions properties. Those materials are not only a venue to study self-assembly, gels and active matter but they also mimics phenomena observed in biology or hard condensed matter.

selected Publications : *PNAS* **114**, E3376 (2017) – *Sci. Adv.* **1**, e1500608 (2015) – *Nature* **481**, 348 (2012)
Soft Matter **13**, 2643 (2017) – *Soft Matter* **12**, 1701 (2016)

[Publications, talks, posters](#) – 31 peer reviewed articles (16 as first author and 14 as corresponding author), 3 invited talk in international conferences, 24 contributed talks/posters in conferences, 40 invited seminars. Google Scholar (7/11/2017) : 808 citations, h-index=15.

[Grants](#) – total : 10 as a PI and 2 as a collaborator, ~ 1.0M€
• ANR JCJC, (2019-2023), 230 k€
• Grant région Auvergne-Rhône-Alpes (2017-2022), 256 k€
• CNRS Emergence 2016, 10 k€
• ANR-11-PDOC-027, (2012-2015), 350 k€

[Supervision and co-Supervision](#) – I have supervised 16 bachelor/master students, 3 PhDs and 4 post-docs. 3 of the post-docs got an academic position following our collaboration.

Teaching

Since 2011, I teach ~ 64h/year at the Ens de Lyon in the bachelor/master *Sciences de la Matière*.

During my ATER position, I taught 140h/year at the at the Ens de Lyon in the *agrégation de physique*.

During my PhD, I taught (70h/year) and set up physics lab for freshman students at the université de Fribourg (CH).

[Outreach](#) : I setup and enlive physics experiments for children at the Discovery Museums of Acton, Ma, USA (2011) and in a Kindergarden class at Bulle, CH (2007). I co-organized the 2005 Einstein year at the physics dept of the University of Fribourg, CH and for the occasion presented two 45 min Physics shows targetted toward the general public.

Non Profit Organisations

Vice president at P'tits Bouts – nursery (2017-)

Treasurer at ENplaStik – art association (2013-2016)

Winter School instructor and leader – MIT Outing Club (2010-2011)

Cofounder of Roul'Mans – Roller blading association (1997-2001)

Sailing Teacher for the Fédération Française de Voile (1997-2001)

Membership :

Société Française de Physique.
European Society of Rheology.

selected Services :

- Local committee organizer for the Conference CFCL2017 – systèmes anisotropes auto-organisés, Lyon (2017).
- Editorial board member for the journal Scientific Reports (2017-present)
- Referee, 4 articles/year (2010-present).
- Organizer of the weekly physics seminar at Brandeis University (2009-2011).

Personal

Born in Le Mans (Fr), 1979 – French.

Civil Union with F. Rhode, 2 children.

References

-  S. Manneville, Ens de Lyon
-  Z. Dogic, Brandeis University
-  D. Bartolo, Ens de Lyon
-  P. Schurtenberger, Lund University

9. Long CV

9.1 Short Biography

I studied Physics in France at the Université du Mans for the bachelor degree and at the Université Pierre et Marie Curie for the master degree. I successfully passed the national teaching exam, 'Agrégation de sciences physiques'. I obtained my PhD at the Université de Fribourg in Switzerland under the supervision of Peter Schurtenberger and Anna Stradner on the interplay between phase separation and the glass transition in globular protein suspensions. After a short postdoc with Sébastien Manneville at the Ens de Lyon (Fr) on the yielding dynamics of colloidal gels, I went to the USA for a second postdoc at Brandeis University with Zvonimir Dogic. There I worked on self-assembly using filamentous phages as colloidal building blocks. In 2012, I was appointed CNRS researcher at the Ens de Lyon in France.

9.2 Research statement

Nature excels at building complex functional materials. Scientists are however far from understanding the structure and mechanism involved and even further from being able to replicate equivalent materials. Here, I use, purify or engineer nanometer to micron particles which serve as building blocks to create innovative soft materials. The particles specific properties cascade to macroscopic scales and are the cornerstone for designing new materials. I then put efforts in understanding the soft material response to external solicitations. To do so, I use devices such as rheometer, optical tweezers or high power ultrasound. I also take advantage of built-in sensitivity of the particles to pH or temperature to continuously morph our dispersions properties. This bottom up approach combined with external solicitation of the self assembled soft materials allows me to tackle fundamental issues in self-assembly, gels and active matter and mimics many phenomena observed in biology or hard condensed matter. Remarkable results:

- Discovery of traveling bands as the instability mechanism in shear thickening [PRX 8, 031006 (2018)]
- New wrinkling mechanism in gels [Science Advances e1500608 (2015)]
- New structures with colloidal rods: colloid membranes to twisted ribbons [Nature 481, 348 (2012)]
- Discovery of a new class of yielding mechanism in gels: fatigue and delayed yielding [Soft Matter 6, 3482 (2010)]
- Arrested phase separation as a new pathway for gelation [PRL 99, 118301 (2007)]

9.3 Scientific production

Peer reviewed articles

- 27 research articles
 - 8 articles focused on teaching physics (30,25, 21, 17, 4-1).
 - 17 articles as first author (35, 30, 28, 26, 19, 17, 16, 14-8, 4-1).
 - 15 articles as corresponding author (32-29, 27-25, 23-21, 17, 16, 3-1).
35. Irreversible hardening of a colloidal gel under shear: the smart response of natural rubber latex gels. G. de Oliveira Reis, T. Gibaud, B. Saint Michel, S. Manneville, M. Leocmach, L. Vaysse, F. Bonfils, C. Sanchez and P. Menut, [xxx xxx, xxx \(2018\)](#)
 34. Direct liquid to crystal transition in a quasi-two-dimensional colloidal membrane. T. Gibaud and D. Constantin, [J. Phys. Chem. Lett. 9, 4302 \(2018\)](#)
 33. Redox-induced metamorphism in a Viologen-based Palladium Coordination Polymer. C. Kahlfuss, T. Gibaud, G. Royal, F. Chevallier, E. Saint-Aman and C. Bucher, [Chem. Eur. J. 24, 1 \(2018\)](#)
 32. Uncovering instabilities in the spatiotemporal dynamics of a shear-thickening cornstarch suspension. B. Saint-Michel, T. Gibaud and S. Manneville, [PRX 8, 031006 \(2018\)](#)
 31. Synthetic Schlieren – application to the visualization and characterization of air convection. N. Taberlet, N. Plihon, L. Auzémery, J. Sautel, G. Panel, T. Gibaud, [EJP 39, 035803 \(2018\)](#)

30. Filamentous phages as building blocks for reconfigurable and hierarchical self-assembly. T Gibaud, *J. Phys. Cond. Mat.* **29**, 493003 (2017)
29. Predicting and assessing rupture in protein gels. B. Saint-Michel, T. Gibaud and S. Manneville, *Soft Matter* **13**, 2643 (2017)
28. Achiral symmetry breaking and positive Gaussian modulus lead to scalloped colloidal membranes. T. Gibaud, C. N. Kaplan, P. Sharma, A. Ward, M. J. Zakhary, R. Oldenbourg, R. B. Meyer, R. D. Kamien, T. R. Powers and Z. Dogic, *PNAS* **114**, E3376 (2017)
27. Local Oscillatory Rheology from Echography. B. Saint-Michel, T. Gibaud, M. Leocmach, and S. Manneville, *Phys. Rev. Applied* **5**, 034014 (2016)
26. Multiple yielding processes in a colloidal gel under large amplitude oscillatory stress. T. Gibaud*, C. Perge*, S. B. Lindstrom, N. Taberlet and S. Manneville, *Soft Matter* **12**, 1701 (2016)
25. Differential dynamic microscopy to characterize Brownian colloids and motile bacteria. D. Germain, M. Leocmach and T. Gibaud, *Am. J. Phys* **84**, 202 (2016)
24. Entropic forces stabilize diverse emergent structures in colloidal membranes, L. Kang, T. Gibaud, Z. Dogic and T. C. Lubensky, *Soft Matter* **12**, 386 (2016)
23. Condensation and dissolution of nematic droplets in colloidal rods dispersions with thermo-sensitive depletants. A. Modlinska, A. M. Alsayed, and T. Gibaud, *Scientific Reports* **5**, 18432 (2015)
22. Hierarchical wrinkling in a confined permeable biogel. M. Leocmach, M. Nespoulous, S. Manneville and T. Gibaud, *Science Advances* **1**, e1500608 (2015)
21. Étude expérimentale du mouvement brownien d'une particule colloïdale. P. Maurer, J. Ferrand, M. Leocmach et T. Gibaud, *B.U.P.* **969**, 1567 (2014)
20. Time dependence in large amplitude oscillatory shear: a rheo-ultrasonic study of fatigue dynamics in a colloidal gel. C. Perge, N. Taberlet, T. Gibaud and S. Manneville, *Journal of Rheology* **58**, 1331 (2014)
19. Imprintable membranes from incomplete chiral coalescence. M. J. Zakhary*, T. Gibaud*, C. N. Kaplan, E. Barry, R. Oldenbourg, R. B. Meyer, and Z. Dogic, *Nature communications* **5**, 3063 (2014)
18. Hierarchical organization of chiral rafts in colloidal membranes. P. Sharma*, A. Ward*, T. Gibaud, M. Hagan and Z. Dogic, *Nature* **513**, 77 (2014)
17. Etude de la période d'un pendule pesant: de la mécanique du point à la mécanique du solide. A. Gibaud, G. Ripault, T. Gibaud, étudiants ISTD, *B.U.P.* **952**, 319 (2013)
16. Unexpected decoupling of stretching and bending modes in protein gels. T. Gibaud, A. Zacccone, E. del Gado, V. Trappe, and P. Schurtenberger, *Phys. Rev. Lett.* **110**, 058303 (2013)
15. Intrinsic curvature determines the crinkled edges of "crenelated disks". C.N. Kaplan, T. Gibaud, R.B. Meyer, *Soft Matter* **9**, 8210 (2013)
14. New routes to food gels and glasses. T. Gibaud, N. Mahmoudi, J. Oberdisse, P. Lindner, J. S. Pedersen, C. L. P. Oliveira, A. Stradner, and P. Schurtenberger, *Faraday Discuss.* **158**, 267 (2012)
13. Self-assembly through chiral control of interfacial tension. T. Gibaud, E. Barry, M. Zakhary, M. Henglin, A. Ward, Y. Yang, C. Berciu, R. Oldenbourg, M. Hagan, D. Nicastro, R. Meyer, Z. Dogic, *Nature* **158**, 267 (2012)
12. Phase separation and dynamical arrest for particles interacting with mixed potentials. T. Gibaud, F. Cardinaux, J. Bergenholtz, A. Stradner, and P. Schurtenberger, *Soft Matter* **7**, 857 (2011)
11. Yielding dynamics of a colloidal gel. T. Gibaud, D. Frelat and S. Manneville, *Soft Matter* **6**, 3482 (2010)
10. Shear-induced fragmentation of Laponite suspensions. T. Gibaud, C. Barentin, N. Taberlet and S. Manneville, *Soft Matter* **5**, 3026 (2009)
9. A closer look at arrested spinodal decomposition in protein systems. T. Gibaud and P. Schurtenberger, *J. Phys. Cond. Mat.* **21**, 32220 (2009)

8. Influence of boundary conditions on the yielding flow of soft glassy material. T. Gibaud C. Barentin, and S. Manneville,
Phys. Rev. Lett. **101**, 258302 (2008)
7. A simple patchy model for the phase behaviour of lysozyme dispersions. C. Gogelein, G. Nagele, R. Tuinier, T. Gibaud, A. Stradner, and P. Schurtenberger,
J. Chem. Phys. **129**, 085102 (2008)
6. Soft Nanotechnology - from Colloid Physics to Nanostructured Functional Materials. H. Dietsch, V. Malik, M. Reufer, A. Shalkevich, M. Saric, T. Gibaud, F. Cardinaux, A. Stradner, P. Schurtenberger,
Chimia **62**, 805 (2008)
5. The interplay between spinodal decomposition and glass formation in proteins exhibiting short range attraction. F. Cardinaux, T. Gibaud, A. Stradner, P. Schurtenberger,
Phys. Rev. Lett. **99**, 118301 (2007)
4. Etude des effets non lineaires observes sur les oscillations d'un pendule simple. T. Gibaud, A. Gibaud,
B.U.P. **891**, 167 (2007)
3. Etude theorique et experimentale de pendules pesants couples : modes normaux de vibration. A. Gibaud, T. Gibaud,
B.U.P. **894**, 577 (2007)
2. Caracterisation experimentale d'un systeme lineaire invariant par translation dans le temps en electronique. T. Gibaud, A. Gibaud ,
B.U.P. **894**, 577 (2007)
1. Vidange d'un reservoir. T. Gibaud, A. Gibaud,
B.U.P. **899**, 1195 (2007)

Invited Conferences

5. Journées des CR1 de l'Institut de chimie du CNRS, CNRS Paris, Fr (2017)
4. Journée émergence, CNRS Paris, Fr (2017)
3. 4th Playing Colloidal Mikado Workshop, Bordeaux, Fr (2016)
2. 9ème JFFoS, Kyoto, Japon (2015)
1. European Conference on Liquid Crystals, Rhodos, Greece (2013)

Talk in Conferences

14. 11th Annual European Rheology Conference, Sorrento, It (2018)
13. Cecam Workshop, Rheology of gel networks: combining experimental, computational and theoretical insights, Lyon, Fr (2017)
12. International Soft Matter Conference, Grenoble, Fr (2016)
11. Stat. Phys., Lyon, Fr (2016)
10. Journées Matière Molle et Sciences des Aliments, Montpellier, Fr (2015)
9. Systèmes anisotropes auto-organisés, Conférence Francaise des Cristaux Liquides, Autran, Fr (2015)
8. 10th Annual European Rheology Conference (2 talks), Nantes, Fr (2015)
7. NanoNano-2015, Workshop Lyonnais sur les Nanosciences et les Nanotechnologies, Lyon, Fr (2015)
6. Les Houches Winter School, Macromolecules in Constrained Environments, Fr (2013)
5. New England Complex Fluids, Brandeis University, USA (2011)
4. MRS fall meeting, Boston, USA, (2010)
3. GDR Mephy, Workshop on localization, shear banding and rupture, ESPCI, Paris, Fr (2008)
2. Workshop on micro and nanoscales flows, Université Claude Bernard, Lyon, Fr (2008)
1. International Congress of Rheology, Monterey, USA (2008)

Poster in Conferences

11. 11th Annual European Rheology Conference, Sorrento, It (2018)
10. Cecam Workshop, Rheology of gel networks: combining experimental, computational and theoretical insights, Lyon, Fr (2017)
9. International Soft Matter Conference (2 posters), Grenoble, Fr (2016)
8. Journées entrants INP, Saint-Pierre-d'Oléron, Fr (2013)
7. Workshop New Mech, MIT, USA (2011)
6. Summer School Dynasoft, Cargèse, Fr (2010)
5. Soft Matter Conference, Aarhen, D (2007)
4. Conference of the European Colloid and Interface Society, Geneva, CH (2007)
3. Workshop, Dynamical arrest of soft matter and colloids, Lugano, CH (2006)
2. Summer School, Scattering methods applied to Soft Matter, Bonbannes, Fr (2006)
1. Summer School, Polyelectrolyte and Colloids, Villars sur Ollon, CH (2004)

Invited Seminars

41. [Université Montpellier 2](#), matière molle (2018)
40. [UJF](#), Laboratoire Rhéologie et Procédés (2016)
39. [UPMC](#), Laboratoire Jean Perrin (2015)
38. [Université Diderot](#), Laboratoire Matière et Systèmes Complexes (2015)
37. [University of Geneva](#), Biochemistry Dpt (2015)
36. [Université Paris Sud](#), Laboratory of Theoretical Physics and Statistical Models (2014)
35. [ESPCI](#), Gulliver (2014)
34. [Università degli Studi di Milano](#), Dep. of Medical Biotechnology and Translational Medicine (2013)
33. [Université de Fribourg](#), Dpt of Physics (2013)
32. [UJF](#), Laboratoire Interdisciplinaire de Physique (2013)
31. [Mahidol University](#), Biophysics (2013)
30. [East China Normal University](#), physics Dpt(2013)
29. [ENS de Lyon](#), Laboratoire de physique (2012)
28. [ENS de Lyon](#), Laboratoire Joliot Curie (2012)
27. [CEA Saclay](#), LIONS (2012)
26. [ESRF](#) (2011)
25. [NYU](#), Center for Soft Matter (2011)
24. [Université Paris Sud](#), Laboratoire de Physique des Solides (2011)
23. [Institut Curie](#) (2011)
22. [ESPCI](#), Séminaire café (2011)
21. [ENS de Lyon](#), Laboratoire de physique (2011)
20. [Brandeis University](#), MRSEC seminar (2010)
19. [CEA Grenoble](#), SPrAM (2010)
18. [Brandeis University](#), Quantitative Biology seminar (2009)
17. [Brandeis University](#), MRSEC seminar (2009)
16. [Université Montpellier 2](#), matière molle (2009)
15. [ENS de Lyon](#), Laboratoire de physique (2008)
14. [Columbia University](#), Dpt of Chemistry (2008)
13. [Yale University](#), Materials Science, USA (2008)
12. [Harvard University](#), Dpt of Chemistry (2008)
11. [Brandeis University](#), Dpt of Physics (2009)
10. [Harvard University](#), Dpt of Physics (2008)
9. [ENS de Lyon](#), Laboratoire de physique (2007)
8. [CEA Grenoble](#), SPrAM (2007)
7. [Institut Charles Sadron](#) (2007)
6. [Université Montpellier 2](#), matière molle (2007)
5. [Université de Fribourg](#), Physics Dpt Day (2006)
4. [EPFL](#), Physics (2006)
3. [University of Aarhus](#), Dpt of Chemistry (2006)
2. [Université de Fribourg](#), Dpt of physics (2004)
1. [Lawrence Berkeley National Lab](#), Avanced Light Source (2002)

9.4 Media coverage

8. [CNRS actualités 2015](#): Les rides hiérarchiques du yaourt
7. [Liquid Crystals Today 24](#), (2015): chiral rafts
6. [CNRS Actualités 2014](#): Comment faire pour que deux gouttes en contact ne fusionnent pas?
5. [Liquid Crystals Today 23](#) (2014): Chiral coalescence
4. [La Recherche 462](#) (2012): Comment changer la forme d'un matériau
3. [Nature 481](#), 268 (2012): A fresh twist for self-assembly
2. [Nature Physics 8](#), 116 (2012): Sleight of handedness
1. [Journal Club for Condensed Matter Physics](#) (2012)

9.5 People

Post-docs

4. [B. Saint-Michel](#) (2015-2018)
 ↳ 2018: Post doc, Imperial College, UK
3. [M. Leocmach](#) (2013-2015)
 ↳ 2015: CNRS researcher, Institut Lumière Matière, Lyon, Fr

2. [A. Modlinska](#) (2013-2014)
 ↳ 2014: assistant professor, Poznan University, Poland
1. [M. Nespoulous](#) (2012-2013)
 ↳ 2013: assistant professor, Aix-Marseille University, Fr

PhD students

3. [N. Dages](#) (2018-...) – co-advised with S. Manneville
2. [M. Zakhary](#) (2009-2014) – co-advised with Z Dogic.
 ↳ 2015: Medical Physics Fellow at Mayo Clinic, Rochester USA
1. [S. Yardimci](#) (2009-2014) – co-advised with Z Dogic.
 ↳ 2015: Senior Scientific Officer at the Francis Crick Institute, London UK

Bachelor/Master students

16. [A. Brossollet](#) from L3 Ens (2018)
15. [N. Dages](#) from M2 Ecole Centrale Lyon (2018)
14. [L. Ahoure](#) from M1 Génie des Procédés, UGA (2018)
13. [L. Auzemery](#) from UPMC and la Sorbonne (2017)
12. [P. H. Delville](#) from ENS de Lyon (2017)
11. [A. Lagarde](#) from école Polytechnique (2016)
10. [G. Jung](#) from ENS de Lyon (2016)
9. [D. Germain](#) from ENS de Lyon (2015)
8. [A. Kumar](#) from National Inst. of Tech. Surat (2013)
7. [S. Goldberg](#) from Brandeis University (2011)
6. [M. Henglin](#) from Williams College (2011)
5. [M. Zakhary](#) from Brandeis University (2009)
4. [S. Yardimci](#) from Brandeis University (2009)
3. [D. Frelat](#) from ENS de Lyon (2008)
2. [F. Guillard](#) from ENS de Lyon (2008)
1. [C. Varghese](#) from Indian Inst. of Tech. Bombay (2007)

9.6 Services

PhD Thesis committee

A. Boire, Sup' Agro, Montpellier, Fr (2013)

Conference organization

CFCL2017 – Colloque sur les systèmes anisotropes auto-organisés, Lyon, Fr (2017)

Board member

Journal editorial board member for Scientific Reports (2017-present)

Referee

~ 5 articles/year for Soft Matter, Scientific Report and PRL

9.7 Teaching and Outreach

University courses taught

9. [Soft Matter – 6h/year lecture](#), Master Sciences de la Matière, ENS de Lyon (2017-present)
8. [Soft interfaces – 8h/year lab course](#), *agrégation de chimie*, ENS de Lyon (2017-present)
7. [Physique expérimentale 1 – 24h/year lab course](#), Bachelor Science de la Matière, ENS de Lyon (2016-present)
6. [Physique expérimentale 2 – 24h/year lab course](#), Bachelor Science de la Matière, ENS de Lyon (2013-present)
5. [Physique des systèmes biologiques – 6h/year lecture](#), Master Science de la Matière, ENS de Lyon (2013-2016)
4. [Bio-Physics – 25h](#), Master of physics, East China Normal University (2014)
3. [Teacher at the *agrégation de physique* – 140h/year](#), ENS de Lyon (2007-2009)
2. [Introduction to physics lab – 70h/year lab course](#), Bachelor of physics, Université de Fribourg (2004-2007)
1. [Classical mechanics – 25h/year exercises](#), Bachelor of physics, Université du Mans (2001)

Conferences

2. [Enseigner la Physique dans le Supérieur 2018](#), Grenoble
1. [Enseigner la physique à l'Université 2015](#), Lyon

Outreach

2. [Setup and enlive physics experiments for children](#) at the Discovery Museums of Acton, Ma, USA (2011) and in a Kindergarden class at Bulle, CH (2007).
1. [co-organized the 2005 Einstein year at the physics dept of the University of Fribourg, CH](#) and for the occasion presented two 45 min Physics shows targetted toward the general public.

9.8 Grants

as Principal Investigator

10. Grand ANR JCJC (2019-2023), 230 k€
9. Grand from Région Auvergne-Rhône-Alpes, co-PI with S. Manneville (2017-2022), 253 k€
8. Grant CNRS Emergence (2016), 10 k€
7. Sponsored fellowship from the French embassy in India and UCBL (2013) for A. Kumar
6. Grant from the Ens de Lyon (2013), 4 k€
5. Grant from the Fédération de recherche A.M. Ampère (2013), 10 k€
4. Grant from the Agence Nationale de la Recherche Francaise (ANR-11-PDOC-027, 2012-2015), 350 k€
3. Marie-Curie collaboration grant with J. Oberdisse, Montpellier (2007), 2 k€
2. Fellowship from the *UPMC* to support my master thesis at *U.C. Berkeley* (2002), 6 k€
1. Fellowship from the French government for my master degree (2001), 4 k€

as Collaborator

2. PI : G. Ovarlez (LOF, Bordeaux, Fr), grant from the ANR (2017-2021), 108 k€
1. PI : M. Leocmach (ILM, Lyon, Fr), grant from the Fédération de recherche A.M. Ampère (2016), 24 k€

VI

Bibliography

Bibliography

- [1] G. M. Whitesides and B. Grzybowski, *Science* **295**, 2418 (2002).
- [2] D. Philp and J. F. Stoddart, *Angewandte Chemie International Edition in English* **35**, 1154 (1996).
- [3] W. B. Rogers, W. M. Shih, and V. N. Manoharan, *Nature Reviews Materials* **1**, 16008 (2016).
- [4] D. Frenkel, *Nature materials* **14**, 9 (2015).
- [5] L. Cademartiri and K. J. Bishop, *Nature materials* **14**, 2 (2015).
- [6] T. Gibaud, *Journal of Physics: Condensed Matter* **29**, 493003 (2017).
- [7] P. W. Majewski and K. G. Yager, *Journal of Physics: Condensed Matter* **28**, 403002 (2016).
- [8] C. J. Drummond and C. Fong, *Current opinion in colloid & interface science* **4**, 449 (1999).
- [9] W. Poon, *Science* **304**, 830 (2004).
- [10] Y. Xia, B. Gates, Y. Yin, and Y. Lu, *Advanced Materials* **12**, 693 (2000).
- [11] S. C. Glotzer, *Science* **306**, 419 (2004).
- [12] S. C. Glotzer and M. J. Solomon, *Nature materials* **6**, 557 (2007).
- [13] D. J. Kraft, J. Groenewold, and W. K. Kegel, *Soft Matter* **5**, 3823 (2009).
- [14] V. N. Manoharan, M. T. Elsesser, and D. J. Pine, *Science* **301**, 483 (2003).
- [15] D. J. Milliron, S. M. Hughes, Y. Cui, L. Manna, J. Li, L.-W. Wang, and A. P. Alivisatos, *Nature* **430**, 190 (2004).
- [16] P. M. Johnson, C. M. van Kats, and A. van Blaaderen, *Langmuir* **21**, 11510 (2005).
- [17] N. Malikova, I. Pastoriza-Santos, M. Schierhorn, N. A. Kotov, and L. M. Liz-Marzán, *Langmuir* **18**, 3694 (2002).
- [18] R. M. Laine, C. Zhang, A. Sellinger, and L. Viculis, *Applied Organometallic Chemistry* **12**, 715 (1998).
- [19] M. Rycenga, J. M. McLellan, and Y. Xia, *Advanced Materials* **20**, 2416 (2008).
- [20] J. N. Israelachvili, *Intermolecular and surface forces* (Academic press, 2011).
- [21] C. Gogelein, G. Nagele, R. Tuinier, T. Gibaud, A. Stradner, and P. Schurtenberger, *J. Chem. Phys.* **8**, 085102 (2008).
- [22] G. van Anders, N. K. Ahmed, R. Smith, M. Engel, and S. C. Glotzer, *ACS Nano* **8**, 931 (2014).
- [23] E. Bianchi, R. Blaak, and C. N. Likos, *Physical Chemistry Chemical Physics* **13**, 6397 (2011).
- [24] A. P. Alivisatos, K. P. Johnsson, X. Peng, T. E. Wilson, *et al.*, *Nature* **382**, 609 (1996).
- [25] C. A. Mirkin, R. L. Letsinger, R. C. Mucic, and J. J. Storhoff, *Nature* **382**, 607 (1996).
- [26] V. T. Milam, A. L. Hiddessen, J. C. Crocker, D. J. Graves, and D. A. Hammer, *Langmuir* **19**, 10317 (2003).
- [27] S. Y. Park, A. K. Lytton-Jean, B. Lee, S. Weigand, G. C. Schatz, and C. A. Mirkin, *Nature* **451**, 553 (2008).
- [28] A. L. Hiddessen, S. D. Rodgers, D. A. Weitz, and D. A. Hammer, *Langmuir* **16**, 9744 (2000).
- [29] G. Zhang, D. Wang, and H. Möhwald, *Nano letters* **5**, 143 (2005).
- [30] S. Sacanna, W. Irvine, P. M. Chaikin, and D. J. Pine, *Nature* **464**, 575 (2010).
- [31] L. Feng, L.-L. Pontani, R. Dreyfus, P. Chaikin, and J. Brujic, *Soft Matter* **9**, 9816 (2013).
- [32] P. Poulin, H. Stark, T. Lubensky, and D. Weitz, *Science* **275**, 1770 (1997).
- [33] N. Geerts and E. Eiser, *Soft Matter* **6**, 4647 (2010).
- [34] R. Dreyfus, M. E. Leunissen, R. Sha, A. V. Tkachenko, N. C. Seeman, D. J. Pine, and P. M. Chaikin, *Physical review letters* **102**, 048301 (2009).
- [35] T. Gibaud, F. Cardinaux, J. Bergenholtz, A. Stradner, and P. Schurtenberger, *Soft Matter* **7**, 857 (2011).
- [36] H. Löwen, *Journal of Physics: Condensed Matter* **13**, R415 (2001).
- [37] J. Lin, W. Zhou, A. Kumbhar, J. Wiemann, J. Fang, E. Carpenter, and C. O'Connor, *Journal of Solid State Chemistry* **159**, 26 (2001).
- [38] V. F. Puentes, K. M. Krishnan, and P. Alivisatos, *Applied Physics Letters* **78**, 2187 (2001).
- [39] M. E. Leunissen, H. R. Vutukuri, and A. van Blaaderen, *Advanced Materials* **21**, 3116 (2009).
- [40] B. Liu, T. H. Besseling, M. Hermes, A. F. Demirörs, A. Imhof, and A. Van Blaaderen, *Nature communications* **5** (2014).
- [41] P. N. Pusey and W. Van Megen, *Nature* **320**, 340 (1986).
- [42] M. Grzelczak, J. Vermant, E. M. Furst, and L. M. Liz-Marzán, *ACS nano* **4**, 3591 (2010).
- [43] Y. Huang, X. Duan, Q. Wei, and C. M. Lieber, *Science* **291**, 630 (2001).
- [44] Y. Xia, Y. Yin, Y. Lu, and J. McLellan, *Advanced Functional Materials* **13**, 907 (2003).

- [45] C. S. Chan, G. De Stasio, S. A. Welch, M. Girasole, B. H. Frazer, M. V. Nesterova, S. Fakra, and J. F. Banfield, *Science* **303**, 1656 (2004).
- [46] B. R. Saunders, N. Laajam, E. Daly, S. Teow, X. Hu, and R. Stepto, *Advances in colloid and interface science* **147**, 251 (2009).
- [47] T. Gibaud, E. Barry, M. J. Zakhary, M. Henglin, A. Ward, Y. Yang, C. Berciu, R. Oldenbourg, M. F. Hagan, D. Nicastro, *et al.*, *Nature* **481**, 348 (2012).
- [48] L. Wan, Q. Chen, J. Liu, X. Yang, J. Huang, L. Li, X. Guo, J. Zhang, and K. Wang, *Biomacromolecules* **17**, 1543 (2016).
- [49] R. Nagpal, in *Proceedings of the first international joint conference on Autonomous agents and multiagent systems: part 1* (ACM, 2002) pp. 418–425.
- [50] D. Salgado-Blanco and C. I. Mendoza, *Soft Matter* **11**, 889 (2015).
- [51] K. Tanaka, G. H. Clever, Y. Takezawa, Y. Yamada, C. Kaul, M. Shionoya, and T. Carell, *Nature nanotechnology* **1**, 190 (2006).
- [52] N. A. Kotov, I. Dekany, J. H. Fendler, *et al.*, *Journal of Physical Chemistry* **99**, 13065 (1995).
- [53] L. Di Michele, F. Varrato, J. Kotar, S. H. Nathan, G. Foffi, and E. Eiser, *Nature communications* **4** (2013).
- [54] W. A. Lopes and H. M. Jaeger, *Nature* **414**, 735 (2001).
- [55] Y. He, T. Ye, M. Su, C. Zhang, A. E. Ribbe, W. Jiang, and C. Mao, *Nature* **452**, 198 (2008).
- [56] J. A. Elemans, A. E. Rowan, and R. J. Nolte, *Journal of Materials Chemistry* **13**, 2661 (2003).
- [57] A. Aggeli, I. A. Nyrkova, M. Bell, R. Harding, L. Carrick, T. C. McLeish, A. N. Semenov, and N. Boden, *Proceedings of the National Academy of Sciences* **98**, 11857 (2001).
- [58] T. Gibaud, N. Mahmoudi, J. Oberdisse, P. Lindner, J. S. Pedersen, C. L. Oliveira, A. Stradner, and P. Schurtenberger, *Faraday Discuss.* **158**, 267 (2012).
- [59] G. Nyström, M. Arcari, and R. Mezzenga, *arXiv preprint arXiv:1704.04936* (2017).
- [60] R. W. Perry, M. C. Holmes-Cerfon, M. P. Brenner, and V. N. Manoharan, *Physical review letters* **114**, 228301 (2015).
- [61] M. Poty, G. Lumay, and N. Vandewalle, *New Journal of Physics* **16**, 023013 (2014).
- [62] J. Fern, J. Lu, and R. Schulman, *ACS nano* **10**, 1836 (2016).
- [63] F. W. Twort, *The Lancet* **186**, 1241 (1915).
- [64] F. d’Herelle, *CR Acad. Sci. Paris* **165**, 373 (1917).
- [65] S. Mc Grath and D. van Sinderen, *Bacteriophage: genetics and molecular biology* (Horizon Scientific Press, 2007).
- [66] K. E. Wommack and R. R. Colwell, *Microbiology and molecular biology reviews* **64**, 69 (2000).
- [67] A. Sulakvelidze, Z. Alavidze, and J. G. Morris, *Antimicrobial agents and chemotherapy* **45**, 649 (2001).
- [68] Z. Dogic, *Frontiers in Microbiology* **7** (2016).
- [69] J. L. Slonczewski and J. W. Foster, *Microbiology: An Evolving Science: Third International Student Edition* (WW Norton & Company, 2013).
- [70] D. A. Marvin, *Nature* **197**, 517 (1963).
- [71] L. A. Day, C. J. Marzee, S. A. Reisberg, and A. Casadevall, *Annual review of biophysics and biophysical chemistry* **17**, 509 (1988).
- [72] J. Sambrook, E. F. Fritsch, and T. Maniatis, *Cold Spring Harbor, NY. VIII. Appendix A. pBIND Vector Sequence (continued) A. pBIND Vector Sequence (continued) B. pBIND Vector Restriction Sites Enzyme# of Sites Location Dra I* **4**, 4877 (1989).
- [73] R. R. Unwin, R. A. Cabanas, T. Yanagishima, T. R. Blower, H. Takahashi, G. P. C. Salmond, J. M. Edwardson, S. Fraden, and E. Eiser, *Phys. Chem. Chem. Phys.* , 8194 (2015).
- [74] M. Baus, L. F. Rull, and J.-P. Ryckaert, *S. Fraden in Observation, prediction and simulation of phase transitions in complex fluids*, Vol. 460 (Springer Science & Business Media, 2012).
- [75] H. N. W. Lekkerkerker, P. Coulon, R. Van Der Haegen, and R. Deblieck, *The Journal of chemical physics* **80**, 3427 (1984).
- [76] K. R. Purdy and S. Fraden, *Physical Review E* **70**, 061703 (2004).
- [77] E. Barry, D. Beller, and Z. Dogic, *Soft Matter* **5**, 2563 (2009).
- [78] P. Sharma, A. Ward, T. Gibaud, M. F. Hagan, and Z. Dogic, *Nature* **513**, 77 (2014).
- [79] K. Zimmermann, H. Hagedorn, C. C. Heuck, M. Hinrichsen, and H. Ludwig, *Journal of Biological Chemistry* **261**, 1653 (1986).
- [80] J. Newman, H. L. Swinney, and L. A. Day, *Journal of molecular biology* **116**, 593 (1977).
- [81] S. Bhattacharjee, M. Glucksman, and L. Makowski, *Biophysical journal* **61**, 725 (1992).
- [82] L. Onsager, *Annals of the New York Academy of Sciences* **51**, 627 (1949).
- [83] D. Frenkel, *Journal of Physics: Condensed Matter* **6**, A71 (1994).

-
- [84] Z. Dogic, P. Sharma, and M. J. Zakhary, *Annu. Rev. Condens. Matter Phys.* **5**, 137 (2014).
- [85] Z. Dogic and S. Fraden, *Langmuir* **16**, 7820 (2000).
- [86] Z. Dogic and S. Fraden, *Current opinion in colloid & interface science* **11**, 47 (2006).
- [87] E. Grelet and S. Fraden, *Physical review letters* **90**, 198302 (2003).
- [88] F. Tombolato, A. Ferrarini, and E. Grelet, *Physical review letters* **96**, 258302 (2006).
- [89] S. Dussi, S. Belli, R. van Roij, and M. Dijkstra, *The Journal of chemical physics* **142**, 074905 (2015).
- [90] J. Maguire, J.-P. McTague, and F. Rondelez, *Physical Review Letters* **45**, 1891 (1980).
- [91] L. Alvarez, M. P. Lettinga, and E. Grelet, *arXiv preprint arXiv:1703.06474* (2017).
- [92] Z. Dogic and S. Fraden, *Philosophical Transactions of the Royal Society of London A: Mathematical, Physical and Engineering Sciences* **359**, 997 (2001).
- [93] K. R. Purdy and S. Fraden, *Physical Review E* **76**, 011705 (2007).
- [94] R. Herrmann, K. Neugebauer, E. Pirkl, H. Zentgraf, and H. Schaller, *Molecular and General Genetics MGG* **177**, 231 (1980).
- [95] L. Specthrie, E. Bullitt, K. Horiuchi, P. Model, M. Russel, and L. Makowski, *Journal of molecular biology* **228**, 720 (1992).
- [96] A. N. Marchi, I. Saaem, B. N. Vogen, S. Brown, and T. H. LaBean, *Nano letters* **14**, 5740 (2014).
- [97] S. Brown, J. Majikes, A. Martínez, T. Girón, H. Fennell, E. Samano, and T. LaBean, *Nanoscale* **7**, 16621 (2015).
- [98] S. Sattar, N. J. Bennett, W. X. Wen, J. M. Guthrie, L. F. Blackwell, J. F. Conway, and J. Rakonjac, *Frontiers in microbiology* **6** (2015).
- [99] K. Zimmerman, H. Hagedorn, C. Heuck, M. Hinrichsen, and H. Ludwig, *J Biol Chem* **261**, 1653 (1986).
- [100] E. Grelet and R. Rana, *Soft matter* **12**, 4621 (2016).
- [101] E. Pouget and E. Grelet, *Langmuir* **29**, 8010 (2013).
- [102] Z. Zhang, N. Krishna, M. P. Lettinga, J. Vermant, and E. Grelet, *Langmuir* **25**, 2437 (2009).
- [103] Z. Ruff, S. H. Nathan, R. R. Unwin, M. Zupkauskas, D. Joshi, G. P. Salmond, C. P. Grey, and E. Eiser, *Faraday discussions* **186**, 473 (2016).
- [104] D. Montalvan-Sorrosa, J. González-Solis, J. Mas-Oliva, and R. Castillo, *RSC Advances* **4**, 57329 (2014).
- [105] K. Szot-Karpinska, P. Golec, A. Lesniewski, B. Palys, F. Marken, J. Niedziolka-Jonsson, G. Wgrzyn, and M. Los, *Bioconjugate Chemistry* (2016).
- [106] Z. Zhang and E. Grelet, *Soft Matter* **9**, 1015 (2013).
- [107] G. Abramov, R. Shaharabani, O. Morag, R. Avinery, A. Haimovich, I. Oz, R. Beck, and A. Goldbourt, *Biomacromolecules* (2017).
- [108] D. Marvin, R. Hale, C. Nave, and M. H. Citterich, *Journal of molecular biology* **235**, 260 (1994).
- [109] D. H. Rowitch, G. J. Hunter, and R. N. Perham, *Journal of molecular biology* **204**, 663 (1988).
- [110] G. J. Hunter, D. H. Rowitch, and R. N. Perham, *Nature* **327**, 252 (1987).
- [111] S. R. Whaley, D. S. English, E. L. Hu, P. F. Barbara, and A. M. Belcher, *Nature* **405**, 665 (2000).
- [112] S.-W. Lee, C. Mao, C. E. Flynn, and A. M. Belcher, *Science* **296**, 892 (2002).
- [113] F. Huang, K. Addas, A. Ward, N. Flynn, E. Velasco, M. Hagan, Z. Dogic, and S. Fraden, *Physical review letters* **102**, 108302 (2009).
- [114] K. T. Nam, B. R. Peelle, S.-W. Lee, and A. M. Belcher, *Nano letters* **4**, 23 (2004).
- [115] S. Asakura and F. Oosawa, *The Journal of Chemical Physics* **22**, 1255 (1954).
- [116] A. Matsuyama and T. Kato, *The European Physical Journal E: Soft Matter and Biological Physics* **6**, 15 (2001).
- [117] Z. Dogic, K. R. Purdy, E. Grelet, M. Adams, and S. Fraden, *Phys. Rev. E* **69**, 051702 (2004).
- [118] I. Ichinose, K. Kurashima, and T. Kunitake, *Journal of the American Chemical Society* **126**, 7162 (2004), PMID: 15186138.
- [119] P. Davidson, *Comptes Rendus Chimie* **13**, 142 (2010).
- [120] A. Kaznacheev, M. Bogdanov, and S. Taraskin, *Journal of Experimental and Theoretical Physics* **95**, 57 (2002).
- [121] L. Tortora and O. D. Lavrentovich, *Proceedings of the National Academy of Sciences* **108**, 5163 (2011).
- [122] J. Jeong, Z. S. Davidson, P. J. Collings, T. C. Lubensky, and A. Yodh, *Proceedings of the National Academy of Sciences* **111**, 1742 (2014).
- [123] T. J. Bunning, L. V. Natarajan, V. P. Tondiglia, and R. Sutherland, *Annual Review of Materials Science* **30**, 83 (2000).
- [124] J. D. Joannopoulos, S. G. Johnson, J. N. Winn, and R. D. Meade, *Photonic crystals: molding the flow of light* (Princeton university press, 2011).
- [125] A. Modlińska, A. M. Alsayed, and T. Gibaud, *Scientific reports* **5** (2015).
- [126] T. Still, K. Chen, A. M. Alsayed, K. B. Aptowicz, and A. Yodh, *Journal of colloid and interface science*

- 405, 96 (2013).
- [127] P. R. ten Wolde and D. Frenkel, *Science* **277**, 1975 (1997).
- [128] E. Barry and Z. Dogic, *Proceedings of the National Academy of Sciences* **107**, 10348 (2010).
- [129] J. Nagle and H. Scott, *Biochimica et Biophysica Acta (BBA)-Biomembranes* **513**, 236 (1978).
- [130] D. Needham and R. S. Nunn, *Biophysical journal* **58**, 997 (1990).
- [131] E. Evans and W. Rawicz, *Physical Review Letters* **64**, 2094 (1990).
- [132] E. Evans and D. Needham, *J. phys. Chem* **91**, 4219 (1987).
- [133] W. Rawicz, K. Olbrich, T. McIntosh, D. Needham, and E. Evans, *Biophysical journal* **79**, 328 (2000).
- [134] W. Helfrich, *Zeitschrift für Naturforschung A* **33**, 305 (1978).
- [135] R. Goetz, G. Gompper, and R. Lipowsky, *Physical Review Letters* **82**, 221 (1999).
- [136] J. Israelachvili and H. Wennerstrom, *Nature* **379**, 219 (1996).
- [137] R. Lipowsky and S. Grotehans, *Europhysics Letters* **23**, 599 (1993).
- [138] T. Gibaud and D. Constantin, *The journal of physical chemistry letters* **9**, 4302 (2018).
- [139] A. J. Balchunas, R. A. Cabanas, M. J. Zakhary, T. Gibaud, P. Sharma, M. H. Hagan, S. Fraden, and Z. Dogic, in preparation (2018).
- [140] Y. Yang, E. Barry, Z. Dogic, and M. F. Hagan, *Soft Matter* **8**, 707 (2012).
- [141] A. Marchand, J. H. Weijs, J. H. Snoeijer, and B. Andreotti, *American Journal of Physics* **79**, 999 (2011).
- [142] R. Oldenbourg and G. Mei, *Journal of microscopy* **180**, 140 (1995).
- [143] D. N. Mastrorarde, *Journal of structural biology* **152**, 36 (2005).
- [144] J. R. Kremer, D. N. Mastrorarde, and J. R. McIntosh, *Journal of structural biology* **116**, 71 (1996).
- [145] R. Oldenbourg, *Journal of microscopy* **231**, 419 (2008).
- [146] L. L. Jia, M. J. Zakhary, Z. Dogic, R. A. Pelcovits, and T. R. Powers, arXiv preprint arXiv:1612.03244 (2016).
- [147] L. Kang, T. Gibaud, Z. Dogic, and T. Lubensky, *Soft matter* **12**, 386 (2016).
- [148] C. Fradin, A. Braslau, D. Luzet, D. Smilgies, M. Alba, N. Boudet, K. Mecke, and J. Daillant, *Nature* **403**, 871 (2000).
- [149] S. A. Safran, *Statistical thermodynamics of surfaces, interfaces, and membranes*, Vol. 90 (Perseus Books, 1994).
- [150] D. G. Aarts, M. Schmidt, and H. N. Lekkerkerker, *Science* **304**, 847 (2004).
- [151] P. G. de Gennes, *Solid State Communications* **10**, 753 (1972).
- [152] S. R. Renn and T. C. Lubensky, *Physical Review A* **38**, 2132 (1988).
- [153] R. D. Kamien and J. V. Selinger, *Journal of Physics: Condensed Matter* **13**, R1 (2001).
- [154] L. Hough, H.-T. Jung, D. Krüerke, M. Heberling, M. Nakata, C. Jones, D. Chen, D. R. Link, J. Zasadzinski, G. Heppke, *et al.*, *Science* **325**, 456 (2009).
- [155] W. Helfrich and J. Prost, *Physical Review A* **38**, 3065 (1988).
- [156] E. Efrati and W. T. Irvine, *Physical Review X* **4**, 011003 (2014).
- [157] Y. V. Zastavker, N. Asherie, A. Lomakin, J. Pande, J. M. Donovan, J. M. Schnur, and G. B. Benedek, *Proceedings of the National Academy of Sciences* **96**, 7883 (1999).
- [158] E. A. Matsumoto, G. P. Alexander, and R. D. Kamien, *Physical review letters* **103**, 257804 (2009).
- [159] D. M. Marini, W. Hwang, D. A. Lauffenburger, S. Zhang, and R. D. Kamm, *Nano Letters* **2**, 295 (2002).
- [160] S. Zhang, D. M. Marini, W. Hwang, and S. Santoso, *Current opinion in chemical biology* **6**, 865 (2002).
- [161] S. Srivastava, A. Santos, K. Critchley, K.-S. Kim, P. Podsiadlo, K. Sun, J. Lee, C. Xu, G. D. Lilly, S. C. Glotzer, *et al.*, *Science* **327**, 1355 (2010).
- [162] H. A. Lashuel, S. R. LaBrenz, L. Woo, L. C. Serpell, and J. W. Kelly, *Journal of the American Chemical Society* **122**, 5262 (2000).
- [163] M. J. Zakhary, *The influence of the membrane-polymer interface on colloidal membrane dynamics and phase behavior* (Brandeis University, 2014).
- [164] D. G. Aarts, H. N. Lekkerkerker, H. Guo, G. H. Wegdam, and D. Bonn, *Physical review letters* **95**, 164503 (2005).
- [165] D. G. Aarts and H. N. Lekkerkerker, *Journal of fluid mechanics* **606**, 275 (2008).
- [166] J. D. Paulsen, J. C. Burton, S. R. Nagel, S. Appathurai, M. T. Harris, and O. A. Basaran, *Proceedings of the National Academy of Sciences* **109**, 6857 (2012).
- [167] J. D. Paulsen, J. C. Burton, and S. R. Nagel, *Physical Review Letters* **106**, 114501 (2011).
- [168] U. Sundararaj, C. Macosko, *et al.*, *Macromolecules* **28**, 2647 (1995).
- [169] J.-C. Loudet, P. Barois, and P. Poulin, *Nature* **407**, 611 (2000).
- [170] L. V. Chernomordik and M. M. Kozlov, *Nature structural & molecular biology* **15**, 675 (2008).
- [171] C. K. Haluska, K. A. Riske, V. Marchi-Artzner, J.-M. Lehn, R. Lipowsky, and R. Dimova, *Proceedings of the National Academy of Sciences* **103**, 15841 (2006).

- [172] R. Jahn and T. C. Südhof, *Annual review of biochemistry* **68**, 863 (1999).
- [173] J. C. Shillcock and R. Lipowsky, *Nature materials* **4**, 225 (2005).
- [174] M. Terrones, H. Terrones, F. Banhart, J.-C. Charlier, and P. Ajayan, *Science* **288**, 1226 (2000).
- [175] J. Goodby, A. Slaney, C. Booth, I. Nishiyama, J. Vuijk, P. Styring, and K. Toyne, *Molecular Crystals and Liquid Crystals* **243**, 231 (1994).
- [176] M. J. Zakhary, T. Gibaud, C. N. Kaplan, E. Barry, R. Oldenbourg, R. B. Meyer, and Z. Dogic, *Nature communications* **5**, 3063 (2014).
- [177] T. Gibaud, C. N. Kaplan, P. Sharma, M. J. Zakhary, A. Ward, R. Oldenbourg, R. B. Meyer, R. D. Kamien, T. R. Powers, and Z. Dogic, *Proceedings of the National Academy of Sciences*, 201617043 (2017).
- [178] M. Suntharalingam and S. R. Wenthe, *Developmental cell* **4**, 775 (2003).
- [179] E. J. Tran and S. R. Wenthe, *Cell* **125**, 1041 (2006).
- [180] P. J. Ackerman, Z. Qi, Y. Lin, C. W. Twombly, M. J. Laviada, Y. Lansac, and I. I. Smalyukh, *Scientific reports* **2**, 414 (2012).
- [181] A. Honglawan, D. A. Beller, M. Cavallaro, R. D. Kamien, K. J. Stebe, and S. Yang, *Proceedings of the National Academy of Sciences* **110**, 34 (2013).
- [182] D. K. Yoon, M. Choi, Y. H. Kim, M. W. Kim, O. D. Lavrentovich, and H.-T. Jung, *Nature materials* **6**, 866 (2007).
- [183] U. Tkalec, M. Ravnik, S. Čopar, S. Žumer, and I. Muševič, *Science* **333**, 62 (2011).
- [184] R. E. Goldstein, H. K. Moffatt, A. I. Pesci, and R. L. Ricca, *Proceedings of the National Academy of Sciences* **107**, 21979 (2010).
- [185] J.-i. Fukuda and S. Žumer, *Nature communications* **2**, 246 (2011).
- [186] S. Mühlbauer, B. Binz, F. Jonietz, C. Pfeleiderer, A. Rosch, A. Neubauer, R. Georgii, and P. Böni, *Science* **323**, 915 (2009).
- [187] L. Brey, H. Fertig, R. Côté, and A. MacDonald, *Physical review letters* **75**, 2562 (1995).
- [188] A. Tonomura, X. Yu, K. Yanagisawa, T. Matsuda, Y. Onose, N. Kanazawa, H. S. Park, and Y. Tokura, *Nano letters* **12**, 1673 (2012).
- [189] M. Ravnik, G. P. Alexander, J. M. Yeomans, and S. Žumer, *Proceedings of the National Academy of Sciences* **108**, 5188 (2011).
- [190] T. H. R. Skyrme, *Nuclear Physics* **31**, 556 (1962).
- [191] N. Nagaosa and Y. Tokura, *Nature nanotechnology* **8**, 899 (2013).
- [192] S. Grigoriev, V. Dyadkin, D. Menzel, J. Schoenes, Y. O. Chetverikov, A. Okorokov, H. Eckerlebe, and S. Maleyev, *Physical Review B* **76**, 224424 (2007).
- [193] S. Grigoriev, D. Chernyshov, V. Dyadkin, V. Dmitriev, S. Maleyev, E. Moskvina, D. Menzel, J. Schoenes, and H. Eckerlebe, *Physical Review Letters* **102**, 037204 (2009).
- [194] X. Yu, Y. Onose, N. Kanazawa, J. Park, J. Han, Y. Matsui, N. Nagaosa, and Y. Tokura, *Nature* **465**, 901 (2010).
- [195] A. Bogdanov, U. Röbner, and A. Shestakov, *Physical Review E* **67**, 016602 (2003).
- [196] P. J. Ackerman, R. P. Trivedi, B. Senyuk, J. van de Lagemaat, and I. I. Smalyukh, *Physical Review E* **90**, 012505 (2014).
- [197] I. I. Smalyukh, Y. Lansac, N. A. Clark, and R. P. Trivedi, *Nature materials* **9**, 139 (2010).
- [198] R. Hornreich and S. Shtrikman, *Liquid Crystals* **5**, 777 (1989).
- [199] G. Heppke, B. Jerome, H. Kitzerow, and P. Pieranski, *Liquid Crystals* **5**, 813 (1989).
- [200] H. Tu and R. A. Pelcovits, *Physical Review E* **87**, 032504 (2013).
- [201] C. N. Kaplan, T. Gibaud, and R. B. Meyer, *Soft Matter* **9**, 8210 (2013).
- [202] M. Hu, J. J. Briguglio, and M. Deserno, *Biophysical journal* **102**, 1403 (2012).
- [203] D. P. Siegel and M. Kozlov, *Biophysical journal* **87**, 366 (2004).
- [204] S. Semrau, T. Idema, L. Holtzer, T. Schmidt, and C. Storm, *Physical review letters* **100**, 088101 (2008).
- [205] T. Baumgart, S. Das, W. Webb, and J. Jenkins, *Biophysical journal* **89**, 1067 (2005).
- [206] E. Cerda and L. Mahadevan, *Physical review letters* **90**, 074302 (2003).
- [207] M. Leocmach, M. Nespoulous, S. Manneville, and T. Gibaud, *Science advances* **1**, e1500608 (2015).
- [208] H. King, R. D. Schroll, B. Davidovitch, and N. Menon, *Proceedings of the National Academy of Sciences* **109**, 9716 (2012).
- [209] L. Pocivavsek, R. Dellsy, A. Kern, S. Johnson, B. Lin, K. Y. C. Lee, and E. Cerda, *Science* **320**, 912 (2008).
- [210] L. Kang and T. C. Lubensky, *Proceedings of the National Academy of Sciences* **114**, E19 (2017).
- [211] A. Stradner, H. Sedgwick, F. Cardinaux, W. C. Poon, S. U. Egelhaaf, and P. Schurtenberger, *Nature* **432**, 492 (2004).
- [212] P. Segre, V. Prasad, A. Schofield, and D. Weitz, *Physical Review Letters* **86**, 6042 (2001).

- [213] J. Groenewold and W. K. Kegel, *The Journal of Physical Chemistry B* **105**, 11702 (2001).
- [214] D. Lingwood and K. Simons, *science* **327**, 46 (2010).
- [215] K. Simons and W. L. Vaz, *Annu. Rev. Biophys. Biomol. Struct.* **33**, 269 (2004).
- [216] J. F. Hancock, *Nature Reviews Molecular Cell Biology* **7**, 456 (2006).
- [217] R. W. Klemm, C. S. Ejsing, M. A. Surma, H.-J. Kaiser, M. J. Gerl, J. L. Sampaio, Q. de Robillard, C. Ferguson, T. J. Proszynski, A. Shevchenko, *et al.*, *The Journal of cell biology* **185**, 601 (2009).
- [218] K. Simons and D. Toomre, *Nature reviews Molecular cell biology* **1**, 31 (2000).
- [219] B. Brügger, B. Glass, P. Haberkant, I. Leibrecht, F. T. Wieland, and H.-G. Kräusslich, *Proceedings of the National Academy of Sciences of the United States of America* **103**, 2641 (2006).
- [220] S. Schuck and K. Simons, *Journal of cell science* **117**, 5955 (2004).
- [221] C. Dietrich, L. Bagatolli, Z. Volovyk, N. Thompson, M. Levi, K. Jacobson, and E. Gratton, *Biophysical journal* **80**, 1417 (2001).
- [222] S. L. Veatch and S. L. Keller, *Physical Review Letters* **89**, 268101 (2002).
- [223] T. Baumgart, S. T. Hess, and W. W. Webb, *Nature* **425**, 821 (2003).
- [224] E. Barry, Z. Dogic, R. B. Meyer, R. A. Pelcovits, and R. Oldenbourg, *The journal of physical chemistry. B* **113**, 3910 (2009).
- [225] C. N. Kaplan, H. Tu, R. A. Pelcovits, and R. B. Meyer, *Physical Review E* **82**, 021701 (2010).
- [226] C. N. Kaplan and R. B. Meyer, *Soft Matter*, DOI (2014).
- [227] R. Sakhardande, S. Stanojeviea, A. Baskaran, A. Baskaran, M. F. Hagan, and B. Chakraborty, *arXiv preprint arXiv:1604.03012* (2016).
- [228] S. Xie, M. F. Hagan, and R. A. Pelcovits, *Physical Review E* **93**, 032706 (2016).
- [229] H. Tu and R. A. Pelcovits, *Physical Review E* **87**, 042505 (2013).
- [230] F. Rohwer, *Cell* **113**, 141 (2003).
- [231] G. Koenderink, G. Vliegthart, S. Kluijtmans, A. Van Blaaderen, A. Philipse, and H. Lekkerkerker, *Langmuir* **15**, 4693 (1999).
- [232] L. Carbone, C. Nobile, M. De Giorgi, F. D. Sala, G. Morello, P. Pompa, M. Hytch, E. Snoeck, A. Fiore, I. R. Franchini, *et al.*, *Nano letters* **7**, 2942 (2007).
- [233] C. Querner, M. D. Fischbein, P. A. Heiney, and M. Drndić, *Advanced Materials* **20**, 2308 (2008).
- [234] A. Kuijk, A. Imhof, M. H. Verkuijlen, T. H. Besseling, E. R. van Eck, and A. van Blaaderen, *Particle & Particle Systems Characterization* **31**, 706 (2014).
- [235] J. C. Zhou, C. M. Soto, M.-S. Chen, M. A. Bruckman, M. H. Moore, E. Barry, B. R. Ratna, P. E. Pehrsson, B. R. Spies, and T. S. Confer, *Journal of nanobiotechnology* **10**, 1 (2012).
- [236] C. Mao, A. Liu, and B. Cao, *Angewandte Chemie International Edition* **48**, 6790 (2009).
- [237] H. E. Jin, W. J. Chung, M. Sena, A. Merzlyak, and S. W. Lee, *Virotronics: Viruses as Tools for Functional Nanomaterials Design. Comprehensive Biomaterials II, 2nd edition* (Elsevier, 2016).
- [238] R. Farr, D. S. Choi, and S.-W. Lee, *Acta biomaterialia* **10**, 1741 (2014).
- [239] S. H. Yang, W.-J. Chung, S. McFarland, and S.-W. Lee, *The Chemical Record* **13**, 43 (2013).
- [240] A. Merzlyak, S. Indrakanti, and S.-W. Lee, *Nano letters* **9**, 846 (2009).
- [241] J.-W. Oh, W.-J. Chung, K. Heo, H.-E. Jin, B. Y. Lee, E. Wang, C. Zueger, W. Wong, J. Meyer, C. Kim, *et al.*, *Nature communications* **5** (2014).
- [242] X. Dang, H. Yi, M.-H. Ham, J. Qi, D. S. Yun, R. Ladewski, M. S. Strano, P. T. Hammond, and A. M. Belcher, *Nature Nanotechnology* **6**, 377 (2011).
- [243] C.-Y. Chiang, J. Epstein, A. Brown, J. N. Munday, J. N. Culver, and S. Ehrman, *Nano letters* **12**, 6005 (2012).
- [244] K. T. Nam, D.-W. Kim, P. J. Yoo, C.-Y. Chiang, N. Meethong, P. T. Hammond, Y.-M. Chiang, and A. M. Belcher, *science* **312**, 885 (2006).
- [245] Y. J. Lee, H. Yi, W.-J. Kim, K. Kang, D. S. Yun, M. S. Strano, G. Ceder, and A. M. Belcher, *Science* **324**, 1051 (2009).
- [246] E. Royston, A. Ghosh, P. Kofinas, M. T. Harris, and J. N. Culver, *Langmuir* **24**, 906 (2008).
- [247] F. Cardinaux, T. Gibaud, A. Stradner, and P. Schurtenberger, *Physical Review Letters* **99**, 118301 (2007).
- [248] B. Saint-Michel, T. Gibaud, and S. Manneville, *Soft Matter* **13**, 2643 (2017).
- [249] T. Gibaud, C. Perge, S. B. Lindstrom, N. Taberlet, and S. Manneville, *Soft Matter* **12**, 1701 (2016).
- [250] B. Saint-Michel, T. Gibaud, and S. Manneville, *Phys. Rev. X* **8**, 031006 (2018).
- [251] G. de Oliveira Reis, T. Gibaud, B. Saint Michel, S. Manneville, M. Leocmach, L. Vaysse, F. Bonfils, C. Sanchez, and P. Menut, *Journal of Colloid and Interface Science* (2018).
- [252] P. Lidon and al., in preparation (2018).
- [253] S. Suresh, *Fatigue of materials* (Cambridge university press, 1998).
- [254] S. Bhat and R. Patibandla, EV Morales (2011).

- [255] T. Erdmann and U. Schwarz, *Physical review letters* **92**, 108102 (2004).
- [256] N. Thompson, N. Wadsworth, and N. Louat, *Philosophical Magazine* **1**, 113 (1956).
- [257] N. E. Frost, K. J. Marsh, and L. P. Pook, *Metal fatigue* (Courier Corporation, 1974).
- [258] Y. Murakami, *Metal fatigue: effects of small defects and nonmetallic inclusions* (Elsevier, 2002).
- [259] A. A. Griffith, *Philosophical transactions of the royal society of london. Series A, containing papers of a mathematical or physical character* **221**, 163 (1921).
- [260] P. C. Paris and F. Erdogan (ASME, 1963).
- [261] H. A. Barnes, *Journal of Non-Newtonian Fluid Mechanics* **81**, 133 (1999).
- [262] Q. Nguyen and D. Boger, *Annual Review of Fluid Mechanics* **24**, 47 (1992).
- [263] P. C. Møller, J. Mewis, and D. Bonn, *Soft matter* **2**, 274 (2006).
- [264] D. Bonn, J. Paredes, M. M. Denn, L. Berthier, T. Divoux, and S. Manneville, arXiv preprint arXiv:1502.05281 (2015).
- [265] T. Divoux, D. Tamarii, C. Barentin, S. Teitel, and S. Manneville, *Soft Matter* **8**, 4151 (2012).
- [266] V. Gopalakrishnan and C. Zukoski, *Journal of Rheology* **51**, 623 (2007).
- [267] J. Sprakel, S. B. Lindström, T. E. Kodger, and D. A. Weitz, *Physical review letters* **106**, 248303 (2011).
- [268] S. B. Lindström, T. E. Kodger, J. Sprakel, and D. A. Weitz, *Soft Matter* **8**, 3657 (2012).
- [269] C. Allain, M. Cloitre, and M. Wafra, *Physical review letters* **74**, 1478 (1995).
- [270] L. Starrs, W. Poon, D. Hibberd, and M. Robins, *Journal of Physics: Condensed Matter* **14**, 2485 (2002).
- [271] P. Bartlett, L. J. Teece, and M. A. Faers, *Physical Review E* **85**, 021404 (2012).
- [272] S. Buzzaccaro, E. Secchi, G. Brambilla, R. Piazza, and L. Cipelletti, *Journal of Physics: Condensed Matter* **24**, 284103 (2012).
- [273] S. Manley, J. Skotheim, L. Mahadevan, and D. A. Weitz, *Physical review letters* **94**, 218302 (2005).
- [274] T. Gibaud, D. Frelat, and S. Manneville, *Soft Matter* **6**, 3482 (2010).
- [275] V. Grenard, T. Divoux, N. Taberlet, and S. Manneville, *Soft Matter* **10**, 1555 (2014).
- [276] T. Brenner, S. Matsukawa, K. Nishinari, and R. Johannsson, *Journal of Non-Newtonian Fluid Mechanics* **196**, 1 (2013).
- [277] V. Trappe and D. Weitz, *Physical review letters* **85**, 449 (2000).
- [278] J.-B. Donnet, *Carbon black: science and technology* (CRC Press, 1993).
- [279] V. Trappe, E. Pitard, L. Ramos, A. Robert, H. Bissig, and L. Cipelletti, *Physical Review E* **76**, 051404 (2007).
- [280] O. Basquin, in *Proc Astm*, Vol. 10 (1910) pp. 625–630.
- [281] F. Kun, H. Carmona, J. Andrade Jr, and H. Herrmann, *Physical review letters* **100**, 094301 (2008).
- [282] O. W. Eshbach and B. D. Tapley, *Eshbach's handbook of engineering fundamentals* (John Wiley & Sons, 1990).
- [283] T. Gibaud, C. Perge, S. B. Lindstrom, N. Taberlet, and S. Manneville, *Soft Matter* **12**, 1701 (2016).
- [284] C. Perge, N. Taberlet, T. Gibaud, and S. Manneville, *Journal of Rheology* **58**, 1331 (2014).
- [285] P. Coussot, J. S. Raynaud, F. Bertrand, P. Moucheron, J. P. Guilbaud, H. T. Huynh, S. Jarny, and D. Lesueur, *Phys. Rev. Lett.* **88**, 218301 (2002).
- [286] P. C. F. Moller, J. Mewis, and D. Bonn, *Soft Matter* **2**, 274 (2006).
- [287] T. Gibaud, C. Barentin, and S. Manneville, *Phys. Rev. Lett.* **101**, 258302 (2008).
- [288] T. Gibaud, C. Barentin, N. Taberlet, and S. Manneville, *Soft Matter* **5**, 3026 (2009).
- [289] T. Gibaud, D. Frelat, and S. Manneville, *Soft Matter* **6**, 3482 (2010).
- [290] T. Divoux, D. Tamarii, C. Barentin, S. Teitel, and S. Manneville, *Soft Matter* **8**, 4151 (2012).
- [291] C. Perge, N. Taberlet, T. Gibaud, and S. Manneville, *J. Rheol.* **58**, 1331 (2014).
- [292] R. Besseling, E. R. Weeks, A. B. Schofield, and W. C. K. Poon, *Phys. Rev. Lett.* **99**, 028301 (2007).
- [293] C. Gilbreth, S. Sullivan, and M. Dennin, *Phys. Rev. E* **74**, 051406 (2006).
- [294] A. Kabla, J. Scheibert, and G. Debregeas, *J. Fluid Mech.* **587**, 45 (2007).
- [295] S. A. Rogers, D. Vlassopoulos, and P. T. Callaghan, *Phys. Rev. Lett.* **100**, 128304 (2008).
- [296] L. Bécu, S. Manneville, and A. Colin, *Phys. Rev. Lett.* **96**, 138302 (2006).
- [297] J. Goyon, A. Colin, G. Ovarlez, A. Ajdari, and L. Bocquet, *Nature* **454**, 84 (2008).
- [298] E. D. Knowlton, D. J. Pine, and L. Cipelletti, *Soft Matter* **10**, 6931 (2014).
- [299] N. J. Balmforth, I. A. Frigaard, and G. Ovarlez, *Annual Review of Fluid Mechanics* **46**, 121 (2014).
- [300] D. Bonn, M. M. Denn, L. Berthier, T. Divoux, and S. Manneville, arXiv:1502.05281 (2015).
- [301] A. S. Szczesniak, *Food Qual. Prefer.* **13**, 215 (2002).
- [302] P. Fischer and E. J. Windhab, *Curr. Opin. Colloid Interface Sci.* **16**, 36 (2011).
- [303] K. Guevorkian, D. Gonzalez-Rodriguez, C. Carlier, S. Dufour, and F. Brochard-Wyart, *Proc. Natl. Acad. Sci. U.S.A.* **108**, 13387 (2011).

- [304] T. Baumberger, C. Caroli, and D. Martina, *Nat. Mater.* **5**, 552 (2006).
- [305] B. Mao, T. Divoux, and P. Snabre, *J. Rheol.* **60**, 473 (2016).
- [306] M. Leocmach, C. Perge, T. Divoux, and S. Manneville, *Phys. Rev. Lett.* **113**, 038303 (2014).
- [307] J. Lin, E. Lerner, A. Rosso, and M. Wyart, *Proc. Natl. Acad. Sci. U.S.A.* **111**, 14382 (2014).
- [308] A. Amon, A. Bruand, J. Crassous, E. Clément, *et al.*, *Phys. Rev. Lett.* **108**, 135502 (2012).
- [309] A. Le Bouil, A. Amon, S. McNamara, and J. Crassous, *Phys. Rev. Lett.* **112**, 246001 (2014).
- [310] K. A. Dahmen, Y. Ben-Zion, and J. T. Uhl, *Nat. Phys.* **7**, 554 (2011).
- [311] M. P. Lettinga and S. Manneville, *Phys. Rev. Lett.* **103**, 248302 (2009).
- [312] S. P. Meeker, R. T. Bonnecaze, and M. Cloitre, *Phys. Rev. Lett.* **92**, 198302 (2004).
- [313] P. Ballesta, G. Petekidis, L. Isa, W. C. K. Poon, and R. Besseling, *J. Rheol.* **56**, 1005 (2012).
- [314] J. R. Seth, C. Locatelli-Champagne, F. Monti, R. T. Bonnecaze, and M. Cloitre, *Soft Matter* **8**, 140 (2012).
- [315] T. Divoux, V. Lapeyre, V. Ravaine, and S. Manneville, *Phys. Rev. E* **92**, 060301 (2015).
- [316] T. Divoux, D. Tamarii, C. Barentin, and S. Manneville, *Phys. Rev. Lett.* **104**, 208301 (2010).
- [317] D. Bonn, H. Kellay, M. Prochnow, K. Ben-Djemaa, and J. Meunier, *Science* **280**, 265 (1998).
- [318] A. Guarino, S. Ciliberto, A. Garcimartín, M. Zei, and R. Scorretti, *Eur. Phys. J. B* **26**, 141 (2002).
- [319] L. Salminen, A. Tolvanen, and M. J. Alava, *Phys. Rev. Lett.* **89**, 185503 (2002).
- [320] J. Rosti, J. Koivisto, L. Laurson, and M. J. Alava, *Phys. Rev. Lett.* **105**, 100601 (2010).
- [321] J. Koivisto, M. Ovaska, A. Miksic, L. Laurson, and M. J. Alava, *Phys. Rev. E* **94**, 023002 (2016).
- [322] H. Nechad, A. Helmstetter, R. E. Guerjouma, and D. Sornette, *Phys. Rev. Lett.* **94**, 045501 (2005).
- [323] M. Heap, P. Baud, P. Meredith, S. Vinciguerra, A. Bell, and I. Main, *Earth Planet. Sci. Lett.* **307**, 71 (2011).
- [324] J. M. Brader, M. Siebenbürger, M. Ballauff, K. Reinheimer, M. Wilhelm, S. J. Frey, F. Weysser, and M. Fuchs, *Phys. Rev. E* **82**, 061401 (2010).
- [325] M. Pouzot, T. Nicolai, L. Benyahia, and D. Durand, *J. Colloid Interface Sci.* **293**, 376 (2006).
- [326] T. Vliet *et al.*, *Farad. Discuss.* **101**, 359 (1995).
- [327] L. G. Bremer, B. H. Bijsterbosch, R. Schrijvers, T. van Vliet, and P. Walstra, *Colloids Surf.* **51**, 159 (1990).
- [328] S. Suresh, *Fatigue of materials* (Cambridge university press, 1998).
- [329] F. Kun, M. H. Costa, R. N. C. Filho, J. S. A. Jr, J. B. Soares, S. Zapperi, and H. J. Herrmann, *J. Stat. Mech.*, P02003 (2007).
- [330] F. Kun, H. A. Carmona, J. S. Andrade, and H. J. Herrmann, *Phys. Rev. Lett.* **100**, 094301 (2008).
- [331] A. Miksic, J. Koivisto, and M. Alava, *J. Stat. Mech.* **2011**, P05002 (2011).
- [332] L. G. Bremer, T. van Vliet, and P. Walstra, *Journal of the Chemical Society, Faraday Transactions 1: Physical Chemistry in Condensed Phases* **85**, 3359 (1989).
- [333] J. Lucey and H. Singh, *Food research international* **30**, 529 (1997).
- [334] T. van Vliet, *Current Opinion in Colloid & Interface Science* **1**, 740 (1996).
- [335] B. Keshavarz, T. Divoux, S. Manneville, and G. H. McKinley, arXiv preprint arXiv:1607.08300 (2016).
- [336] B. Saint-Michel, T. Gibaud, M. Leocmach, and S. Manneville, *Phys. Rev. Applied* **5**, 034014 (2016).
- [337] K. Hyun, M. Wilhelm, C. O. Klein, K. S. Cho, J. G. Nam, K. H. Ahn, S. J. Lee, R. H. Ewoldt, and G. H. McKinley, *Prog. Polym. Sci.* **36**, 1697 (2011).
- [338] M. D. Graham, *J. Rheol.* **39**, 697 (1995).
- [339] M. J. Reimers and J. M. Dealy, *J. Rheol.* **40**, 167 (1996).
- [340] C. O. Klein, H. W. Spiess, A. Calin, C. Balan, and M. Wilhelm, *Macromolecules* **40**, 4250 (2007).
- [341] Y. Guo, W. Yu, Y. Xu, and C. Zhou, *Soft Matter* **7**, 2433 (2011).
- [342] G. Gough, C. Elam, G. Tipper, and N. De Bruyne, *The Aeronautical Journal* **44**, 12 (1940).
- [343] P. Bijlaard, *R. Dutch Acad. Sci. Proc.* **49**, 1189 (1946).
- [344] M. A. Biot, *Proc. R. Soc. Lond. A* **242**, 444 (1957).
- [345] N. Bowden, S. Brittain, A. G. Evans, J. W. Hutchinson, and G. M. Whitesides, *nature* **393**, 146 (1998).
- [346] J. Genzer and J. Groenewold, *Soft Matter* **2**, 310 (2006).
- [347] D. Bissett, D. Hannonand, and T. Orr, *Photochemistry and photobiology* **46**, 367 (1987).
- [348] T. Savin, N. A. Kurpios, A. E. Shyer, P. Florescu, H. Liang, L. Mahadevan, and C. J. Tabin, *Nature* **476**, 57 (2011).
- [349] P. Ciarletta, V. Balbi, and E. Kuhl, *Physical review letters* **113**, 248101 (2014).
- [350] A. E. Shyer, T. Tallinen, N. L. Nerurkar, Z. Wei, E. S. Gil, D. L. Kaplan, C. J. Tabin, and L. Mahadevan, *Science* **342**, 212 (2013).
- [351] M. Trejo, C. Douarche, V. Bailleux, C. Poulard, S. Mariot, C. Regeard, and E. Raspaud, *Proceedings of the National Academy of Sciences* **110**, 2011 (2013).

-
- [352] M. Asally, M. Kittisopikul, P. Rué, Y. Du, Z. Hu, T. Çağatay, A. B. Robinson, H. Lu, J. Garcia-Ojalvo, and G. M. Süel, *Proceedings of the National Academy of Sciences* **109**, 18891 (2012).
- [353] K. Efimenko, M. Rackaitis, E. Manias, A. Vaziri, L. Mahadevan, and J. Genzer, *Nature materials* **4**, 293 (2005).
- [354] M. Guvendiren, J. A. Burdick, and S. Yang, *Soft Matter* **6**, 5795 (2010).
- [355] P. Kim, M. Abkarian, and H. A. Stone, *Nature materials* **10**, 952 (2011).
- [356] F. Brau, H. Vandeparre, A. Sabbah, C. Poulard, A. Boudaoud, and P. Damman, arXiv preprint arXiv:1006.2404 (2010).
- [357] Z. Hu, Y. Chen, C. Wang, Y. Zheng, and Y. Li, *Nature* **393**, 149 (1998).
- [358] J. Kim, J. Yoon, and R. C. Hayward, *Nature materials* **9**, 159 (2010).
- [359] E. Dickinson and L. M. Merino, *Food hydrocolloids* **16**, 321 (2002).
- [360] C. Bechinger, R. Di Leonardo, H. Löwen, C. Reichhardt, G. Volpe, and G. Volpe, *Reviews of Modern Physics* **88**, 045006 (2016).
- [361] J. Schwarz-Linek, C. Valeriani, A. Cacciuto, M. Cates, D. Marenduzzo, A. Morozov, and W. Poon, *Proceedings of the National Academy of Sciences* **109**, 4052 (2012).
- [362] T. Sanchez, D. T. Chen, S. J. DeCamp, M. Heymann, and Z. Dogic, *Nature* **491**, 431 (2012).
- [363] P. J. Lu, E. Zaccarelli, F. Ciulla, A. B. Schofield, F. Sciortino, and D. A. Weitz, *Nature* **453**, 499 (2008).
- [364] E. Bianchi, J. Largo, P. Tartaglia, E. Zaccarelli, and F. Sciortino, *Physical review letters* **97**, 168301 (2006).
- [365] J. Dunkel, S. Heidenreich, K. Drescher, H. H. Wensink, M. Bär, and R. E. Goldstein, *Physical review letters* **110**, 228102 (2013).
- [366] H. H. Wensink, J. Dunkel, S. Heidenreich, K. Drescher, R. E. Goldstein, H. Löwen, and J. M. Yeomans, *Proceedings of the National Academy of Sciences* **109**, 14308 (2012).
- [367] C. Dombrowski, L. Cisneros, S. Chatkaew, R. E. Goldstein, and J. O. Kessler, *Physical review letters* **93**, 098103 (2004).
- [368] K. Wong, A. Ayuso-Sacido, P. Ahyow, A. Darling, J. A. Boockvar, and M. Wu, *Journal of visualized experiments: JoVE* (2008).
- [369] M. Dahan, M. Morel, J.-C. Galas, V. Studer, and D. Bartolo, “Microfluidic system for controlling the concentration of molecules for stimulating a target,” (2015), uS Patent 9,164,083.
- [370] M. Morel, J.-C. Galas, M. Dahan, and V. Studer, *Lab on a Chip* **12**, 1340 (2012).
- [371] O. Sipos, K. Nagy, R. Di Leonardo, and P. Galajda, *Physical review letters* **114**, 258104 (2015).
- [372] R. Di Leonardo, L. Angelani, D. Dell’Arciprete, G. Ruocco, V. Iebba, S. Schippa, M. Conte, F. Mecarini, F. De Angelis, and E. Di Fabrizio, *Proceedings of the National Academy of Sciences* **107**, 9541 (2010).
- [373] S. E. Spagnolie, G. R. Moreno-Flores, D. Bartolo, and E. Lauga, *Soft Matter* **11**, 3396 (2015).
- [374] X.-L. Wu and A. Libchaber, *Physical review letters* **84**, 3017 (2000).
- [375] D. Germain, M. Leocmach, and T. Gibaud, *American Journal of Physics* **84**, 202 (2016).
- [376] P. Maurer, J. Ferrand, M. Leocmach, and T. Gibaud, *Bulletin de l’Union des Physiciens* **108**, 1567 (2014).
- [377] C. Kahlfuss, T. Gibaud, S. Denis-Quanquin, S. Chowdhury, G. Royal, F. Chevallier, E. Saint-Aman, and C. Bucher, *Chemistry—A European Journal* **24**, 13009 (2018).
- [378] N. Taberlet, N. Plihon, L. Auzémery, J. Sautel, G. Panel, and T. Gibaud, *European Journal of Physics* **39**, 035803 (2018).
- [379] A. Gibaud and T. Gibaud, *Bulletin de l’Union des Physiciens* **101**, 167 (2007).
- [380] T. Gibaud and A. Gibaud, *Bulletin de l’Union des Physiciens* **101**, 141 (2007).
- [381] T. Gibaud and A. Gibaud, *Bulletin de l’Union des Physiciens* **101**, 1195 (2007).
- [382] A. Gibaud and T. Gibaud, *Bulletin de l’Union des Physiciens* **101**, 894 (2007).
- [383] A. Gibaud, G. Ripault, T. Gibaud, and e. ISTD, *Bulletin de l’Union des Physiciens* **107**, 319 (2013).
- [384] T. Gibaud, F. Cardinaux, J. Bergenholtz, A. Stradner, and P. Schurtenberger, *Soft Matter* **7**, 857 (2011).
- [385] T. Gibaud, N. Mahmoudi, J. Oberdisse, P. Lindner, J. S. Pedersen, C. L. Oliveira, A. Stradner, and P. Schurtenberger, *Faraday Discuss.* **158**, 267 (2012).
- [386] T. Gibaud and P. Schurtenberger, *Journal of Physics: Condensed Matter* **21**, 322201 (2009).
- [387] T. Gibaud, A. Zacccone, E. Del Gado, V. Trappe, and P. Schurtenberger, *Phys. Rev. Lett.* **110**, 058303 (2013).